

CHEMICAL GENETIC APPROACHES FOR ELUCIDATING PROTEASE
FUNCTION AND DRUG-TARGET POTENTIAL IN *PLASMODIUM*
FALCIPARUM

Michael B. Harbut

A DISSERTATION

in

PHARMACOLOGY

Presented to the Faculties of the University of Pennsylvania

in

Partial Fulfillment of the Requirements for the

Degree of Doctor of Philosophy

2012

Supervisor of Dissertation:

Doron C. Greenbaum, PhD
Assistant Professor of Pharmacology

Graduate Group Chairperson:

Vladimir R. Muzykantov, PhD
Professor of Pharmacology

Dissertation Committee:

John B. Hogenesch, PhD, Associate Professor of Pharmacology (Chair)

Scott L. Diamond, PhD, Arthur E. Humphrey Professor of Chemical and
Biomolecular Engineering

David S. Roos, PhD, E. Otis Kendall Professor of Biology

David W. Speicher, PhD, Caspar Wistar Professor in Computational and Systems
Biology

Acknowledgements

Presented herein is work that could only have come to fruition with the support, both scientifically and otherwise, of numerous individuals. My most immediate gratitude is dedicated towards my mentor, Doron Greenbaum. His support facilitated this work in a variety of ways. Just as importantly, he fostered an intellectually rigorous and enthusiastic scientific environment, the consequences of which I will appreciate long after I've left the lab. I am also grateful to the various members of the Greenbaum lab over the past five years who always made the lab lively and enjoyable to be in.

I am appreciative of the time and guidance provided by my committee, Drs. Scott Diamond, John Hogenesch, David Roos, and David Speicher. I am grateful for support and funding provided by the Pharmacology Graduate Group as well as the Parasitology Training Grant. This work was produced in collaboration with many scientists, both at Penn and elsewhere, whose efforts, advice, and outstanding science I am thankful for.

I have numerous friends who have provided a cathartic outlet from the stress of lab for which I am extremely grateful. My family has always provided support but never pushed me in any one direction, and for this deft touch, I am and will always be extremely thankful. Finally, Laura has been the one variable that has remained constant during the last five years, for which I am more appreciative than I can express here.

Abstract

CHEMICAL GENETIC APPROACHES FOR ELUCIDATING PROTEASE FUNCTION AND DRUG-TARGET POTENTIAL IN *PLASMODIUM* *FALCIPARUM*

Michael B. Harbut

Advisor: Doron C. Greenbaum, PhD

Plasmodium falciparum is a protozoan parasite and the causative agent of malaria, which kills upwards of 1 million people annually. With the increasing prevalence of drug-resistant parasites, considerable interest now exists in the identification of new biological targets for the development of new malaria chemotherapeutics. However, given the genetic intractability inherent in studying *P. falciparum*, it is imperative that novel approaches be developed if we are to understand the role of essential enzymes. My work presented here focuses on the development and use of chemical tools to study malarial proteases, a class of enzymes that have been shown to play essential roles throughout the parasite lifecycle, but the majority of which though are still uncharacterized. In Chapter 2 I develop a novel set of activity-based probes (ABPs) based on the natural product metallo-aminopeptidase (MAP) inhibitor bestatin. I show the bestatin-based ABP allows the functional characterization of MAP activity within a complex proteome. In Chapter 3, I utilize an extended library of bestatin-based ABPs to define the function of two essential malarial MAPs, PfA-M1 and Pf-LAP. I find that PfA-M1 is necessary in the proteolysis of hemoglobin and that lethal inhibition starves parasites of amino acids. I also show that Pf-LAP has a role other than hemoglobin digestion, as parasites are susceptible to its inhibition prior to the onset of this process. In Chapter 4, I use a suite of specific small molecules to validate the *P. falciparum* signal peptide peptidase (PfSPP) as a drug target. This work shows that PfSPP is a druggable enzyme and that parasites are extremely vulnerable to its inhibition. Evidence is also presented that suggests this enzyme

may play an important role in the parasite's endoplasmic reticulum stress-response.

Table of Contents

| | |
|---|------|
| TITLE..... | i |
| ACKNOWLEDGEMENTS..... | ii |
| ABSTRACT..... | iii |
| TABLE OF CONTENTS..... | iv |
| LIST OF TABLES..... | vii |
| LIST OF FIGURES..... | viii |
| LIST OF SCHEMES..... | x |
| <u>CHAPTER 1: INTRODUCTION</u> | 1 |
| 1.1 Malaria | 1 |
| 1.2 The <i>Plasmodium falciparum</i> life cycle | 4 |
| 1.3 Proteolytic enzymes and their roles during the erythrocytic stage of <i>P. falciparum</i> | 7 |
| 1.4 Understanding protein function in <i>P. falciparum</i> : a chemical-genetics approach | 11 |
| 1.5 Using chemical genetics to study protease function in <i>P. falciparum</i> | 13 |
| 1.6 Proteases as drug targets in <i>P. falciparum</i> | 16 |
| <u>CHAPTER 2: DEVELOPMENT OF BESTATIN-BASED ACTIVITY-BASED</u> | |
| <u>PROBES FOR METALLO-AMINOPEPTIDASES</u> | 21 |
| 2.1 Introduction | 20 |
| 2.2 Results and Discussion | 25 |
| 2.3 Experimental procedures | 36 |
| <u>CHAPTER 3: A BESTATIN-BASED CHEMICAL BIOLOGY STRATEGY</u> | |
| <u>REVEALS DISTINCT ROLES FOR MALARIAL M1 AND M17 FAMILY</u> | |
| <u>AMINOPEPTIDASES</u> | 38 |
| 3.1 Introduction | 3 |

| | |
|--|------------|
| 3.2 Results | 41 |
| 3.3 Discussion | 64 |
| 3.4 Experimental procedures | 68 |
| <u>CHAPTER 4: CHEMICAL VALIDATION OF SIGNAL PEPTIDE PEPTIDASES AS</u> | |
| <u>POTENTIAL ANTI-PROTOZOAN DRUG TARGET</u> | 78 |
| 4.1 Introduction | 78 |
| 4.2 Results | 81 |
| 4.3 Discussion | 98 |
| 4.4 Experimental procedures | 101 |
| <u>CHAPTER 5: CONCLUSIONS AND FUTURE DIRECTONS</u> | |
| 105 | |
| 5.1 A bestatin-based chemical biology strategy reveals distinct roles for M1 and M17 family aminopeptidases | 105 |
| 5.2 Chemical validation of signal peptide peptidases as potential anti-protozoan targets | 109 |
| <u>REFERENCES</u> | 116 |

List of Tables

| | |
|---|----|
| Table 3.1: Data Collection and refinement statistics..... | 73 |
|---|----|

List of Figures

| | |
|---|----|
| Figure 1.1: The malaria parasite erythrocytic pathway..... | 6 |
| Figure 2.1: General mode of binding of bestatin..... | 24 |
| Figure 2.2: Anatomy of ABPs and labeling of aminopeptidase N..... | 28 |
| Figure 2.3: Aminopeptidase N ABP labeling by fluorophore-containing bestatin..... | 30 |
| Figure 2.4: “Click” chemistry-based ABP labeling of aminopeptidase N..... | 33 |
| Figure 2.5: ABP labeling of the malarial M1 metallo-aminopeptidase in cell lysates..... | 34 |
| Figure 3.1: Identification of PfA-M1 and Pf-LAP as the targets of the anti-parasitic MAP inhibitor bestatin..... | 44 |
| Figure 3.2: Bestatin-based ABP libraries reveal distinct chemotypes produced by ABPs with increased specificity for either PfA-M1 or Pf-LAP..... | 48 |
| Figure 3.3: Biochemical and structural characterization of BTA and PNAP specificity against PfA-M1 and Pf-LAP..... | 53 |
| Figure 3.4: DV-localised endoproteases are not inhibited by BTA..... | 54 |
| Figure 3.5: Inhibition of PfA-M1 kills parasites via disruption of Hb digestion whereas Pf-LAP kills via a distinct mechanism..... | 58 |
| Figure 3.6: Inhibition of PfA-M1 causes DV swelling but does not prevent proteolytic cleavage of full length Hb..... | 61 |
| Figure 3.7: Inhibition of PfA-M1 blocks proteolysis of specific Hb oligopeptides..... | 62 |
| Figure 3.8: Small dipeptide species accumulate in BTA-treated parasites..... | 63 |
| Figure 4.1: SPP/PS Inhibitor pharmacology against protozoan parasites and photolabeling of PfSPP with a (Z-LL) ₂ -based probe..... | 84 |

| | |
|--|----|
| Figure 4.2: Yeast activity-based SPP assay..... | 87 |
| Figure 4.3: Generation of parasites resistant to potent PfSPP inhibitors..... | 91 |
| Figure 4.4: PfSPP localizes to the parasite ER and is important during the trophozoite stage..... | 94 |
| Figure 4.5: Inhibition of PfSPP synergizes with ER stress in <i>P. falciparum</i> and potentiates the antimalarial effect of an inhibitor of the ERAD pathway..... | 97 |

List of Schemes

Scheme 2.1: Synthesis of bestatin-based ABPs.....27

Scheme 2.2: Synthesis of a clickable bestatin-based ABP.....33

Chapter 1: Introduction

1.1 The burden of malaria

Plasmodium is the etiological agent of malaria, a devastating global public health burden that each year leaves over 400 million people infected and up to 1 million dead, over 75% of them African children [1]. The disease manifests itself as a serious illness characterized by recurrent fevers, metabolic acidosis, respiratory distress, and anemia, and fatal cases occur disproportionately in young children [2]. Four species of *Plasmodium* infect humans and all are transmitted through the bite of the female *Anopheles* mosquito. The species *Plasmodium falciparum* is the most severe, accounting for the vast majority of malaria-associated deaths. This is largely the result of its propensity to produce surface changes upon the infected erythrocyte that cause cytoadherence and disruption of the microvasculature in organs such as the lungs, kidneys, and brain. [3]. While over 50% of the world's population is exposed to malaria, the African continent shows the greatest burden from this disease and accounts for more than 90% of all malaria deaths. This, along with the compounding burdens of tuberculosis and HIV/AIDS within these populations, has had catastrophic socio-economic consequences for sub-Saharan South Africa [4].

While malaria is today perceived as a tropical disease, it is only in the last century that malaria has been eliminated from most developed Western nations. Elimination of malaria from North Africa and Europe was achieved primarily through the systematic control or elimination of the mosquito vector, such as through the use of anti-insecticidal agents (mainly DDT) and the elimination of

breeding habitats [5]. The World Health Organization launched the Global Malaria Eradication Program in 1955, was key to this accomplishment in Europe, but similar success was not shared in sub-Saharan Africa [6]. In the second half of the nineteenth century eradication efforts were largely abandoned due to diminishing resources, strife, concern about DDT, insecticide resistance, and the growing thought that eradication in Africa was virtually impossible.

Today, where it is endemic, malaria is managed by two primary methods: 1) vector control (indoor residual spraying, insecticide treated nets) and 2) treatment. While a significant effort has been put towards the development of a malaria vaccine, the most advanced candidate (RTS,S) has shown only modest success in clinical trials and is not likely to see widespread use until 2015 [7]. In addition, almost complete vector coverage will still necessitate the use of drug administration to help eliminate malaria in high transmission areas.

Quinine, derived from the bark of the tree *Cinchona calisaya*, has been used to treat malaria since the 17th Century. Due to its low cost and ease of use, the quinine-related drug chloroquine remained a constant in the control of acute uncomplicated malaria for over 40 years since the discovery of its antimalarial properties in 1946 [8]. Chloroquine inhibits the parasite's mechanism for heme detoxification, likely resulting in lethal lysis of the lysosome-like organelle where this occurs. Other frequently used antimalarials target parasite-essential metabolic pathways, such as the tetrahydrofolic acid synthesis (sulfadoxine-pyrimethamine).

Unfortunately, *P. falciparum* resistance to chloroquine arose within 20 years of its introduction and by the 1980s widespread resistance was reported in most high-transmission areas, virtually nullifying the effectiveness this drug. Resistance to drugs with specific enzyme targets such as sulfadoxine-pyrimethamine arose at an even quicker pace [9].

Modern malaria chemotherapy relies on the active ingredient of the Qinghao plant, a sesquiterpene lactone called artemisinin, and its use in combinations with other antimalarials. The mechanism of action of artemisinin and artemisinin derivatives is still debated, but its properties have facilitated its use as a frontline defense, including rapid activity against existing drug-resistant strains and blood stages of the parasite, in addition to mature sexual stage gametocytes, which helps reduce transmission. By using artemisinin in combination therapy (ACT), that is, two medicines with different mechanisms of action, the probability for the emergence of parasite resistance is drastically reduced. Indeed, in areas where artemisinin monotherapy has predominated, reports of resistance are beginning to emerge [10].

The global spread of resistance to current antimalarial standards has spurred an innovation in malaria research over the last 20 years. The current antimalarial drug-development pipeline is mostly devoid of newly defined molecular targets, being dominated by alternative artemisinin-based combination therapies or new generations of validated inhibitors (www.mmv.org). Thus, it is essential that more information is gathered on the parasite's essential biological

pathways and enzymes. This way, a more rational approach to the validation of novel targets may be achieved to further the development of new antimalarials.

1.2 The *Plasmodium falciparum* life cycle

Plasmodium spp are obligate intracellular protozoan parasites, and progress through a complicated life cycle both in a mosquito vector and human host. The asexual erythrocytic cycle, which in *P. falciparum* is synchronous and lasts 48 hrs, is the cause of morbidity and mortality associated with malaria [11]. Transmission occurs via the bite of an *Anopheles* mosquito, which injects sporozoite forms that migrate to the liver. After multiple rounds of replication in hepatocytes, merozoites are released into the blood stream and the erythrocytic life cycle of the parasite begins. This cycle is initiated by the invasion of host red blood cells by the merozoites and the formation of a parasitophorous vacuole inside the erythrocyte within which the new ring stage parasite resides. Parasites progress through the ring stage for approximately 20 hrs. This is followed by a highly metabolically active growth stage, the trophozoite stage, which is accompanied by the uptake and degradation of host hemoglobin. At about 36 hrs post invasion, parasites begin a process of asexual reproduction leading to the formation of 16-32 daughter merozoites. Finally, the merozoite-containing red blood cells are lysed around 48 hrs post infection, releasing the parasites, and the process begins anew upon invasion of erythrocytes by merozoites.

Catabolic processes are known to mediate a number of events during the parasite's life cycle. Essential to those processes are protease enzymes, both derived from the parasite and human host.

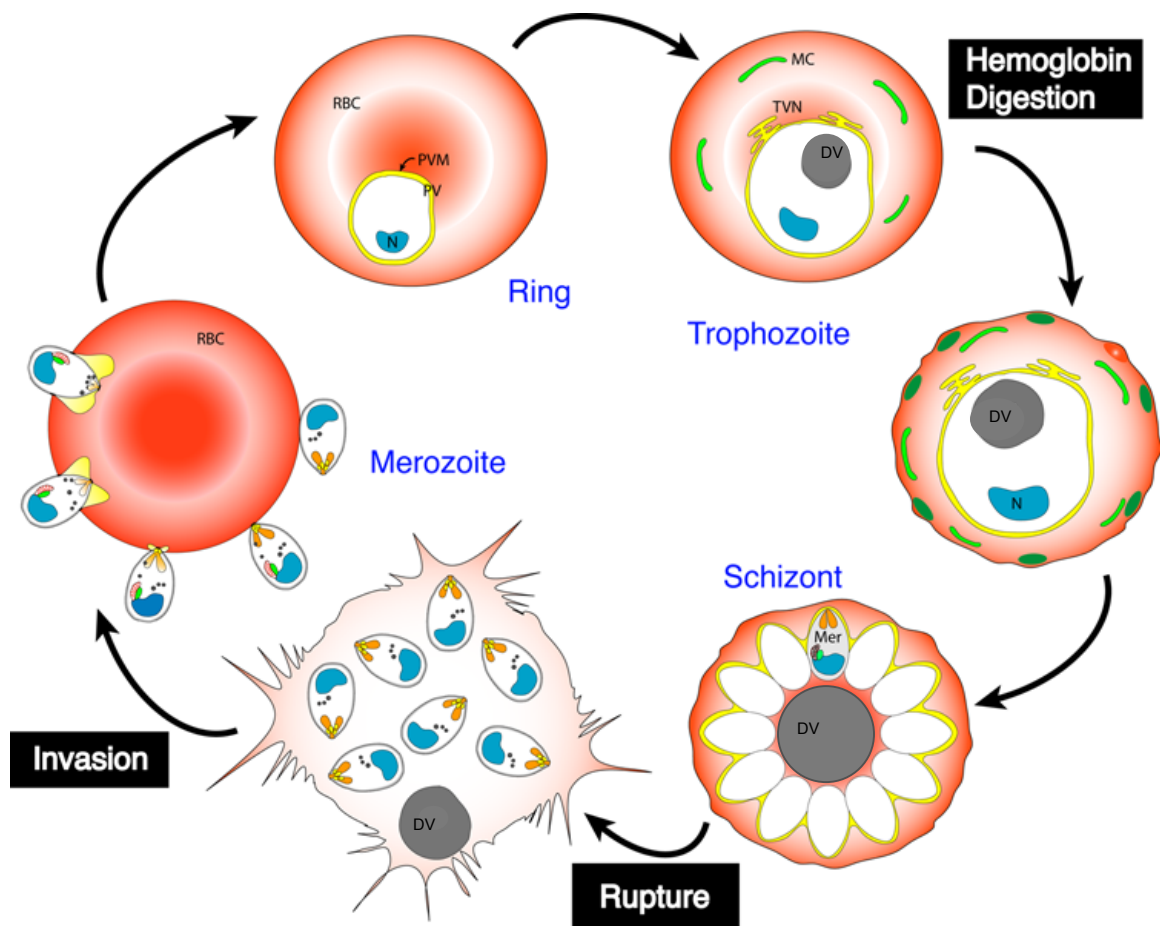


Figure 1.1: The malaria parasite erythrocytic pathway. Merozoite parasites invade the erythrocyte (RBC) and develop into ring stage parasites within the parasitophorous vacuole (PV). The peak of the parasite's metabolic activity occurs during the growing trophozoite stage, during which host cell cytoplasm is endocytosed and large-scale hemoglobin proteolysis is carried out within the digestive vacuole (DV). In addition, the parasite sets up a complex secretory pathway during this stage for delivering proteins to the PV and host cell. During the schizont stage multiple rounds of nuclear division occur, which results in the formation of daughter merozoites. At roughly 48 hrs post infection (for *P. falciparum*), the parasite ruptures from the host cell.

1.3 Proteolytic enzymes and their roles during the erythrocytic stage of *P. falciparum*

Proteolytic enzymes, or proteases, catalyze the degradation of proteins or peptides and have wide-ranging and important roles from single-cell prokaryotes to metazoans. There are approximately 100 predicted proteases in the *Plasmodium* genome that span all classes and several proteases are thought to participate in critical pathways during the life cycle of *P. falciparum* [12]. As such, proteases and the biological events they mediate have been considered potential anti-malarial drug targets. Specifically, three events during the erythrocytic life cycle have been extensively studied so as to uncover the proteolytic events necessary: 1) merozoite invasion of the erythrocyte, 2) hemoglobin degradation, and 3) egress from the erythrocyte [13-15].

Early evidence for the importance of proteolysis during invasion was uncovered using purified *P. knowlesi* merozoites. Pre-treatment of the merozoites with a variety of protease inhibitors significantly decreased the invasion capacity of the parasite [16]. Follow-up work in *P. falciparum* has focused on primarily on the role of proteases that process merozoite-associated proteins. During invasion, sets of adhesin molecules are released from the parasite apical secretory organelles, the micronemes, which facilitate high affinity binding of the host cell and parasite. The most abundant of these is a glycosyl phosphatidylinositol (GPI)-anchored protein named merozoite surface protein-1 (MSP1) [17]. MSP1 is synthesized during development of intracellular merozoites

and at the end of schizogony is proteolytically processed by a serine protease called PfSUB1, resulting in a non-covalent complex of several polypeptides. Two other proteins are also part of this complex (MSP6 and MSP7) and are processed as well. The importance of this primary processing event is still unclear, but it is possible that it allows a conformational change that enables the complex to function on the free merozoite at the time of invasion. During subsequent invasion events, the N-terminus is shed from the merozoite surface by a membrane-bound subtilisin-like protease, PfSUB2 [18].

Apical membrane antigen 1 (AMA-1) is another important adhesin whose function depends on proteolytic processing [19,20]. Like MSP1, AMA-1 is synthesized in the apical complex of the merozoite and undergoes multiple rounds of proteolytic maturation prior to circumferential redistribution on the merozoite surface. In addition, once it is translocated from the apical complex to the parasite surface it is then shed from the membrane by PfSUB2. Additional cleavage is carried out by an intramembrane serine protease, rhomboid 1 (PfROM1), the biological relevance of which is still being assessed [21].

Once established inside the erythrocyte, the parasite begins to endocytose host hemoglobin (Hb) and proteolytically digests it into its constituent amino acids within a lysosome-like organelle called the digestive vacuole (DV) [15]. This process peaks during the parasite's most active metabolic stage, between 20-36 hours post infection, and is likely carried out to relieve osmotic pressure for the growing parasite and for utilization of individual amino acids derived from Hb [22,23]. Hb degradation is necessary for the survival of the

parasite, and has long been considered an “Achilles heel” of the parasite. Thus the putative proteases involved have been focus of intense study for their drug target potential.

The upstream endoproteases that catalyze the initial cleavage of the Hb molecule are the aspartyl protease plasmepsins (I-IV) and the cysteine protease falcipains (2, 2', 3) [24,25]. The roles for cysteine and aspartyl protease activity were originally identified by biochemical characterization of whole DVs and purified enzymes, where the hydrolysis of native and denatured hemoglobin was analyzed under assumed physiologic conditions [26-28]. The discovery of additional proteases was facilitated by the *P. falciparum* genome sequencing project. The active roles of the individual enzymes are still uncertain. Some have described it as an ordered process, initiated by the plasmepsins at the α Phe33-Leu34 conserved hinge region of Hb, whereas others have suggested that the falcipains initially cleave rapidly at multiple sites in intact hemoglobin [15,29]. A striking functional redundancy exists amongst these proteases, suggesting the importance of this process to the parasite. For instance, the falcipains appear to be able to compensate for the loss of all four DV plasmepsins [30]. A metalloprotease, falcilysin, has also been localized to the DV and is capable of cleaving small Hb peptides 11-15 residues in length, suggesting it has a role downstream of the plasmepsins and falcipains [31]. Finally, exopeptidases release individual amino acids from the N-terminus of Hb, and their roles are discussed in depth in Chapter 3.

At the end of its erythrocytic life cycle, the parasite disrupts both the membrane to the parasitophorous vacuole and the host erythrocytes to allow egress from the cell. That protease inhibitors can block egress tells us that rupture is indeed an active process and not a passive consequence of parasite growth [32]. The SERA family of proteins have been a primary focus of protease-mediated rupture in *P. falciparum* based on the evidence that the *P. berghei* ortholog to *SERA8* is essential for egress from the oocyst wall of the mosquito midgut [33]. The gene products of all the *SERA* family members have been detected in the asexual blood stage during late schizogony. In addition, *SERA5*, an essential gene product, is proteolytically processed during rupture. Processed products of *SERA5* precursor are found in culture supernatants, and only the precursor could be detected in unruptured schizonts [34,35]. Mechanical disruption of parasites releases unprocessed *SERA5*, suggesting that a specific pathway of events is necessary during rupture for *SERA* processing. The mechanistic importance of this processing has yet to be uncovered. Intriguingly, the *SERA* proteins all share a conserved papain-like cysteine protease domain, suggesting that proteolytic processing of the respective *SERAs* may represent an activation event of a non-catalytic zymogen precursor. While a refolded papain domain of *SERA5* has shown weak chymotrypsin-like activity, the role of *SERAs* during egress remain to be elucidated [36].

Even with our current limited understanding of protease function in *P. falciparum* biology, the critical role these enzymes have in the biology of the parasite is clear. Further characterization of malarial proteases will likely uncover

novel essential functions, the results of which may lead to putative drug target candidates. To facilitate these discoveries, tools beyond classical genetic approaches, which remain burdensome in *P. falciparum*, must be developed and utilized.

1.4 Understanding protein function in *P. falciparum*: a chemical-genetics approach

Significant biochemical and biological work has helped to elucidate essential protease-mediated events during the *P. falciparum* life cycle. Yet, of the approximately 100 proteases encoded by the parasite genome, fewer than 15 have been fully characterized, making this biological system ripe for study. Unfortunately, the systematic approaches used today to study gene function in other organisms, such as RNAi, are not available in *P. falciparum*, leaving classical gene disruption, via homologous recombination, the main genetic technique [37]. Additionally, the procedure for targeted gene disruption is inherently labor-intensive, slow, and inefficient, due to difficulties in the culturing of the parasite and extremely low transfection rates. These technical limitations and the fact that the parasite is grown as a haploid renders it currently difficult to genetically disrupt essential genes. The development of a tetracycline-based conditional gene expression system in the related apicomplexan organism *Toxoplasma gondii* has not been successfully applied for functional studies in *P. falciparum* [38].

One approach to circumvent these problems is through the use of small

molecules to modulate the activity of protein families or individual proteins to provide insight into protein function and validate potential therapeutic targets. This assemblage of techniques is broadly called “chemical-genetics” [39]. As opposed to manipulation of DNA, as in classical chemical genetics, small molecules usually modulate protein function, such as by active site binding or preventing protein-protein interactions. In addition, small molecules offer greater temporal control, allowing for the discrimination of effects at restricted stages.

Two approaches to chemical-genetics can be undertaken to discover small molecules that modify protein function. The first approach is analogous to classical reverse genetics, in which a gene of interest is permanently or conditionally disrupted or modified in such a way that protein it codes for ceases to function. The knockout or knockdown of the gene can give functional insights as to its role in the system under study. Reverse chemical genetic strategies aim to identify small molecules that target a specific protein. These are often carried out through traditional medicinal chemistry efforts with significant underlying knowledge about the protein of interest. Recently, the Wandless lab developed a novel reverse chemical genetics strategy, that allows for the regulatable control of protein stability [40]. The approach relies on FK506-binding protein (FKBP) mutants that contain a degron that normally destabilizes the protein, but is stabilized by a small molecule. This degron can be appended to a protein of interest and will destabilize the protein in the absence of the small molecule. Application or removal of the small molecule allows for the conditional expression of the targeted protein. This approach has recently been used with success in *P.*

falciparum to validate the role of a calcium dependent kinase (PfCDPK5) in egress [41]. Parasites expressing the kinase with the destabilization domain failed to rupture from the host erythrocyte when the stabilizing small molecule was removed from culture. This phenotype was rescued upon application of the small molecule and subsequent stabilization of the kinase.

The second chemical genetics approach is known as forward chemical genetics. This technique seeks to identify a protein responsible for a phenotype or pathology under study. This is often done through the use of small molecule libraries in phenotypic screens. Upon the small molecule-mediated production of a phenotype of interest, the target(s) of the small molecule that produces the phenotype is identified. High throughput screens in *P. falciparum* are still primarily focused on parasite replication, and informative assays such as protein export to the erythrocyte surface are complex and not as amenable to high throughput screening. As such, phenotypic screens are rare for *P. falciparum*.

1.5 Using chemical genetics to study protease function in *P. falciparum*

Small-molecule based approaches have been critical to the understanding of protease function in *P. falciparum*. In a study to assess the role of proteases during invasion, Dluzewski and colleagues uncovered the first evidence for the proteolytic breakdown of hemoglobin within the digestive vacuole (DV) after discovering the accumulation of undegraded hemoglobin within the swollen DV of parasites treated with leupeptin (a general cysteine and serine protease inhibitor) [42]. Following up on this, the Leech group confirmed the necessity of cysteine

protease activity by inhibiting Hb degradation in parasites with cysteine protease inhibitors [28]. Biochemical characterization of Hb digestion from purified DVs also facilitated the discovery of aspartyl protease activity in this process [26]. These studies, using inhibitors with broad selectivity, could at best suggest a role for a specific class of proteases involved in Hb degradation. Only with extensive studies, including expression analysis, immunofluorescence localization, biochemical purification and characterization, and finally genetic knockout, could the individual roles of the endoproteases involved in Hb catabolism be ascribed to particular proteins. Further study of the putative downstream exopeptidases in the Hb catabolic pathway has been hindered because they are genetically essential and refractory to knockout [31,43,44].

More recently, much progress has been made in identifying the proteases required for rupture from the host erythrocyte, using specific inhibitors and both reverse and forward chemical genetic approaches. The Bogoy lab recently undertook a forward chemical genetics screen that utilized a facile and rapid method for the assessment of parasite staging by flow cytometry [45]. This allowed the authors to screen a library of over 1,200 covalent serine and cysteine protease inhibitors that blocked parasite egress. Upon identification of a serine protease inhibitor that blocked egress (JCP-104), they then undertook a chemical-genetics approach known as activity-based protein profiling (ABPP). ABPP is a chemical strategy that utilizes mechanism-based, tagged small molecule inhibitors. Appending a reporter tag such as a biotin or fluorophore to the mechanism-based inhibitor allows for the profiling of activity via avidin blot (or

fluorescent scanning) and the identification of the inhibitor target(s) by biotin-(strept)avidin chromatography capture, gel separation, and mass spectrometry analysis. Using JCP-104 as an ABP allowed the identification of the protein target of the inhibitor, PfSUB1. In addition, it was shown that JCP-104 inhibited the processing of SERA5, the blocking of which prevented egress.

In this same study, a cysteine protease capable of blocking rupture was also identified. Again, the suitability of ABPP in *P. falciparum* was illustrated when the authors were able to identify the target of the inhibitor, JCP-405, by utilizing the inhibitor as an ABP, and showed that it targeted two cysteine proteases, dipeptidyl-aminopeptidases 1 and 3 (DPAP3). DPAP1 was previously implicated as a hemoglobinase, while the function of DPAP3 was unknown. Using a forward chemical genetics strategy, the authors screened a focused library of dipeptide vinylsulfone inhibitors similar to JCP-405 to identify selective inhibitors of DPAP1 and DPAP3. Upon identification of specific inhibitors, they showed that selective inhibition of DPA3 resulted in a block of parasite rupture, prior to PfSUB1 processing of SERA5.

The treatment of late-stage parasites with the cysteine protease inhibitor E64 results in the accumulation of merozoites locked in the erythrocyte. E64 is a general cysteine protease inhibitor and thus targets multiple cysteine proteases [46]. The Greenbaum lab recently utilized chemical genetics combined with biochemical and cell-biological approaches to reveal a role for the host-erythrocyte calpain protease in rupture [47]. Using an activity-based probe (ABP) based on E64 they showed that human calpain 1 was active during late

schizogony and localized that the host cell membrane upon activation. Using an endogenous inhibitor specific for calpain 1, calpastatin, along with immunodepletion of calpain 1 the authors showed that human calpain 1 activity was coopted by the parasite and necessary for degradation of the host cell.

Proteases that mediate invasion have also been uncovered using chemical genetic approaches. Using a chemical screen, the Bogoy lab showed that falcipain 1 was the only active parasite cysteine protease during the invasive merozoite stage [48]. In a reverse chemical genetics approach, they identified a specific inhibitor of falcipain 1 by screening a small chemical library. Use of this specific inhibitor showed that inhibition falcipain 1 had no effect on parasite growth or hemoglobin degradation, but did result in unruptured schizonts, illustrating that falcipain 1 was indeed necessary for egress.

These studies demonstrate the promise and feasibility of using chemical tools in forwarding the understanding of protease roles in *P. falciparum* biology. Furthermore, they also help to provide proof of principle in the druggability of protease targets and identify putative starting points for drug development initiatives.

1.6 Proteases as drug targets in *P. falciparum*

The validity of targeting proteases to alleviate a pathology as a therapeutic strategy is illustrated by the clinical success of a number of protease inhibitor drugs, including inhibitors of HIV aspartyl protease, dipeptidyl peptidase IV (diabetes), and angiotensin converting enzyme (ACE) inhibitors (hypertension)

[49]. As the roles of many proteases in *P. falciparum* are essential for the parasite's life cycle, it is not unreasonable to consider the parasite proteases as potential drug targets. Moreover, extensive biochemical knowledge of protease mechanism and structure in addition to the existence of focused inhibitor libraries allows for a rational approach to the design of potential drugs.

Though the sequencing of the *P. falciparum* genome has led to the identification of at least 100 putative proteases, viewing proteases of *P. falciparum* as drug targets is a strategy that predates that long predates the genome-sequencing effort [50]. Two of the most significant efforts were directed towards the hemoglobin-catabolizing proteases, the cysteine protease falcipains and aspartyl protease plasmepsin. Efforts to identify optimal inhibitors to these enzymes were facilitated through screening of existing cysteine and aspartyl protease inhibitor libraries and through the development of novel inhibitors based on scaffolds known to inhibit the respective protease families [24,51]. Genetic approaches were also utilized, and numerous labs showed through the knockout of the individual genes that exceptional functional redundancy existed amongst all four plasmepsins and also falcipains (only falcipain-3 was shown to be essential) [30,52,53]. Unfortunately, plasmepsin inhibitors with high potency towards the recombinant enzyme often showed limited potency against cultured parasites [24]. In addition, inhibitors for both the falcipains and plasmepsins showed problems with bioavailability, undermining their effectiveness [54]. The combination of these issues has recently limited enthusiasm for these enzymes as therapeutic targets.

Multiple other proteases are expected to have a role in hemoglobin degradation, working downstream on the peptide products of Hb produced by plasmepsin, and may represent improved drug targets over falcipains or plasmepsins. These proteases include falcilysin, a metallo-aminopeptidases (PfA-M1), a proline aminopeptidase (PfAPP), and a cathepsin C-like cysteine protease DPAP1. All four have been validated as genetically essential during the erythrocytic stage. DPAP1 and PfA-M1 are the only proteases of the group shown to be amenable to chemical inhibition. A recent study utilizing ABPs to characterize DPAP1 activity identified nonpeptidic covalent inhibitors of DPAP1 lethal to parasites at low nanomolar concentrations. Unfortunately, the most potent inhibitors of DPAP1 were toxic in mice, while a less potent but non-toxic inhibitor did decrease parasite levels in a mouse model.

Given the parasite-essential nature, proteases involved in rupture and invasion may also represent attractive drug targets. DPAP3, SERA5, PfSUB1, and PfSUB2 have each been shown to be genetically essential. In addition, DPAP3 and PfSUB1 are amenable to chemical inhibition in live parasites. PfSUB2 has not been targeted by small molecules, but a PfSUB2 propeptide inhibits PfSUB2 sheddase activity in parasites. SERA5 represents an unusual cysteine protease in that a cysteine-to-serine replacement has occurred within its putative canonical catalytic site. Its protease-like domain has been expressed and, upon renaturing, shown to have weak chymotrypsin-like protease activity that was reversible with a serine protease inhibitor, although the biological relevance of these activities remains unclear. Furthermore, recent structural

characterization of SERA5 revealed a number of anomalies in addition to the non-canonical active site, further complicating any rational drug discovery efforts centering on SERA5.

Proteases represent a highly druggable class of parasite enzymes, based both on our present knowledge of their enzymology and keys to inhibition as well as their importance in numerous biological processes during the *P. falciparum* life cycle. With the increase of data from analysis of the *P. falciparum* genome project our awareness of putative protease targets is great. At the same time, translating these potential targets into validated targets requires not just knowledge of the enzyme's existence, but a better foundational understanding of the biology and biochemistry of the protease within the context of the parasite's life cycle, which will allow us to fully exploit this class of enzymes. This understanding will only come about with the development of novel technologies, such as activity-based protein profiling, coupled with classical cell biological, biochemical, and genetic techniques. Herein, work is presented that exploits these and other approaches in an attempt to forward our knowledge of *P. falciparum* protease biology while testing potential as drug-target. In Chapter 2 I present work on the development of a novel activity-based probe based on the metallo-aminopeptidase inhibitor, bestatin, as published in Harbut et al., (2008). This novel chemical reagent is then utilized in a study on metallo-aminopeptidases in *P. falciparum*, in which we identify the protease parasite targets of bestatin. Upon identification of bestatin-based specific inhibitors to two *P. falciparum* aminopeptidases, PfA-M1 and Pf-LAP, I show that inhibition of PfA-

M1 results in a block of hemoglobin peptide degradation, implicating this PfA-M1 in this process. Inhibition of Pf-LAP is lethal to parasites prior to the onset of bulk hemoglobin degradation, suggesting a role beyond the release of Hb amino acids. The latter observations are presented in Chapter 3 and were published in Harbut et al., (2011). In Chapter 4, I present work that chemically validates the malarial signal peptide peptidase (PfSPP) as a drug target along with data that indicates the *P. falciparum* endoplasmic-reticulum associated degradation (ERAD) pathway represents an untapped parasite vulnerability. Parasites are sensitive to SPP inhibitors, and utilizing a variety of approaches I show that the PfSPP protein is indeed targetable by small molecules. Data is also presented that parasites are sensitized to SPP inhibitors under conditions that produce endoplasmic reticulum stress and that SPP inhibitors combined with inhibitors of other ERAD pathway components may represent a new antimalarial chemotype.

Chapter 2: Development of bestatin-based activity-based probes for metallo-aminopeptidases*

2.1 Introduction

Metallo-aminopeptidases (MAPs) are exopeptidases that catalyze the hydrolysis and cleavage of a single N-terminal amino acid from a peptide or protein substrate. The families of MAPs are a large and diverse set of peptidases and comprise the M1, M17, and M18 families, which in humans totals 16 potential enzymes (www.merops.org). MAPs are widely distributed in organisms from bacteria to humans and play essential roles in protein maturation and regulation of the metabolism of bioactive peptides [55-57]. In addition, MAPs have been linked to several pathophysiological states including cancer and hypertension [58,59].

A major challenge in elucidating the function of peptidases during normal or pathological processes lies in their complex post-translational regulation. Peptidase activity is usually tightly controlled post-translationally, with mRNA levels frequently showing little correlation to active protein levels. In addition, peptidases can be localized to any part of a cell and are frequently found in multiple locations with different functions. A targeted proteomics approach whereby only active proteins are enriched by the use of activity-based probes (ABPs) can address these complicating issues and provide complementary data to more traditional genetic and biochemical approaches. These ABPs typically

* The text of this chapter has been published (Harbut et al. Development of bestatin-based activity-based probes for metallo-aminopeptidases. *Bioorg Med Chem Lett*. 2008 Nov 15;18(22)5932-6). It is printed here with permission.

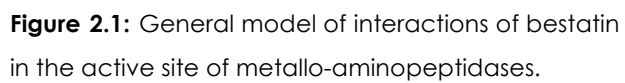
possess three main structural components: (i) a mechanism-based inhibitor scaffold to covalently or non-covalently target catalytic residues or the active site of peptidases, (ii) a linker, and (iii) a reporter tag, such as a fluorophore or biotin, for the visualization and characterization of labeling events, and eventual affinity purification of target proteins. The mechanism-based inhibitor scaffold ensures that the ABP binds to the peptidase in an activity-dependent manner. Therefore these ABPs can identify peptidases with differential levels of activity during a biological process and potentially identify candidate enzymes that regulate the specific phenotype under study. In addition, ABPs allow for screening of small molecule libraries and identification of specific inhibitors that can be used to validate the role of the target enzyme. To date, ABPs have been developed for more than a dozen enzyme classes including: peptidases, kinases, phosphatases, glycosidases and oxidoreductases [60-64].

Although the MAP superfamily is quite large and divergent, MAPs utilize a common catalytic mechanism by the coordination of one or two Zn atoms in the active site to activate water for nucleophilic attack of a peptide or protein substrate. To exploit this mechanism several classic inhibitor scaffolds have been developed to target the MAP family including, most prominently, phosphinic acids, hydroxamic acids and the bestatin family [65-69]. Both phosphinic acids and hydroxamic acids have the capacity to inhibit metallo-endopeptidases and peptide deformylase while the bestatin scaffold appears specific for MAPs.

We have thus chosen to explore the bestatin scaffold to develop ABPs to specifically target the MAP superfamily. Bestatin is a natural product of

Actinomycetes that inhibits most MAP families, including the M1, M17, and M18 families. Bestatin was originally found to be a potent aminopeptidase B and leucine aminopeptidase inhibitor and has been crystallized with leucine aminopeptidase, leukotriene A4 hydrolase, and aminopeptidase N [70-72]. Bestatin is thought to modulate many biological pathways, including the induction of apoptosis in tumors [73,74]. It is also known to possess anti-inflammatory properties [75]. Therefore a MAP-specific ABP would be a powerful tool to tease apart the functions of multiple MAP pathways. In the present study, we set out to develop the first MAP-specific ABP, exploiting bestatin for use as the inhibitor scaffold.

Bestatin resembles a Phe-Leu dipeptide substrate. However, the first residue contains a α -hydroxy group that, along with the neighboring carbonyl, coordinates the catalytic zinc atom resulting in a competitive active site-directed inhibitor (Fig. 2.1). In addition, the free amine of bestatin is coordinated by one or more glutamate residues in the MAP active site [72]. Bestatin family members are slow- and tight-binding inhibitors with well-defined interactions with the S1 and S1' active site pockets [69]. Thus bestatin represents an ideal candidate for ABP development for MAPs due to its family specificity, potency in the low nanomolar to micromolar range, synthetic tractability and potential for expansion through variation of the amino acid side chains in its core structure.

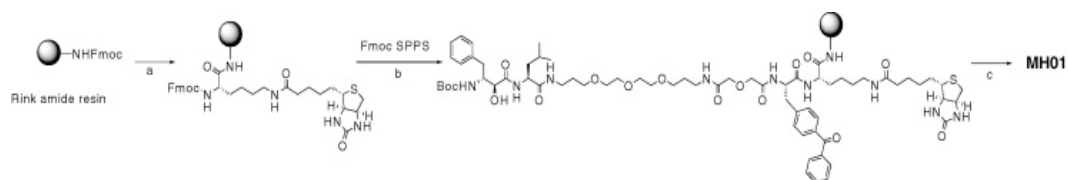


2.2 Results and Discussion

To design an ABP family for MAPs, we chose to derivatize the core bestatin inhibitor scaffold using a solid-phase synthetic strategy (Scheme 2.1). Bestatin has a free carboxyl group available for functionalization and previous x-ray crystal structures of MAP-bestatin complexes indicated that extension at this carboxylate was unlikely to perturb inhibitor binding [72]. Thus we attached the inhibitor scaffold to solid-phase resin at the carboxyl end of the molecule. Our first attempt to develop a MAP-directed ABP probe involved the addition of a spacer, a UV crosslinker, and a biotin affinity tag to the C-terminus of the core bestatin scaffold (Scheme 2.1). We included a benzophenone UV crosslinker since this is a non-covalent, reversible inhibitor scaffold. Synthesis was accomplished on solid-phase using Rink amide resin and, to our knowledge, represents the first reported solid-phase synthesis of this class of molecules.

We initially explored the placement of the spacer and UV crosslinker relative to the core bestatin scaffold (MH01 and MH02, Fig. 2.2) and found that there was little difference in labeling efficiency of a model enzyme, purified porcine aminopeptidase N (Fig. 2.2A). We then assessed the ability of MH01 to label the model aminopeptidase in an activity-dependent manner (Fig. 2.2B). Our results show that, indeed, the bestatin-based probe is an activity-dependent probe of MAPs. Firstly, competition with the unbiotinylated parental compound, bestatin, blocked all labeling seen in lane 1, indicating that the probe was

competitive and therefore binding at the active site (Fig. 2.2C, lane 2). Preheating of the sample, a process that denatures all protein targets, abrogated labeling (Fig. 2.2C, lane 3), indicating that this labeling was dependent on properly folded, active enzyme. Lastly, UV exposure was necessary for labeling owing to the fact that bestatin is a non-covalent, reversible inhibitor (Fig. 2.2C, lane 4).



Scheme 2.1: Synthesis of bestatin-based ABPs. Reagents and conditions: a) i) 20% Piperidine/DMF; ii) FmocLys(Biotin)OH, HBTU, HOBT, DIEA; iii) 20% Piperidine/DMF; iv) FmocBpaOH, HBTU, HOBT, DIEA; v) 20% Piperidine/DMF; vi) FmocNHPEGOH (20 atoms), HBTU, HOBT, DIEA; vii) 20% Piperidine/DMF; viii) FmocLeuOH, HBTU, HOBT, DIEA; ix) 20% Piperidine/DMF; x) *N*-Boc-(2*S*,3*R*)-3-amino-2-hydroxy-4-phenyl butyric acid, HATU, DIEA; xi) 95%TFA:2.5%TIS:2.5%H₂O.

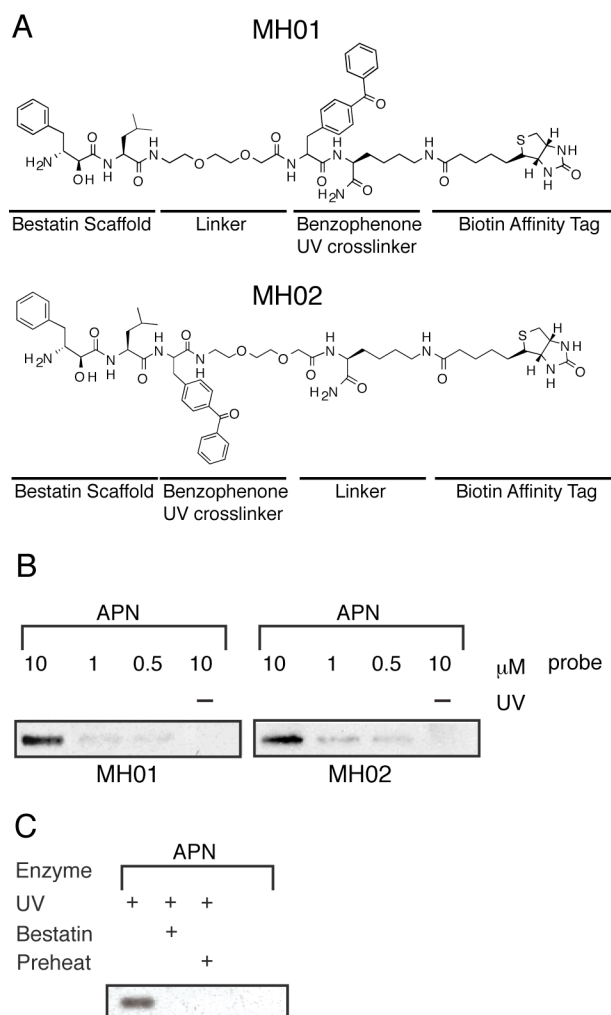


Figure 2.2: Anatomy of ABPs and labeling of aminopeptidase N. (a) Structure of ABPs MH01 and MH02. **(b)** Aminopeptidase N (0.13 U) was treated with 10, 1, or 0.5 μ M of either MH01 or MH02 for 1 hr in 50mM Tris-HCl, pH 7.8, 0.5 μ M ZnCl_2 (buffer A). Certain reaction mixtures were UV crosslinked for 1 hr on ice. Reactions were quenched with SDS-PAGE buffer, and labeled protein was visualized via SDS-PAGE and western blotting for biotin. **(c)** Aminopeptidase N was treated with 100 μ M of the aminopeptidase inhibitor bestatin or DMSO for 1 hr in buffer A followed by labeling with MH01 for 1 hr. Reactions were UV crosslinked (or not) for 1 hr on ice, and labeled protein was visualized as in Fig. 2.2B.

While a biotin tag is ideal for affinity tagging purposes, its use is not optimal for higher throughput activity-based profiling due to the time and labor involved in producing western blots. Additionally, many cells and tissues contain endogenously biotinylated proteins that complicate analysis of biotinylated probe-based western blots. To circumvent these shortcomings we synthesized a fluorophore-tagged version of the bestatin-based probe, which would allow for direct detection of labeled targets in a gel-based read-out. For the fluorescent bestatin-based probe we added a TAMRA group in addition to the biotin, creating a dual function ABP, MH03, making it suitable for both affinity purification and fluorescence applications (Fig. 2.3). Labeling of purified porcine aminopeptidase N with the dual label probe was performed under the same conditions as with the original biotinylated MH01 (Fig. 2.3B). Labeled proteins were analyzed by SDS-PAGE coupled with in-gel fluorescent scanning (Typhoon, GE). MH03 showed similar activity-dependent labeling as MH01 (Fig. 3B) demonstrating the robustness of this ABP scaffold. Some residual labeling was observed (Fig 2.3B, lane 2), which is normal in ABP labeling experiments, although this may have been enhanced since bestatin is a slow- and tight-binding inhibitor.

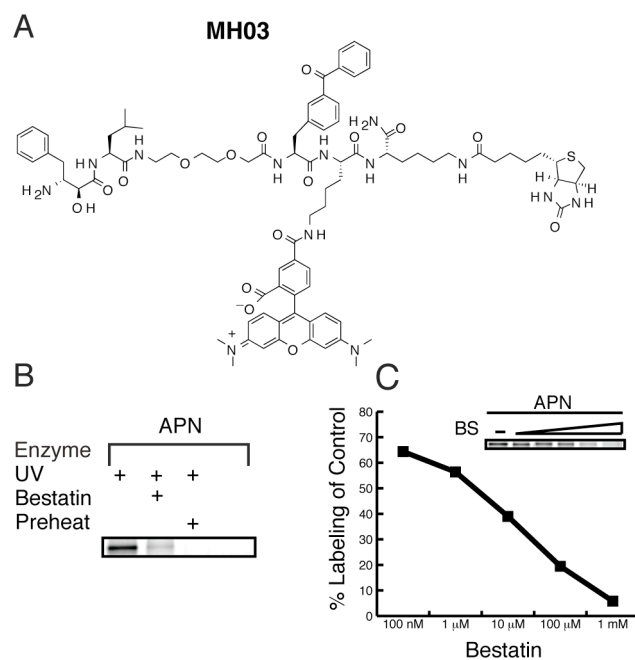
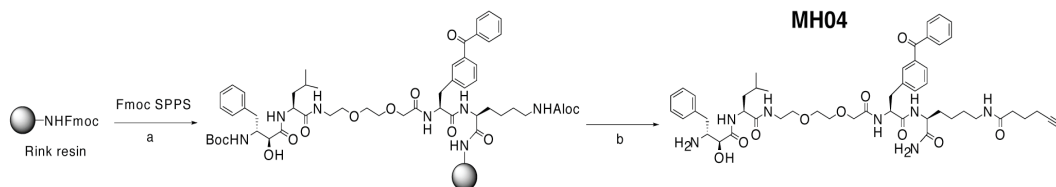


Figure 2.3: Aminopeptidase N labeling by fluorophore-containing bestatin-based ABP. (a) Structure of MH03 probe. **(b)** Labeling of aminopeptidase N was performed as described in Figure 2.2, but using MH03 and visualized using SDS-PAGE and in-gel fluorescent scanning. **(c)** Aminopeptidase N was pretreated with multiple concentrations of bestatin for 1 hr and then labeled with 10 μ M fluorescent MH03. After in-gel fluorescent scanning labeling was quantified using ImageQuant software (GE).

Next, we wanted to demonstrate that utility of the fluorescent MH03 for relative quantification of enzyme labeling. To do this, porcine aminopeptidase N was preincubated with increasing concentrations of bestatin followed by the addition of a single concentration of the fluorescent MH03. The densities of each labeled band, representing active enzyme, were quantified using a Typhoon flatbed fluorescent scanner (GE). In-gel fluorescent scanning of the labeled peptidase band showed a decrease in aminopeptidase N labeling by MH03 relative to increasing concentration of bestatin preincubation (insert in Fig. 2.3C). Percent competition values were calculated by dividing the density of the bestatin preincubated aminopeptidase N band relative to the untreated band in lane 1 (Fig. 2.3C). We demonstrate a dose dependent relationship that is amenable to relative quantification with a dynamic range of several orders of magnitude and will allow future screening efforts of derivative libraries.

One of the technical challenges facing the development and use of ABPs with biotin or fluorophore tags is limited or biased uptake by live cells. In some cases, ABPs have been used to label enzymes in living cells, but a more universal system for labeling would employ a small, hydrophobic tag. We therefore chose to add a small alkyne tag to our MAP probe in order to utilize the popular “click” bio-orthogonal chemistry, which employs a 1,3-dipolar azide/alkyne cycloaddition [76,77]. We thus replaced the biotin of MH01 with a C-terminal alkyne resulting in a click probe, MH04 (Scheme 2.2 and Fig. 2.4). We observed facile “click” addition of a biotinylated azide following labeling of porcine aminopeptidase N with MH04. Importantly the activity-dependent labeling of the

enzyme was not affected by this procedure, as illustrated by bestatin preincubation, UV, and preheat controls.



Scheme 2.2: Synthesis of a clickable bestatin ABP. Reagents and conditions: a) i) 20% Piperidine/DMF; ii) FmocLys(Aloc)OH, HBTU, HOBT, DIEA; iii) 20% Piperidine/DMF; iv) FmocBpaOH, HBTU, HOBT, DIEA; v) 20% Piperidine/DMF; vi) FmocNHPEGOH (9 atoms), HBTU, HOBT, DIEA; vii) 20% Piperidine/DMF; viii) FmocLeuOH, HBTU, HOBT, DIEA; ix) 20% Piperidine/DMF; x) *N*-Boc-(2*S*,3*R*)-3-amino-2-hydroxy-4-phenyl butyric acid, HATU, DIEA; b) i) Pd(PPh₃)₄, PhSiH₃, DCM; ii) hexynoic acid, HBTU, HOBT, DIEA; iii) 95%TFA:2.5%TIS:2.5%H₂O.

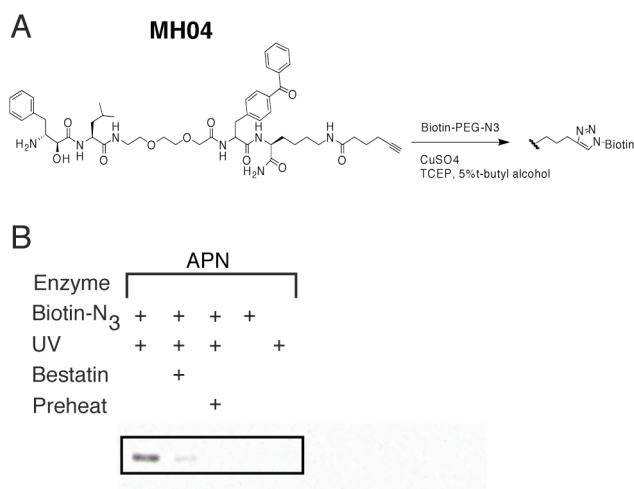


Figure 2.4: “Click” chemistry-based ABP labeling of aminopeptidase N. (a) Structure of MH04 probe. (b) Aminopeptidase N labeling was performed as described in Figure 2.2C using MH04. The ligation of the biotin-azide reporter tag was performed by adding 100 μ M of the biotin-azide tag, followed by 1 mM TCEP (tris(2-carboxyethyl) phosphine hydrochloride), 100 mM ligand (tris[(1-benzyl-1*H*-1,2,3-triazol-4-yl)methyl]amine) (17x stock in DMSO:t-butanol 1:4), and 1 mM CuSO₄. Reactions were allowed to proceed for 1 h at room temperature, then quenched with equal volume of SDS-PAGE loading buffer. Labeled protein was visualized as in Fig. 2.2B.

Finally, to validate the utility of the probe as an ABP for MAPs in the context of a complex proteome, we assessed labeling of an aminopeptidase N homolog from the malarial parasite (PfA-M1) from whole cell lysates. To facilitate the identification of PfA-M1 from *P. falciparum* we utilized a parasite line that expresses the endogenous PfA-M1 as a YFP C-terminal fusion. Homogenized whole cell lysates from *P. falciparum* were labeled with MH01. The resulting proteome was separated by SDS-PAGE and western blot analysis was performed to first visualize biotinylated proteins. A 150 kD protein was labeled by MH01, which corresponds to the approximate weight of the PfA-M1-YFP fusion protein (Fig. 2.5A). Preincubation of the protein lysate with unbiotinylated bestatin (Fig. 2.5A, lane 2) resulted in loss of labeling of the 150 kD band illustrating that bestatin was competitive with MH01 for this protein target. Additionally, the target was labeled in an activity-dependent manner, as preheating of the proteome prior to labeling abrogated any labeling (Fig. 2.5A, lane 3). Finally, to identify this target the blot was stripped and reprobed using an anti-YFP antibody (Fig. 2.5B). The anti-YFP revealed the presence of the expected 150kD fusion protein in all lanes and this band overlaid the exact position where the biotinylated protein appeared. It should be noted that PFA-M1-YFP fusion appeared in all lanes with the anti-YFP antibody, whereas the biotinylated species only appeared when the active peptidase was labeled. This data thus confirmed the specific activity-based labeling of the PFA-M1 aminopeptidase by MH01 within a complex malarial parasite proteome.

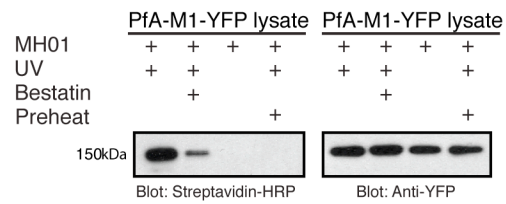


Figure 2.5: ABP labeling of the malarial M1 metallo-aminopeptidase in cell lysates. (a) *P. falciparum* cells (in buffer A) were freeze/thawed 3x on dry ice. Cell debris was removed by centrifugation, and the lysate was retained for labeling. MH01 was incubated with parasite lysate for 1 hr and then UV crosslinked for 1 hr. In one reaction, 100 μ M unbiotinylated bestatin was preincubated with the lysate prior to probe addition. Labeled protein was visualized via a western blot for biotin. (b) The same blot was then stripped and reprobed using anti-YFP.

In conclusion, we have developed a novel activity-based probe class, with specificity for MAPs, based on the bestatin inhibitor scaffold. The use of a biotin, fluorophore, or alkyne moiety did not alter the activity-dependent labeling profile for the scaffold and, thus, the suite of ABPs presented in this manuscript should allow for a variety of labeling methodologies. We therefore believe that this ABP may prove to be a valuable tool for future characterization of MAP activity in a wide variety of biological systems. We are now currently pursuing the expansion and application of these probes for use against the malarial parasite.

2.3 Experimental Procedures

General method for solid-phase peptide synthesis of ABPs: Standard solid-phase peptide synthesis was performed on Rink amide resin, using HBTU/HOBt/DIEA in an equimolar ratio in DMF for 30 min at RT. Coupling of the α -hydroxy- β -amino acid required HATU for 1 hr. Each amino acid was double coupled. Fmoc protecting groups were removed with 20% piperidine/DMF for 30 min. To cleave products from resin, a solution of 95%TFA:2.5%TIS:2.5%H₂O was added to the resin. After standing for 2 hrs, the cleavage mixture was collected, and the resin was washed with fresh cleavage solution. The combined fractions were evaporated to dryness and the product was purified by reverse phase-HPLC. Fractions containing product were pooled and lyophilized. Reverse phase HPLC was conducted on a C18 column using an Agilent 1200 HPLC. Purifications were performed at room temperature and compounds were eluted

with a concentration gradient 0-70% of acetonitrile (0.1% Formic acid). LC/MS data were acquired using LC/MSD SL system (Agilent). Solid-phase peptide chemistry was conducted in polypropylene cartridges, with 2-way Nylon stopcocks (Biotage, VA). The cartridges were connected to a 20 port vacuum manifold (Biotage, VA) that was used to drain excess solvent and reagents from the cartridge. MH01: $C_{62}H_{90}N_{10}O_{14}S$, predicted mass 1230.64, observed $[M+H]$ 1231.4. MH02: $C_{57}H_{81}N_9O_{12}S$, predicted mass 1115.57, observed $[M+H]$ 1116.3.

The synthesis of the dual function ABP MH03 was accomplished using standard solid phase peptide synthesis as detailed above, However, the TAMRA was added after product cleavage from resin due to the instability of TAMRA to TFA. This was accomplished using a Boc protected lysine and addition of TAMRA using HBTU/HOBt/DIEA in DMF after resin cleavage for 3 h. MH03: $C_{85}H_{107}N_{13}O_{16}S$, predicted mass 1597.77, observed $[M+2H]$ 799.8.

Synthesis of MH04 was accomplished as depicted in Scheme 2.2. The deprotection of the Alloc group was conducted under a positive flow of argon. The resin was solvated with dichloromethane for 5 min. The solvent was drained, and $PhSiH_3$ (24 eq.) in CH_2Cl_2 was added to the resin followed by $Pd(PPh_3)_4$ (0.25 eq.) in CH_2Cl_2 . After agitating the resin for 1 hr by bubbling with argon, the solution was drained, and the resin was washed with CH_2Cl_2 (3x). Synthesis of the biotin-azide was accomplished using standard solid-phase synthesis using a bromo-acetic acid as the final group. The replacement of the bromo group by the azide was achieved by heating with NaN_3 at 60°C. MH04: $C_{50}H_{67}N_7O_{10}$, predicted mass 925.49, observed $[M+H]$ 926.5.

Chapter 3: A bestatin-based chemical biology strategy reveals distinct roles for malarial M1 and M17 family aminopeptidases[†]

3.1 Introduction

Malaria is a global disease causing at least 500 million clinical cases and more than 1 million deaths each year [78]. While significant efforts to control malaria via insect vector elimination have been pursued, chemotherapy remains the principal means of malaria control. Moreover, the emergence of drug resistance in *Plasmodium falciparum*, the causative agent of most malaria-associated deaths, necessitates the discovery of novel antimalarials.

P. falciparum has a complex life cycle involving mosquito and human hosts. This life cycle involves both sexual and asexual stages of growth, wherein the human asexual erythrocytic phase (blood stage) is the cause of malaria-associated pathology. The erythrocytic stage begins when extracellular parasites, initially released from the liver, invade red blood cells. Once established in a specialized vacuole inside the host erythrocyte, parasites grow from the initial ring stage to the trophozoite stage, wherein much of the host hemoglobin (Hb) is proteolyzed. Parasites then replicate during the schizont stage to produce expanded populations of invasive merozoites that then rupture from the host cell approximately 48 hours post-invasion and go on to recapitulate the life cycle [79].

[†] The text of this chapter has been published (Harbut et al. A bestatin-based chemical biology strategy reveals distinct roles for malarial M1 and M17 aminopeptidases. Proc Natl Acad Sci USA. 2011 Aug 21;108(234)E526-34. Epub 2011 Aug 15). It is republished here with permission.

Peptidases are critical to parasite development throughout the life cycle and therefore are considered to be potential antimalarial drug targets [45,80,81].

One proteolytic pathway that has received significant attention is the multi-step degradation of host Hb [15]. While residing inside the host red blood cell, malaria parasites endocytose and proteolytically digest host Hb in a specialized lysosomal-like digestive vacuole (DV). This process liberates amino acids that the parasite can utilize for protein synthesis and general metabolism [22] and may reduce pressure on the host cell produced by the growing parasite [23]. Multiple endoproteases make initial cuts in full-length Hb; however, genetic knockout studies of these enzymes, plasmepsins 1-4 and falcipain 2/2', have revealed that all are non-essential and functionally redundant [52,53,82]. While falcipain 3 has not been shown to be dispensable, it is expressed later in the parasite lifecycle and may have roles beyond Hb degradation. On the other hand, several exopeptidases, some of which may have roles in Hb degradation, are likely genetically essential [43,44]. Among these non-redundant enzymes are cysteine dipeptidyl aminopeptidase 1 (DPAP1) and three metallo-aminopeptidases (MAPs): aminopeptidase N (PfA-M1), aminopeptidase P (PfAPP), and leucyl aminopeptidase, (Pf-LAP) [44].

MAPs have been postulated to be important for the parasite life cycle. Early studies suggested that MAP activities were absent from the DV lumen, leading to the proposal that Hb peptides are exported to the cytosol for further degradation by MAPs [83-85]. However, more recent localization and biochemical evidence suggest that PfA-M1 and PfAPP are located inside the DV,

while Pf-LAP is located in the parasite cytosol and has been proposed to act on exported globin peptides [86-88]. A cytosolic aspartyl MAP, PfDAP, has been shown to hydrolyze substrates with an amino-terminal Asp or Glu residue, but its contribution to blood-stage peptide catabolism appears to be dispensable as genetic disruption causes no overt phenotype [44]. Importantly, none of these studies provide any biological evidence, most importantly in live parasites, for a direct role for MAPs during Hb peptide catabolism.

Unfortunately in *P. falciparum*, genetic approaches to study essential genes are limited and thus direct evidence for the biological roles of these MAPs is still lacking [37]. As a complementary approach, we have developed a MAP-specific chemical genetics platform that utilizes activity-based protein profiling (ABPP) based on the natural product inhibitor bestatin to study the roles of MAPs [89]. ABPP is a chemical strategy that utilizes mechanism-based, tagged small molecule inhibitors to discover new enzymes, profile their activity state in complex proteomes, and identify potential functions for these enzymes during a specific biological process [90]. ABPP has been utilized for a variety of enzyme classes, including serine hydrolases, peptidases, histone deacetylases and kinases [60,61,91,92].

(-)-Bestatin is a natural product dipeptide analog of actinomycetes that potently inhibits multiple families of MAPs including the M1 and M17 families [70-72,93] (Fig. 3.1A). Importantly, bestatin has been shown to inhibit growth of *P. falciparum* parasites in culture and in mouse models of malaria [94-96]. In addition, a recent study has indirectly implicated aminopeptidases in hemoglobin

catabolism showing that parasites treated with bestatin had decreased levels of hemazoin formation, the detoxified biomineral byproduct of Hb digestion [97]; likewise, isoleucine uptake was decreased in these bestatin treated parasites. However, the MAP(s) targeted by bestatin, which are responsible for these processes, were not identified.

Herein, we report on a multidisciplinary effort combining bestatin-based, small molecule ABPs with biochemical and peptidomic approaches to functionally analyze two essential aminopeptidases, PfA-M1 and Pf-LAP.

3.2 Results

*Identification of bestatin targets in *P. falciparum**

Because of the paucity of genetic tools for analysis of essential proteins in *P. falciparum* and a lack of highly specific inhibitors with which to probe the individual roles of MAPs, we chose to study the functions of these essential parasite MAPs through the development and application of a MAP specific ABPP platform. ABPP utilizes tagged mechanism-based inhibitors, or activity-based probes (ABPs), to characterize families or individual active peptidases within complex proteomes. ABPs typically possess two main structural components that contribute to their target specificity: (i) a mechanism-based inhibitor scaffold to covalently or noncovalently target catalytic residues or the active site of peptidases and (ii) a reporter tag, such as a fluorophore or biotin, for the visualization, characterization of labeling events, and eventual affinity purification

of target proteins. The mechanism-based inhibitor scaffold ensures that ABPs bind to the enzyme(s) in an activity-dependent manner.

We decided to use the natural product, bestatin, as the scaffold for the development of ABPs for MAPs since it is a general MAP inhibitor, kills *Plasmodium* parasites, and is synthetically tractable using both solution and solid-phase chemistry [69,89,98]. To identify the target(s) of bestatin in *P. falciparum*, we utilized a previously published bestatin-based ABP, MH01 (Fig.3.1B) [89]. MH01 contains a biotin moiety to allow for monitoring of protein binding and affinity purification for target identification and also utilizes a benzophenone for irreversible UV crosslinking to protein targets, as the inhibition of MAPs with bestatin is noncovalent [89]. Asynchronous cultures of 3D7 parasites were treated with saponin to lyse the erythrocyte and parasitophorous vacuole membranes and isolated whole parasites were harvested by centrifugation. Crude parasite lysates, including both soluble and membrane proteins, were treated with 5 μ M MH01, exposed to UV light, and analyzed by western blot using streptavidin-HRP to detect biotinylated proteins. The observed labeling pattern consisted of four bands at approximately 100 kDa, 70 kDa, 55 kDa, and 25 kDa (Fig. 3.1C). Western blot analysis with PfA-M1 or Pf-LAP antibodies of parasite lysates labeled with MH01 showed that all four labeled species could be accounted for with these two antibodies: three bands corresponded to different species of PfA-M1 and one to Pf-LAP (Fig. 3.1C). PfA-M1 is known to be proteolytically processed from a 120 kDa proform to a 115 kDa intermediate yielding the p96 and p68 forms, both of which contain the

catalytic domains and are labeled by MH01 [85]. The labeled p25 band is likely a secondary proteolytic breakdown product. We further confirmed that MH01 bound PfA-M1 and Pf-LAP using individual parasite lines expressing YFP-tagged versions of these proteins [44]. After incubation of each YFP-tagged transgenic line with MH01, immunoprecipitation using streptavidin and western blotting for YFP revealed that both PfA-M1-YFP and Pf-LAP-YFP were targeted by MH01 (Fig. 3.1D and E). Likewise, the reciprocal experiment involving the immunoprecipitation of YFP and western blotting for biotin revealed that each YFP-tagged peptidase protein was biotinylated by MH01 (Fig. 3.1D and E). Specificity of the interaction was confirmed by pretreatment with unlabeled bestatin, which blocked labeling. These results indicate that PfA-M1 and Pf-LAP are likely the only targets of bestatin in *P. falciparum* parasites. In addition, they highlight the difficulty in understanding the mechanism of bestatin toxicity, which could be due to the inhibition of either PfA-M1 or Pf-LAP or both.

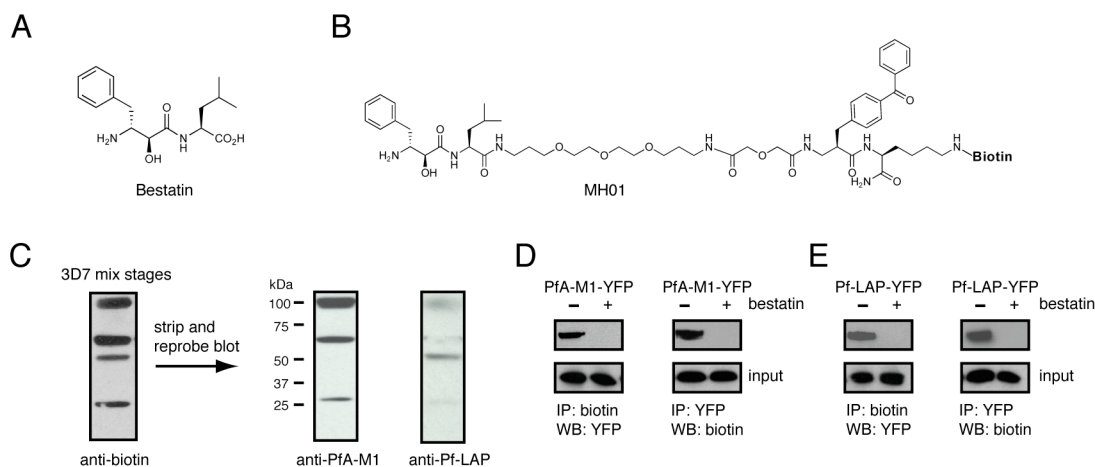


Figure 3.1: Identification of PfA-M1 and Pf-LAP as the targets of the anti-parasitic MAP inhibitor bestatin. (a) Structure of bestatin. **(b)** Structure of MH01. **(c)** Identification of PfA-M1 and Pf-LAP as the parasite targets of bestatin. Parasite lysates were prepared by freeze-thaw lysis and subsequently labeled with 5 μ M MH01, UV crosslinked, and analyzed by western blot for biotin. Four proteins were labeled by MH01. The same blot was stripped and reprobed sequentially with antibodies for PfA-M1 and Pf-LAP; three MH01 labeled proteins were accounted for by anti-PfA-M1 and fourth by anti-Pf-LAP. **(d)** A parasite line expressing a YFP-tagged PfA-M1 protein was incubated with MH01 followed by immunoprecipitation for biotin (MH01) and western blot analysis for YFP, which confirmed that PfA-M1 is targeted by MH01 (first panel). The reciprocal experiment involving the immunoprecipitation of PfA-M1-YFP (after incubation of parasites with MH01) using a YFP-specific antibody confirmed PfA-M1-YFP is biotinylated and thus labeled by MH01 (second panel). **(e)** Likewise, the same analysis was performed using a parasite line expressing a YFP-tagged Pf-LAP protein; incubation of these parasites with MH01, followed by immunoprecipitation of biotin (MH01) and western blot analysis for YFP confirmed that MH01 labels PF-LAP. The reciprocal experiment involving immunoprecipitation of Pf-LAP-YFP and analysis by western blot for biotin confirmed that Pf-LAP-YFP is biotinylated by MH01. Lastly, MH01 labeling of YFP-tagged MAPs, in both cases, is blocked by pretreatment with unbiotinylated bestatin as seen as a lack of labeling. Input lanes below each panel show western blot analysis using anti-YFP of total parasite lysate just before immunoprecipitation.

MAP ABP library design and in vitro analysis against PfA-M1 and Pf-LAP

To investigate the individual functions of the two MAP targets of bestatin and to gain insight into the mechanism of how bestatin kills parasites, we synthesized several libraries of bestatin-based ABPs with the intention of generating specific ABPs for both PfA-M1 and Pf-LAP. Bestatin has two side chains that can be diversified, which are derived from the constituent α -hydroxy- β -amino acid and a natural α -amino acid (Fig. 3.1A). These side chains straddle the active sites of MAPs where the α -hydroxy- β -amino acid side chain (termed P1) fits into the S1 pocket of the enzyme (N-terminal to the scissile bond) and the adjacent natural amino acid side chain (P1') interacts with the S1' pocket (C-terminal to the scissile bond) [99,100]. In our initial library, the P1' leucine residue in bestatin was replaced with a series of natural amino acids (except cysteine and methionine which are prone to oxidation; norleucine was included as an isostere for methionine) and a limited number of non-natural amino acids (Fig. 3.2A). Each library member was designed to incorporate a benzophenone to enable covalent attachment of the ABP to its targets and a terminal alkyne at the C-terminus, to allow for the later addition of a variety of reporter tags using the bio-orthogonal copper(I)-catalyzed [3+2] azide/alkyne cycloaddition ('click reaction') [101-103]. This library construction strategy increases the flexibility of downstream applications as each member has a "taggable" arm; thus, they can be used to directly treat live cells (as well as cellular lysates or recombinant enzymes) for target identification and activity profiling using a reporter tag, without any necessity for re-synthesis or troubleshooting of tag placement.

We initially screened a P1' diverse library against both recombinant PfA-M1 and Pf-LAP via standard fluorescence protease activity assays. Results of this experiment are presented as a heat map based on percent inhibition of PfA-M1 and Pf-LAP for each ABP (Fig. 3.2A). The S1' pocket of Pf-LAP tended to favor aromatic side chains such as Phe, Tyr, and Naphthyl. One probe, Phe-Naphthyl (PNAP), showed strong specificity for Pf-LAP over PfA-M1. In addition, several sidechains favored binding towards PfA-M1 over Pf-LAP, which tended to be either small (Ser, Ala) or positively charged (Lys, Arg). The probes Phe-Ala, Phe-Lys and Phe-Arg showed moderate specificity for PfA-M1; however we decided not to pursue further studies with the positively charged probes because of potential issues with cell permeability. Although the Phe-Ala ABP was somewhat specific for PfA-M1, we felt it was not yet suitably specific for further biological studies; thus we investigated modifications to the P1 sidechain to achieve higher specificity.

To increase specificity for PfA-M1, we synthesized a second bestatin-based library that diversified the α -hydroxy- β -amino acid side chain (P1 position) using a fixed alanine at the P1' position. Given structural information indicating that the S1 pocket of the PfA-M1 enzyme was hydrophobic the P1 library was synthesized with a variety of natural and non-natural hydrophobic P1 side chains including: Ala, Leu, Diphenyl, Naphthyl, Biphenyl, and (Benzyl)Tyr; (Fig. 3.2B) [100]. Again each library member had a clickable alkyne C-terminal to the benzophenone. This secondary ABP library was profiled against recombinant

PfA-M1 and Pf-LAP and from the initial heat map analysis, the (Benzyl)Tyr-Ala ABP (BTA) gave the highest specificity of PfA-M1 over Pf-LAP.

To determine the morphological effects of inhibition using the probe libraries, parasite development was monitored throughout the entire lifecycle by Giemsa staining of thin blood smears (Fig. 3.2C). Three chemotypes (small molecule-induced morphological changes) were observed from this analysis: i) no overt effect, ii) early parasite death at the ring/trophozoite transition marked by pyknotic bodies, and iii) swelling of the DV with parasite death occurring at the trophozoite/schizont transition. Importantly, the swollen DV as observed with these bestatin-based ABPs appeared translucent in Giemsa-stained smears, which distinguishes them from the dark swollen DV containing undigested Hb seen after treating parasites with papain family cysteine protease inhibitors such as E64 that target DV falcipains 2 and 3 [28].

Correlating the *in vitro* results with the live cell morphological screening results revealed that ABPs that produced the swollen DV chemotype displayed a high degree of specificity for PfA-M1 while ABPs more specific for Pf-LAP produced the early death/pyknosis chemotype. Compounds that failed to inhibit both MAPs, such as Phe-Asp (P1'-Asp) showed no chemotypes and were useful as negative control compounds (Fig. 3.2C). The contrasting chemotypes displayed by parasites treated with the most specific compounds, BTA or PNAP, suggested that PfA-M1 and Pf-LAP have essential yet distinct roles in the parasite.

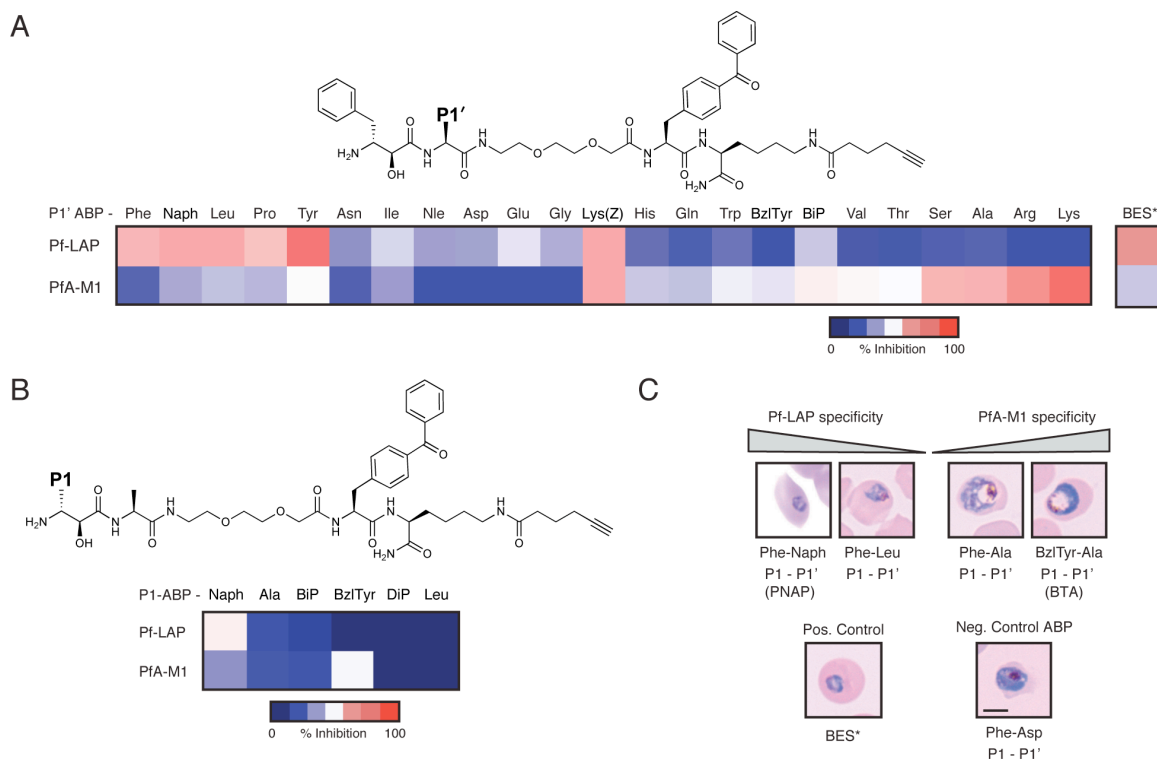


Figure 3.2: Bestatin-based ABP libraries reveal distinct chemotypes produced by ABPs with increased specificity for either PfA-M1 or Pf-LAP. (a) Representative structure of the bestatin-based ABP scaffold showing the point of diversification at the P1' position. This ABP library was screened against recombinant PfA-M1 and Pf-LAP in single fixed concentrations. Results of the assay are displayed as a heat map: red indicates higher potency; blue indicates lower potency. The Phe-Naph ABP showed high specificity for Pf-LAP. (BES* indicates parental bestatin) (b) A library of ABPs was synthesized to identify a probe with increased specificity for PfA-M1. Representative structure of the bestatin-based ABP scaffold showing the point of diversification at the P1 position. All compounds had an Ala at the P1' position. Results of the assay are displayed as a heat map: red indicates higher potency; blue indicates lower potency. The (Benzyl)Tyr-Ala ABP showed high specificity for PfA-M1. (c) Synchronized parasites were treated with each compound at 1 μ M and assayed for morphological changes by light microscopy of Giemsa stained blood smears through the erythrocytic lifecycle. Bar, 5 μ m. ABPs more specific for PfA-M1 showed swelling of the DV, while probes more specific for Pf-LAP showed an early death chemotype. *In collaboration with Seema Dalal and Mike Klemba.*

Evaluation of BTA and PNAP potency and specificity

To quantitatively assess the relative specificity of BTA and PNAP, inhibition constants against recombinant PfA-M1 and Pf-LAP were determined (Fig. 3.3A). All ABPs bound rapidly to PfA-M1; in contrast, binding to Pf-LAP was slow, as has been reported for bestatin [69]. Analysis of BTA inhibition revealed that the substitution of the P1' Leu for Ala shifted the specificity moderately towards PfA-M1. With the substitution of the P1 Phe with (Benzyl)Tyr in BTA, the affinity of the ABP was only moderately changed for PfA-M1 (Fig. 3.3A), while the inhibition constant for Pf-LAP radically dropped nearly 100-fold resulting in an ABP with an estimated micromolar K_i^* (an estimate was necessary due to insolubility at high micromolar concentrations). Thus the overall change in the ratio of inhibition constants of PfA-M1 over Pf-LAP from bestatin to BTA was approximately 75-fold and the absolute specificity difference for PfA-M1 over Pf-LAP was at least 15-fold making BTA a useful biological tool to study PfA-M1 function. Likewise, the substitution of a naphthyl group for the P1' leucine of PNAP increased the affinity of PNAP for Pf-LAP, resulting in a 170-fold change in the specificity of PNAP for Pf-LAP relative to BTA and approximately a 12-fold difference in absolute specificity, creating a relatively specific inhibitors for both enzymes.

Although *in vitro* data suggested that BTA and PNAP were quite specific for PfA-M1 and Pf-LAP, respectively, these data do not rule out the possibility that the ABPs have other targets in parasites. To confirm the specificity of each probe in parasites, we utilized the alkyne on each ABP to 'click' on a fluorophore

(BODIPY) tag, to identify target(s) of BTA and PNAP in crude *P. falciparum* proteomes. The fluorescent ABPs were incubated with parasite lysates, UV-crosslinked and targets analyzed via in-gel fluorescent scanning. As predicted from the *in vitro* kinetic assays, BTA exclusively labeled bands identical in migration on gels to those recognized by antibodies to PfA-M1 in this complex proteome, while PNAP was specific for a band that correlated in migration with Pf-LAP (Fig. 3.3B).

To investigate the structural basis for the specificity of BTA for PfA-M1 we solved the X-ray co-crystal structure of PfA-M1 bound to the BTA probe. The co-crystal structure was solved to 1.8 Å and electron density clearly resolved the BTA probe and linker but lacked any visible density for the “clickable” alkyne C-terminal tag (Fig. 3.3C, left panel; see Table 3.1 for statistics). The BTA ABP bound to the essential active site zinc ion via the hydroxyl and carbonyl groups (O2/O3) and central nitrogen of the bestatin scaffold. The S1 pocket showed a slight movement (~1.2 Å between C-α atoms between the key S1 residue, Glu572, of the two structures) to accommodate the (Benzyl)Tyr at the P1 position. The P1' Ala moiety did not reach far into the S1' pocket of PfA-M1 as the remaining probe positioned itself close to the S1 pocket (Fig. 3.3C, left panel). We also modeled BTA into the X-ray crystal structure of Pf-LAP bound to bestatin (PDB ID 3KR4). Superposition of BTA onto the bestatin core showed that the large (Benzyl)Tyr residue at the P1 position clashed with the narrow S1 pocket of the active site in Pf-LAP (Fig 3.3C, right panel).

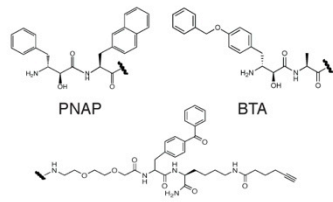
We also solved the co-crystal structure of Pf-LAP bound to PNAP (Fig. 3D, right panel). The 2.0 Å X-ray structure resolved the structural basis for the PNAP specificity and potency for Pf-LAP. As expected the PNAP ABP bound in a similar manner to the parent bestatin dominated by coordination of two Zn²⁺ ions of the active site [104]. The P1-Phe ring of PNAP fit neatly into the small hydrophobic S1 pocket of Pf-LAP and the P1' naphthyl group also formed a series of hydrophobic interactions in the S1' cleft. The only alteration noted to accommodate the P1' naphthyl group was the movement of Ser550 (~2.9 Å between c-α atoms of the Pf-LAP-PNAP structure versus the Pf-LAP-bestatin structure). This residue is located in a loop that lines the S1' cleft and the movement noted in the Pf-LAP-PNAP structure effectively flips the serine residue away from the naphthyl group, dragging the loop and preventing any close contacts with the P1' residue. It was also possible to model PNAP into the X-ray crystal structure of Pf-LAP bound to bestatin (PDB ID 3EBH). Superposition of PNAP onto the bestatin core showed that the naphthyl side chain at the P1' position clashed with the wall of the S1' pocket of the active site in Pf-LAP (Fig. 3.3D, left panel).

Although we saw no evidence of labeling of any other peptidase in parasite proteomes (Figs. 3.1 and 3.3), we wanted to further confirm that the BTA-derived DV chemotype was not caused by inhibition of other proteases; thus we assayed for inhibition of other DV peptidases: DPAP1, PfAPP and falcipain 2. No inhibition of any enzyme was seen at a concentration up to 30 μM BTA,

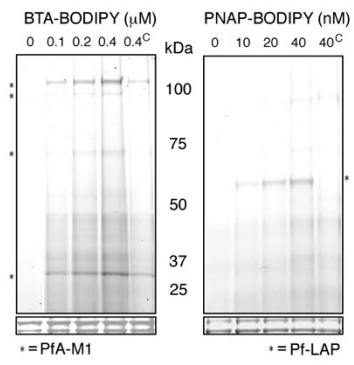
indicating that there is likely no cross-reactivity of BTA with these enzymes in live parasites and that the DV swelling is caused solely by inhibition of PfA-M1

A

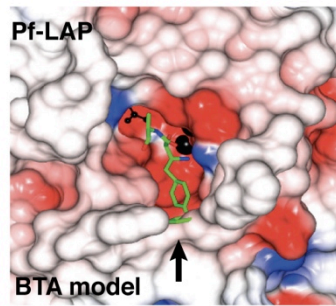
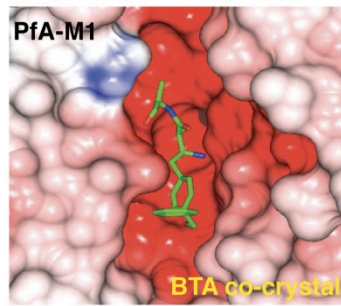
| ABP | K_i (PfA-M1) | K_i^* (Pf-LAP) | K_i^*/K_i |
|------|----------------|------------------|-------------|
| PNAP | 330 nM | 29 nM | 0.088 |
| BTA | 260 nM | ~4000 nM | 15 |



B



C



D

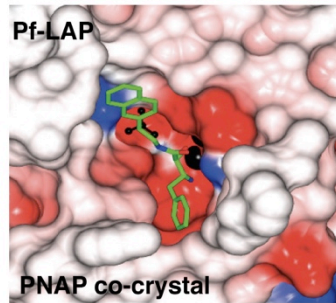
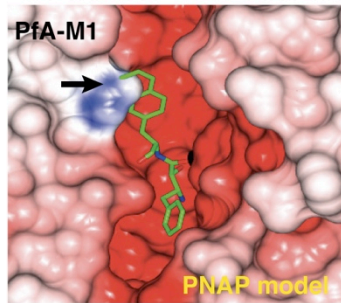


Figure 3.3: Biochemical and structural characterization of BTA and PNAP specificity against PfA-M1 and Pf-LAP. **(a)** Kinetic evaluation of inhibition for PNAP and BTA on recombinant PfA-M1 and Pf-LAP reveal over 15-fold specificity for PfA-M1 over Pf-LAP by BTA; PNAP showed greater than 10 fold specificity for Pf-LAP over PfA-M1. K_i^* for BTA for Pf-LAP was estimated due to solubility issues. **(b)** Activity-based probe profiling using “click” fluorescent versions of BTA or PNAP show that each probe specifically targets PfA-M1 or Pf-LAP, respectively (as indicated by an asterisk). (The superscript “C” in lane 4 of both panels indicates pretreatment with 10x of the non-fluorescent version of the respective ABP). **(c)** The electrostatic potential surface of the co-crystal of PfA-M1 with BTA (left panel) and model of Pf-LAP with BTA bound in active site (right panel). **(d)** The electrostatic potential surface of the model of PfA-M1 with PNAP (left panel) and surface of the co-crystal of Pf-LAP with PNAP (right panel). The zinc ion is shown as black sphere, the carbon atoms of inhibitors in green. Residues 755-1090 of PfA-M1 are excluded for clarity and a single monomer active site is shown for Pf-LAP. Surfaces were color coded according to electrostatic potential. Arrows show points at which either PNAP or BTA sterically clash with the enzyme. *In collaboration with Seema Dalal, Mike Klemmba, Sheena McGowan, and James Whistock.*

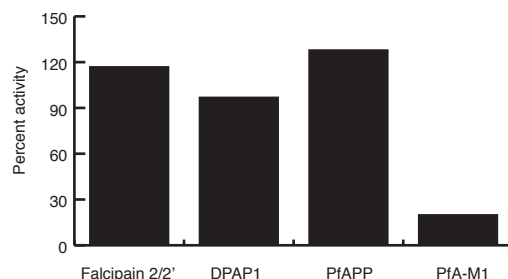


Figure 3.4: DV-localised endoproteases are not inhibited by BTA. Activity assays for falciparin 2/2', DPAP1 and PfAPP show that no inhibition occurs at 30 μ M BTA. *In collaboration with Seema Dalal and Mike Klemmba.*

Inhibition of PfA-M1 kills parasites via disruption of Hb digestion whereas Pf-LAP kills via a distinct mechanism

After confirming the specificities of BTA and PNAP, we next wanted to more fully characterize the effects of these ABPs on parasites through their life cycle. To do this, synchronized parasites were treated at the ring stage and followed by light microscopy evaluation of Giemsa stained thin blood smears (Fig. 3.5A). We found that treating parasites with BTA at its IC₉₉ caused a delay in the life cycle and swelling of the DV at the trophozoite stage with eventual parasite death around 60 hours post-treatment. As a comparison, parasites treated with E64-d, a cysteine protease inhibitor that blocks DV falcipains (and initial endoproteolytic cleavage of Hb) had a similar delay and swollen DV (darkly stained rather than translucent), but remained alive at the 60-hour timepoint. In contrast, PNAP-treated parasites were arrested at the transition to the trophozoite stage; therefore it appeared that PNAP exerted its effect on parasites significantly earlier than the time of major Hb digestion. PNAP treatment caused no prominent morphological features (other than death), thus complicating hypothesis generation as to its mechanism of action. To our knowledge the only other inhibitor that kills rings is artesunate and the other members of the artemisinin family (also shown in Fig. 3.5A for comparative purposes); although the mechanism of action for artesunate may be different than PNAP it is intriguing that there could be overlap amongst these two structurally divergent inhibitor classes [105].

Inhibition of PfA-M1 by BTA treatment of parasites caused a novel swollen DV chemotype. To investigate this phenomenon more closely we visualized the swelling of the DV in live parasites using a parasite line expressing YFP-tagged plasmepsin II that serves as a DV marker [106]. Transgenic parasites were treated with increasing concentrations of BTA and evaluated by fluorescent microscopy (Fig. 3.5B). From these images, we estimated the relative average DV size (measuring 10 DVs) after each treatment. Parasites treated with as little as 250 nM BTA (the K_i of BTA for PfA-M1) showed a statistically significant increase in DV size relative to untreated parasites, with saturation of this swelling at 1 μ M (Fig. 3.5B and C). The observation that the degree of DV swelling is dose-dependent and saturable is consistent with the hypothesis that, within this concentration range, PfA-M1 is likely the sole target and performs a key function in the DV. In contrast, parasites treated with PNAP at a concentration over 8 fold greater than its K_i against Pf-LAP did not show any significant DV swelling (Fig. 3.4B).

Since disruption in the endocytosis or subsequent catabolic breakdown of Hb is thought to be lethal to parasites we hypothesized that PfA-M1 inhibition by BTA leads to starvation of the parasite via blockage of proteolysis of Hb peptides [82]. To test this idea, we assayed whether parasites forced to rely only on Hb catabolism are more sensitive to BTA than parasites cultured with exogenous amino acids, by assaying the potency of BTA on parasites cultured in media lacking all amino acids except isoleucine (the only amino acid not present in Hb). Indeed, parasites were sensitized by approximately 2.4-fold to inhibition by BTA

in media with only isoleucine (Fig. 3.5D). In contrast, parasites treated with PNAP or the antimalarial artesunate, which kills ring stage parasites prior to initiation of large-scale Hb degradation and thus acts as a negative control, showed statistically insignificant differences in sensitization to either compound in the isoleucine media. This evidence suggests a role for PfA-M1 in the Hb digestion pathway and also provides further evidence that the primary role of Pf-LAP is not within the Hb digestion pathway.

Initial proteolytic events are thought to be carried out by the redundant endopeptidases falcipains 2/2'/3, plasmepsins I, II, IV, and HAP [107]. Hb-derived oligopeptides are then broken down by exopeptidases. Considering that PfA-M1 is an aminopeptidase, its likely role in the DV would occur after initial Hb proteolysis by the endopeptidases. To confirm this, we treated synchronous cultures of parasites during the trophozoite stage, in which the majority of Hb degradation takes place. Figure 3.6 shows that parasites treated with E64-d leads to an accumulation of full-length Hb and causes the swelling of the DV with undigested Hb [28,108]. Conversely, parasites treated with BTA showed no inhibition of proteolysis of full-length Hb but still caused the DV to swell. Treatment of parasites with PNAP was similar to DMSO.

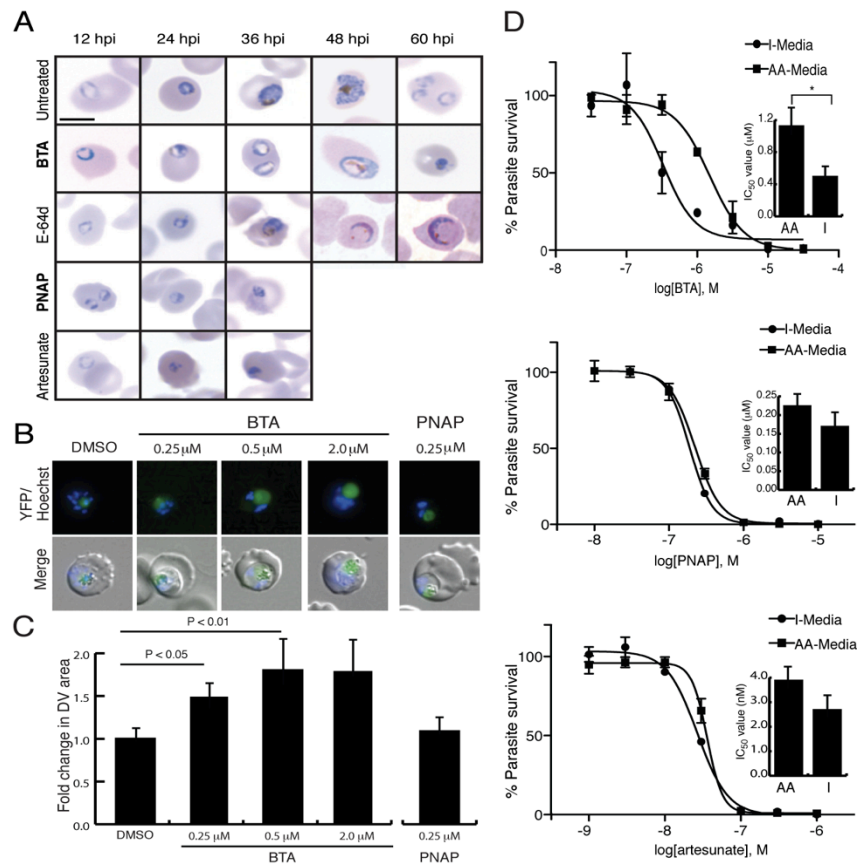


Figure 3.5: Inhibition of PfA-M1 kills parasites via disruption of Hb digestion whereas Pf-LAP kills via a distinct mechanism. (a) Parasites were treated with BTA (10 mM), E64-d (10 μM), PNAP (3 μM), bestatin (10 μM), and artesunate (10 nM) at concentrations roughly equivalent to their IC₉₉, and followed by Giemsa staining and light microscopy throughout the lifecycle. Bar, 5 μm. **(b)** DV swelling was confirmed by the dose-dependent enlargement of the average DV area. Parasites expressing YFP-tagged plasmepsin II (PMII-YFP), which localizes to the DV, were treated with increasing concentrations of BTA (and 250 nM PNAP) and imaged by fluorescence microscopy. **(c)** DV swelling was determined to be saturable and quantified by treating the PMII-YFP parasites with increasing concentrations of BTA (PNAP was also used at 250 nM) at mid-ring stage and measuring fluorescent DV area 20 hrs later using a minimum of 10 parasites (+/- standard deviation). **(d)** Treatment of parasites with BTA in media lacking exogenous amino acids, except for isoleucine, results in more than two-fold decrease in the IC₅₀ of BTA, while parasites treated with PNAP or artesunate show a non-significant difference. Shown are representative IC₅₀ plots for each compound in both I-Media (lacking exogenous amino acids except for isoleucine), and AA-Media (containing all natural amino acids). The inlay bar graphs show differences of the mean IC₅₀ of three experiments carried out in triplicate (**P* < 0.05, Student's *t* test).

Inhibition of PfA-M1 blocks proteolysis of specific Hb-derived oligopeptides

To obtain direct evidence for the role of PfA-M1 in the proteolysis of Hb-derived oligopeptides, we endeavored to find peptide substrates for this enzyme. We used a mass spectrometry-based peptidomics approach to assay the relative abundance of peptides (<10 kDa) in parasites either untreated or treated with the specific PfA-M1 inhibitor BTA. To do this, trophozoite stage parasites were treated with BTA or DMSO for 24 hr. Whole parasite extracts were prepared and peptides were enriched by an acid extraction followed by a filtration through a 10 kDa filter column. Resulting peptide extracts were analyzed by nano LC-MS/MS. Mass spectrometry analysis of the peptide peaks against both Hb α and β sequences revealed that the great majority of these oligopeptides showed no difference between the treated and untreated samples; however, several oligopeptides, from both the α and β chains of Hb, appeared to accumulate after treatment of parasites with BTA (Fig. 3.7A and B).

Further sequence analysis of the accumulated Hb-derived oligopeptides revealed that the majority were likely poor substrates for DPAP1, the other essential aminopeptidase with broad substrate specificity found in the DV [108]. We thus hypothesized that PfA-M1 was necessary for proteolysis of these oligopeptides. To test this idea, a highly enriched peptide that was identified from the peptidomics study of BTA-treated samples was re-synthesized and shown to be resistant to cleavage by DPAP1, yet efficiently cleaved by PfA-M1 (Fig. 3.7C). This data provides the first direct evidence of a role for the genetically essential

enzyme, PfA-M1, in the digestion of small Hb-derived oligopeptides in *P. falciparum*.

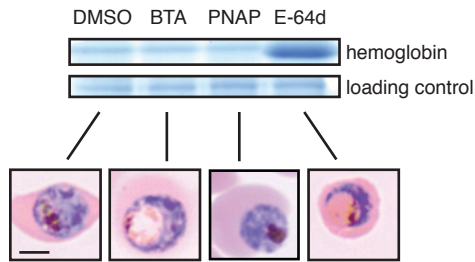


Figure 3.6: Inhibition of PfA-M1 causes DV swelling but does not prevent proteolytic cleavage of full length Hb. Parasites treated with BTA (1 μ M) and PNAP (0.25 μ M) are capable of initiating Hb degradation, as shown by an absence of full length Hb subunits (17 kDa) in both untreated and BTA-treated parasites, in contrast to parasites treated with E-64d, which disrupts the initial endoproteolytic cleavage of Hb.

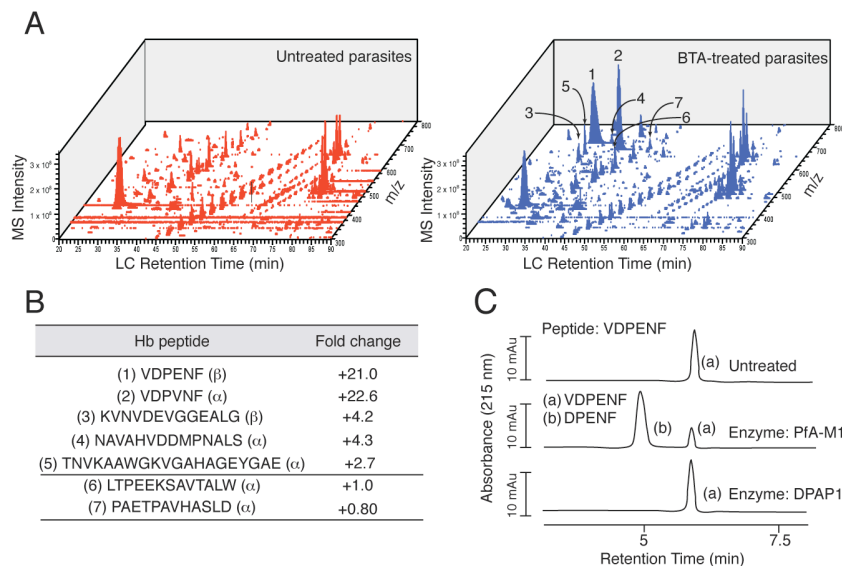


Figure 3.7: Inhibition of PfA-M1 blocks proteolysis of specific Hb oligopeptides. (a) Global peptide profiling of treated parasites identifies a subset of peptides that accumulate in BTA-treated parasites relative to DMSO. Peptides were extracted from either DMSO or BTA-treated parasites and peptides analyzed by LC-MS/MS. Peptides identified are displayed according to elution time, intensity, and M/Z . Area of the peptide peak corresponds to relative abundance **(b)** LC-MS/MS sequencing of the peptides reveals accumulated peptides are derived from Hb. Ratio of peptide abundance was calculated by determining the area of peptide intensity of BTA-treated vs untreated **(c)** A synthesized version of an abundantly accumulated peptide, identified in the prior LC-MS/MS analysis, was efficiently proteolyzed at the N-terminal valine by PfA-M1; while DPAP1, the other likely essential DV aminopeptidase, failed to catalyze any proteolysis. Shown are HPLC traces displaying the synthetic peptide without enzyme (top trace), with PfA-M1 (middle trace), or with DPAP1 (lower trace). Insets show peptide sequences corresponding to HPLC peaks.

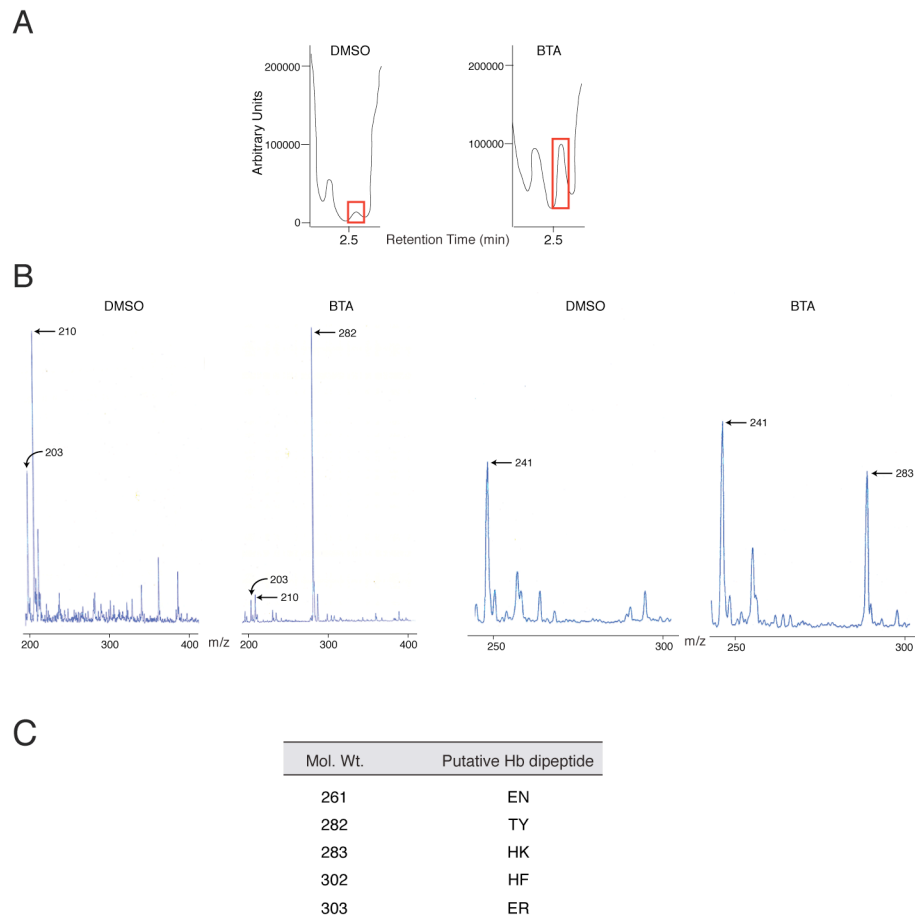


Figure 3.8: Small dipeptide species accumulate in BTA-treated parasites. (a) The LC trace identifies a peak that increases in the lysates of BTA-treated parasites. (b) The MS profile identifies the species with a molecular weight of 282 Da, which may corresponds to a Thr-Tyr dipeptide from Hb. Another MS trace identifies a putative Hb-derived His-Lys dipeptide, with a molecular weight of 283. (c) A table of the putative dipeptides species identified in BTA-treated parasites.

3.3: Discussion

Peptidases likely have many essential functions in *P. falciparum*, yet the biological roles of the majority of putative proteases encoded by the parasite genome remain to be characterized. One reason for this rests in the difficulty in genetically manipulating essential parasite genes. To circumvent this deficit in genetic tools, a small molecule approach may be used to perturb and thus investigate essential protein functions in the parasite. Several issues arise from the use of small molecule probes, including i) target identification, ii) specificity, and iii) permeability in live cells. To address some of these issues, we generated a library of MAP-specific, 'clickable' ABPs. Replacement of a bulky reporter tag with an alkyne group resulted in smaller, more versatile ABPs that allowed for their use in live cells for phenotypic analysis along with more traditional lysate-based ABPP.

Using this set of chemical tools, we first identified the targets of bestatin in *P. falciparum* to be PfA-M1 and Pf-LAP; although there are limitations to this ABPP approach, i.e., it is hard to determine with absolute certainty that there are no low abundance targets, further diversification of the MAP inhibitor scaffold to generate structure-activity relationship (SAR) trends can strengthen functional conclusions. Thus, through diversification of the bestatin scaffold, we were able to create a suite of ABPs with increasing specificity for both PfA-M1 and Pf-LAP and used these ABPs to further understand the functions of these essential enzymes.

The aggregate data using the BTA ABP strongly suggests that PfA-M1 plays a key role in oligopeptide proteolysis in the DV. The most prominent morphological feature of PfA-M1 inhibition was the novel swollen, translucent DV chemotype, which was likely due to the accumulation of oligopeptides that created hyperosmotic conditions. DV swelling also occurs after E64-d inhibition of DV falcipains; yet these parasites do not die until they attempt to egress, which suggests that swelling alone is not lethal to parasites, and that there must be enough amino acids generated (perhaps by plasmepsins) or obtained from the medium in the presence of this inhibitor to allow life cycle progression. We therefore propose that the likely cause of death upon PfA-M1 inhibition is a severe deprivation of the DV production of amino acids in the parasite. (Although we cannot rule out that killing may be due to indirect effects distinct to PfA-M1 inhibition, such as the accumulation of small peptides in the DV, which could potentially be toxic). To support the hypothesis that inhibition of PfA-M1 disrupts Hb degradation, we demonstrated that the effects of BTA were enhanced when parasites were forced to rely solely on Hb degradation. Why the amino acids present in complete media do not allow for the parasite to completely complement for the genetic or pharmacological loss of PfA-M1 via the utilization of exogenous amino acids is an interesting question. This sensitivity may be explained by the fact that the parasite is particularly dependent on leucine generated in the DV from Hb, which is thought to be exchanged for isoleucine via an antiport mechanism [109].

From our peptidomics experiments we showed that Hb oligopeptides were substrates for PfA-M1 proteolysis. One issue with this analysis is that small peptides were not found using our mass spectrometry method, which was limited to the identification of peptides greater than four amino acids in length. It is likely that the concerted action of DV endo- and exoproteases also produced smaller tri- and di-peptides, which are substrates for PfA-M1 in the DV. In support of this idea, we also attempted to identify small peptide species using a single Quad LC/MS (which allows for profiling peptides between 200 and 400 Da) that accumulated in BTA-treated parasites (Fig. 3.8). These low molecular weight species all matched to predicted dipeptide molecular weights, and more than half were the molecular weight of dipeptides found in Hb. This method precluded the definitive identification of these molecules as peptides (as opposed to metabolites) and their origin (i.e., Hb). However, we believe these data are suggestive that several dipeptides, in addition to oligopeptides, are likely important substrates for the PfA-M1 enzyme.

Our data using the PNAP ABP for Pf-LAP indicated that this enzyme has an important role quite early in the intra-erythrocytic life cycle rather than during the major period of Hb digestion. Formulating a testable hypothesis about a specific role for Pf-LAP is complicated by the fact that its inhibition did not yield any overt morphological change in the parasite other than death. However, we suspect Pf-LAP may have an essential housekeeping function in the cytosolic turnover of dipeptides [110], and perhaps acts in concert with the parasite proteasome, as has been shown for other neutral cytosolic leucine

aminopeptidases pathways [111]. Like PNAP, lethal amounts of proteasome inhibitors exert their effect in the ring-trophozoite transition and parasites do not progress into the later trophozoite stage [112]. Our data does not completely rule out the possibility of a minor role for Pf-LAP in the Hb degradation pathway via proteolysis of Hb-derived dipeptides that have been transported from the DV into the cytoplasm. However, the fact that PNAP-treated parasites die prior to the major period of Hb degradation suggests that the essential role for Pf-LAP is not within the Hb digestion pathway.

Our collective data suggest that these two MAPs are both potential anti-parasitic drug targets. In fact, PNAP is, to our knowledge, the most potent parasite MAP inhibitor with an IC_{50} in the 200 nM range which gives us hope that these types of inhibitors could be further developed into more drug-like therapeutics. In addition, *P. falciparum* MAPs share little homology with their human counterparts; less than 35% in the case of the M1 family proteases. It is therefore reasonable to suggest that potent, specific inhibitors of *P. falciparum* MAPs can be designed over human MAPs. In addition, information gleaned from our preliminary SAR and crystallography efforts may provide a jumping off point for future medicinal chemistry efforts against both enzymes. Our data here suggest that combination therapy involving endopeptidase inhibitors, such as those for falcipains, and PfA-M1-specific inhibitors might provide an opportunity for a synergistic drug combination [113]. Ultimately, this strategy may represent a good way to reduce the chance of parasite resistance.

3.4: Experimental procedures

Parasite culture and IC₅₀ determination for bestatin-based ABPs.

Briefly, 3D7 parasites were cultured in RPMI 1640 (Invitrogen) supplemented with Albumax II (Invitrogen). For synchronization, schizont stage parasites were magnet purified using a SuperMACS™ II Cell Separation Unit (Miltenyi Biotech). For IC₅₀ determinations, synchronized parasites were plated at 1% parasitemia and 6% hematocrit in 96-well plates at a total volume of 50 μ L. Serial dilutions of 2x concentration of the respective compound were added to the wells to bring the total volume up to 100 μ L and 0.5% parasitemia and 3% hematocrit. Compounds were assayed for a 72 h period, after which 2x Vybrant DyeCycle Green DNA (Invitrogen) in PBS was added for a final concentration of 10 μ M and incubated at 37 °C for 30 min. DNA content, as an indicator of parasitemia, was analyzed on an Accuri C6 Flow Cytometer with C-Sampler. IC₅₀ curves were generated using GraphPad Prism (GraphPad Software).

Labeling of parasite MAPs with activity based probes.

For parasite labeling, mixed stage parasites were harvested and released from erythrocytes with 1% saponin followed by centrifugation at 1,500xg for 5 min and 3 washes in cold PBS. Parasite lysates were prepared by freeze-thaw in 50 mM Tris-HCl pH 7.0, 50 mM NaCl, 10 μ M ZnCl₂, and protease inhibitor cocktail (EDTA-free) (Roche) and extracts were clarified by centrifugation at 1,100 x g for 10 min at 4 °C. Labeling was performed with indicated concentrations of the ABP for 1 hr at 37 °C followed by UV crosslinking (365 nm) for 1 hr on ice.

Competition of labeling was carried out by preincubating lysates for 1 hr at 37 °C. For immunoprecipitation, lysates were passed through 7K MWCO desalting columns (Pierce) after UV crosslinking then incubated overnight with streptavidin Ultralink Resin (Pierce). Proteins were visualized by standard western blotting and VECTASTAIN ABC kit (Vector Labs) or rabbit anti-GFP (ab6556, Abcam). For fluorescent probes, labeled proteins were visualized in-gel using a Typhoon flatbed scanner (GE Healthcare).

Fluorescence imaging

Trophozoite state parasites were treated for 12 hr with the compounds and concentrations as shown in the figure. Images were obtained using a Leica DMI6000 B microscope and Leica LAS AF software. Parasite and DV sizes were quantified using ImageJ.

Synthesis of bestatin-based ABP libraries.

Standard solid-phase peptide synthesis was performed on Rink amide resin, using HBTU/HOBt/DIEA in an equimolar ratio in DMF for 30 min at RT. Coupling of the α -hydroxy- β -amino acid required HATU for 1 hr. Each amino acid was double coupled. Fmoc protecting groups were removed with 20% piperidine/DMF (30 min). The deprotection of the Alloc group was conducted under a positive flow of argon. The resin was solvated with dichloromethane for 5 min. The solvent was drained, and PhSiH_3 (24 eq.) in CH_2Cl_2 was added to the resin followed by $\text{Pd}(\text{PPh}_3)_4$ (0.25 eq.) in CH_2Cl_2 . After agitating the resin for 1 h

by bubbling with argon, the solution was drained, and the resin was washed with CH_2Cl_2 (3x). To cleave products from resin, a solution of 95%TFA:2.5%TIS:2.5% H_2O was added to the resin. After standing for 2 h, the cleavage mixture was collected, and the resin was washed with fresh cleavage solution. The combined fractions were evaporated to dryness and the product was purified by reverse phase-HPLC. Fractions containing product were pooled and lyophilized. Reverse phase HPLC was conducted on a C18 column using an Agilent 1200 HPLC. Purifications were performed at room temperature and compounds were eluted with a concentration gradient 0-70% of acetonitrile (0.1% Formic acid). LC/MS data were acquired using LC/MSD SL system (Agilent). HRMS was recorded at the UCRiverside mass spectrometry facility. Solid-phase peptide chemistry was conducted in polypropylene cartridges, with 2-way Nylon stopcocks (Biotage, VA). The cartridges were connected to a 20 port vacuum manifold (Biotage, VA) that was used to drain excess solvent and reagents from the cartridge. The scheme for the synthesis of ABPs of bestatin may be depicted as follows.

Recombinant proteins

Details of the expression in *E. coli* and purification of recombinant PfA-M1 (residues 192 to 1085) are described in [114]. Pf-LAP lacking the N-terminal Asn-rich region (residues 79 - 605) was expressed with a C-terminal hexahistidine tag in *E. coli* and purified as previously described [104]. The estimated molecular mass of the purified species from size exclusion chromatography (343 kDa) was

in good agreement with the predicted mass for the hexameric enzyme (357 kDa). The purification of recombinant DPAP1 has been published [108].

X-ray Crystallography

PfA-M1 and Pf_LAP enzymes were purified and crystallized as previously described [100]. Crystals of the PfA-M1-BTA complex were obtained by cocrystallisation of BTA with PfA-M1 in mother liquor containing 1 mM ligand. Crystals of the Pf-LAP-PNAP complex were obtained by cocrystallisation of PNAP with Pf-LAP in mother liquor containing 1 mM ligand. Prior to data collection, Pf-LAP-PNAP co-crystals were soaked in mother liquor containing 1 mM ligand and 1 mM ZnSO₄. Data were collected at 100K using synchrotron radiation at the Australian synchrotron micro crystallography beamline 3ID1. A summary of statistics is provided in Table 3.1. The coordinates and structure factors will be available from the Protein Data Bank (3T8V and 3T8W). Raw data and images will be available from TARDIS [115].

The inhibitor complex was initially solved and refined against the unbound PfA-M1 and Pf-LAP structure (protein atoms only) as described previously [100] and clearly showed unbiased features in the active site for both structures. After placement of inhibitors into unbiased density, CNS composite omit maps were calculated using all atoms. Supplementary Figure S3 shows inhibitor density contoured at 1.0 σ . Supplementary Figure S3 was generated using MacPymol and uses a 2.0 carve value around each inhibitor and zinc ion for clarity. Superposition of BTA into the Pf-LAP active site was performed using the X-ray

crystal structure of Pf-LAP-bestatin (3KR4) where the bestatin scaffold was used to superpose BTA.

Table 3.1 | Data Collection and refinement statistics

| Data collection | rPfA-M1_BTA | Pf-LAP-PNAP |
|----------------------------------|---|--|
| Space Group | $P2_12_12_1$ | $P2_12_12_1$ |
| Cell dimensions (Å) | a=75.5, b=108.8, c=118.3, b=90.0° | a=173.8, b=177.1, c=231.2, b=90.0° |
| Resolution (Å) | 46.57 – 1.8 (1.90- 1.80) | 88.64 – 2.0 (2.11 – 2.0) |
| Total number of observations | 1109709 | 5836680 |
| Number of unique observations | 90083 | 477295 |
| Multiplicity | 12.3 (11.4) | 12.2 (12.2) |
| Data Completeness (%) | 99.1 (96.6) | 100.0 (100.0) |
| $\langle I/\sigma_I \rangle$ | 14.7 (2.3) | 6.3 (2.1) |
| $R_{pim} (\%)^b$ | 4.2 (30.5) | 10.9 (43.4) |
| Structure refinement | | |
| Non hydrogen atoms | | |
| Protein | 7233 | 47062 |
| Solvent | 1006 | 4536 |
| Ligand | 40 | 876 |
| Zn ²⁺ ions | 1 | 24 |
| PEG/SO ₄ | - | 512 |
| $R_{free} (\%)$ | 19.8 | 20.0 |
| $R_{cryst} (\%)$ | 16.0 | 16.4 |
| Bond lengths (Å) | 0.01 | 0.01 |
| Bond angles (°) | 0.99 | 1.09 |
| Ramachandran plot | | |
| Favoured (%) | 98.4 | 98.3 |
| Allowed (%) | 100.0 | 99.9 |
| B factors (Å²) | | |
| Mean main chain | 16.6 | 16.3 |
| Mean side chain | 21.8 | 22.4 |
| Mean ligand | 42.4 | 53.0 |
| Mean water molecule | 32.2 | 28.2 |
| r.m.s.d. bonded Bs | | |
| Main chain | 1.61 | 1.80 |
| Side chain | 3.94 | 4.47 |

^aValues in parentheses refer to the highest resolution shell.

^bAgreement between intensities of repeated measurements of the same reflections and can be defined as: $\sum(I_{h,i} - \langle I_h \rangle) / \sum I_{h,i}$, where $I_{h,i}$ are individual values and $\langle I_h \rangle$ is the mean value of the intensity of reflection h .

Anti-PfA-M1 sera

Details of the production of rabbit anti-sera against recombinant PfA-M1 have been previously described [114].

Screening of P1 and P1' ABP libraries

Screens of relative ABP potencies were conducted at single fixed ABP concentrations for the P1 (PfA-M1- 250 nM; Pf-LAP- 750 nM), P1' natural (PfA-M1- 1 μ M; Pf-LAP- 250 nM) P1' non-natural (0.37 μ M for both enzymes) libraries. PfA-M1 assays contained 50 mM HEPES pH 7.5, 100 mM NaCl, 25 mM leucyl-7-amido-4-methylcoumarin (Leu-AMC) and 0.1% Triton X-100; Pf-LAP assays contained 50 mM HEPES pH 7.5, 100 μ M ZnCl₂, 50 - 250 μ M Leu-AMC and 0.1% Triton X-100. For Pf-LAP, steady-state rates were approximated by linear fits to the progress curves after a one hour equilibration period in the presence of substrate and inhibitor.

Determination of K_i and K_i^ values*

Bestatin has been shown to be a slow-binding inhibitor of leucine aminopeptidases, including Pf-LAP, with the slow step involving a conformational change of the initially-formed low affinity enzyme-inhibitor complex (EI) to form a tight complex (EI*); K_i is the dissociation constant for the initial enzyme-inhibitor complex whereas K_i^* is the overall inhibition constant and is defined as $[E][I]/([EI]+[EI*])$. K_i^* values were determined for the di-Zn form of Pf-LAP[116] in

50 mM Tris-HCl pH 8.0 containing 50 mM ZnCl₂, 250 mM Leu-AMC, 0.1% Triton X-100, 180 ng/mL Pf-LAP and inhibitor at 25 °C. Changes in fluorescence upon mixing of substrate and inhibitor with enzyme were monitored in 96 well plates using a Victor³ microplate fluorometer. Progress curves were followed for 160 minutes and fit to the equation for slow-binding inhibition $[P] = v_s t + (v_o - v_s)(1 - e^{(-k_{obs} t)})/k_{obs}$, where v_o is the initial rate, v_s is the steady-state rate and k_{obs} is an apparent first-order rate constant for the formation of the high affinity enzyme-inhibitor complex, EI*. At the inhibitor concentrations necessary to produce well-defined progress curves (at least two half-times), v_s was typically < 5% of the uninhibited velocity making steady-state approaches to determining K_i^* (i.e. Dixon plot) unfeasible. Instead K_i^* was determined from plots of k_{obs} vs. $[I]$. In the case of bestatin, the data defined a hyperbolic curve. k_6 was determined from the relationship $k_6 = v_s/v_o * k_{obs}$ and was added to the data set ($k_{obs} = k_6$ when $[I] = 0$) to better define the hyperbolic curve. Data were fit by non-linear regression to the equation $k_{obs} = k_6 + k_5[I]/(K_i^{app} + [I])$, where $K_i^{app} = K_i(1 + [S]/K_m)$. Under our assay conditions the K_m for Leu-AMC was 1.1 mM. K_i^* was calculated from the relationship $K_i^* = k_6 K_i / (k_5 + k_6)$ where K_i and $(k_5 + k_6)$ were determined from curve fits and k_6 was determined as described above. For bestatin probe, Phe-Ala probe and BTA probe, plots of k_{obs} vs. $[I]$ were linear, a situation that can arise if K_i is much greater than the inhibitor concentrations used in the assay. In these cases k_{obs} vs. $[I]$ plots were fit by linear regression yielding a slope of k_6/K_i^{app} ; determination of k_6 as described above enabled calculation of K_i^{*app} and thus K_i^* . With BTA probe, the combination of low affinity for Pf-LAP and insolubility at high

micromolar concentrations restricted the range of k_{obs} values that could be determined compared to those for bestatin and Phe-Ala probes. However, sufficient K_i values for inhibition of PfA-M1 were determined by Dixon plots and a detailed protocol for determining Pf-LAP K_1^* values may be found in Supporting Information.

Mass spectrometry-based peptide profiling

Briefly, parasites were treated with 2 μM BTA or DMSO at the mid-ring stage. Parasites were treated for 24 hr at which point they were harvested by saponin treatment, centrifuged, and stored at -80°C in the presence of protease inhibitors. To isolate peptides, parasite samples were boiled in water for 10 minutes and then centrifuged for 10 min at $18,000 \times g$. The supernatant was saved, and the pellet was resuspended in 0.25% acetic acid and disrupted by freeze-thaw and microsonicated. All fractions were combined and centrifuged at $20,000 \times g$ at 4°C for 20 min. The supernatant was passed through a 10 kDa molecular weight cutoff filter (Millipore).

The retention times and m/z values of the peptides identified were used to map corresponding peptide peaks in the chromatograms generated from nano-HPLC–ESI-MS (LCQ-DecaXP Plus). These peptide peaks were manually aligned and then for semi-quantitative assessment of the abundances of individual peptides, the total peak areas were determined using the Bioworks algorithm PepQuan (the Area/Height Calculation) with parameters set to area, mass tolerance of 1.5, minimum threshold of 5,000, five smoothing points, and

including all proteins. The alignment was based on retention times, m/z values, and patterns of peaks in close proximity.

Peptide Synthesis

The peptide VDPENF was synthesized on an Argonaut synthesizer using standard Fmoc solid phase peptide synthesis on Rink-amide resin. Peptides were purchased from Bachem (Switzerland). Rink-amide resin (0.69 mmol/g) was purchased from Novabiochem (San Diego, CA). All other chemicals and reagents were purchased from Fisher Scientific (Pittsburgh, PA). Peptide assembly was performed using HBTU (2-(1H—benzotriazole-1-yl)-1,1,3,3-tetramethyluronium hexafluorophosphate) activation (5 and 10 equivalents respectively) of amino acids (5 eq) in DIEA (N,N'-diisopropylethylamine) and NMP (N-methylpyrrolidone). The Fmoc protecting group was removed with 20% piperidine in DMF, for 5 min. After deprotection and again after amino acid coupling, the reaction vessel was rinsed 3 times with NMP followed by 3 rinses with DMF. The N-terminus of the peptide was not capped. The peptide was cleaved from the resin using 93% TFA (trifluoroacetic acid), 2% TIPS (triisopropylsilane), and 5% water. The peptide was precipitated twice in 40 mL cold diethyl ether and dried overnight. To purify, the peptide was dissolved in 95% water, 5% acetonitrile and 0.1% formic acid (Solvent A) and run on a semi-preparative C18 column on an Agilent HPLC (15% to 35%, Solvent B) (Agilent Technologies). Pure fractions were confirmed by ES-API (calculated m/z 719.31, found m/z 719.2).

Chapter 4: Chemical validation of signal peptide peptidase as a potential anti-protozoan drug target[‡]

4.1 Introduction

Protozoan pathogens cause significant disease worldwide and constitute one of the most substantial global public health problems faced today. *Toxoplasma gondii* has a widespread throughout the world, chronically infecting an estimated 30% of the world's population [117]. Treatment options are limited, especially for congenital disease and those who may require chronic therapy (e.g. immune-compromised patients). The related *Plasmodium* parasites that cause malaria are collectively responsible for >400 million clinical cases and up to 1 million deaths each year [1]. While vector control may reduce parasite transmission, and extensive effort is being devoted to vaccine development, chemotherapy remains the principal means of disease treatment. The emergence and spread of drug resistant parasites has rendered many of the traditional antimalarials (e.g. chloroquine and sulfadoxine-pyrimethamine) clinically ineffective in many cases. Infection by *Trypanosoma brucei* is potentially lethal to both humans (trypanosomiasis) and livestock, and treatment relies on antiquated drugs that are difficult to administer and potentially toxic [118]. Like *Plasmodium*, *Trypanosoma brucei* utilizes complicated immune avoidance strategies that have thus far hampered effective vaccine development [119]. Therefore, the validation of novel anti-protozoan drug targets is of an

[‡] This chapter is currently in preparation for publication.

urgent need, and efforts that synergize a strategy towards target identification in multiple parasite classes may be particularly beneficial.

Proteases are known to participate in several critical pathways during the life cycle of protozoan parasites, including host-protein degradation, rupture from the host cell, and invasion of new cells, and thus have been considered a protein family of therapeutic interest [120]. Signal peptide peptidase (SPP) is a recently identified aspartyl protease family that performs proteolytic cleavage within the cell membrane (intramembrane proteolysis) [121]. SPP (or SPP1), the prototypic member of this family, is a ~40 kDa presenilin-like aspartyl protease found in the ER membrane with protease active site motifs (YD and LGLGD) located within opposing transmembrane regions. The orientation of the transmembrane domains that contain the catalytic aspartates in SPP family members is opposite that found in the intramembrane aspartyl protease gamma-secretase/presenilin (GS/PS) [122]. This topological difference provides a structural basis for the observation that SPP cleaves type II transmembrane domains, while PSs cleave type I transmembrane domains.

There are five human genes encoding SPPs (SPP1, SPPL3, SPPL2a,b,c), which have been referred to as presenilin homologs (PSH), intramembrane proteases (IMPAS) and signal peptide peptidase like (SPPL) [123]. Although there are no major human diseases associated with SPPs, recent work suggests that SPPs may play important developmental roles in *C. elegans*, *D. melanogaster*, and *D. rerio* [124-126]. Originally it was hypothesized SPPs provided housekeeping role in processing residual signal peptide nubs in the

endoplasmic reticulum (ER) membrane left after signal peptide cleavage. More recently, it has been demonstrated that SPP participates in a virus-induced ERAD pathway and can bind misfolded proteins [127-130]. Thus, from the aggregate literature, it appears that SPPs play several roles in the secretory system including: i) cleaving residual signal peptides and ii) binding and possibly cleaving misfolded transmembrane domains for ERAD-based destruction and iii) regulated proteolysis of select type II secretory substrates.

A recent search by our lab of the available pathogenic protozoan genomes, including the *P. falciparum*, *T. gondii*, *E. histolytica*, *G. lamblia*, and *C. parvum*, has identified a single, conserved SPP homologue in each organism. The *P. falciparum* SPP (PfSPP) is most closely related to the human SPP and SPPL3 proteins, though the homology it shares with them is less than 50%. The protein is most conserved in its C-terminal region, which includes the aspartyl active site motifs and a highly conserved PAL domain. Importantly, these parasites lack PS orthologs and thus SPP is their sole aspartyl iCLIP. The observation that the pathogenic protozoans contain a single copy of this gene, while humans have five copies, offers a compelling reason to hypothesize that inhibition of SPP in these organisms would be lethal and therefore an attractive therapeutic target for a broad range of pathogenic protozoans. Indeed, recent efforts by the Chishti group have concluded the *P. falciparum* copy of SPP is an essential gene [131].

Here, in a multidisciplinary effort, we validate SPP as a suitable pan-protozoan therapeutic target. We show SPP inhibitors of multiple chemical

scaffolds are lethal to protozoan parasites and confirm their SPPs are active and druggable enzymes using *in vitro* assays. Focusing on the malarial parasite *P. falciparum*, we are able to generate *in vitro* resistant parasites to SPP inhibitors, and show that resistance is conferred by a mutation in the SPP gene, confirming that SPP inhibitors target SPP in live parasites. Finally, we show that PfSPP is vital in coping with ER-stress in malarial parasites, and that the heightened protozoan sensitivity to SPP inhibition is likely due to a greatly streamlined unfolded protein response/degradation pathways in these parasites.

4.2 Results

PS/SPP inhibitors kill multiple protozoan parasites

Small molecular inhibitors have been useful tools in the understanding the role and mechanism of the intramembrane aspartyl proteases SPP and gamma-secretase/presenilin (PS) [132,133]. In addition, because of its central role in the pathology of Alzheimer's disease, a large number of inhibitors from several different classes have been developed towards PS, with varying degrees of potency and selectivity towards SPP [134,135]. We took advantage of this pharmacological abundance to chemically validate the requirements of SPP in protozoan parasites.

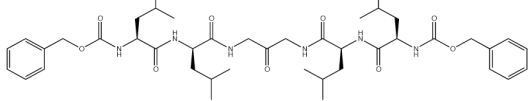
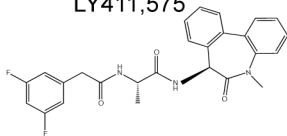
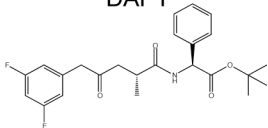
P. falciparum cultures were treated with several SPP inhibitors including: (Z-LL)₂, helical peptide mimics, and LY411,575 [132,135,136]. (Z-LL)₂ is an SPP-specific transition-state analog inhibitor and binds to the active site. Helical peptide-based inhibitors (denoted as the ES and AK inhibitors) mimic the transmembrane structure of a putative substrate and bind to a substrate docking

site distinct from the active site. The benzodiazepine-like inhibitor LY411,575 inhibits both SPP and PS in a manner distinct from transition-state analogues and helical peptides. (DAPT is specific for PS and represents a negative control). As a means of comparison and robustness of inhibitor effects we show data from inhibitor screening against other protozoan parasites, *T. gondii* and *T. brucei*. Initial testing with these SPP inhibitors on *P. falciparum*, *T. gondii*, and *T. brucei* revealed that the SPP inhibitors killed parasites with potent IC₅₀s (Fig. 4.1A). The PS-specific inhibitor, DAPT, showed no activity. Importantly, these inhibitors represent unique chemical scaffolds with a single common target of SPP. This raises our confidence that the parasite killing effects were not due to off-target events, but rather from the specific inhibition of the respective parasite SPP. In addition, the potency of the compounds suggests that SPP is indeed an essential protease in each of the protozoan parasites tested.

To help link parasite death due to the administration of SPP inhibitors to SPP, we synthesized an activity-based probe (ABP) based on the SPP inhibitor (Z-LL)₂. A similar ABP was originally used by the Martoglio group to discover the SPP class of proteases [121]. The (Z-LL)₂ ABP contains a benzophenone moiety to allow covalent crosslinking of the probe to its target as well as a biotin moiety to allow purification by streptavidin. Our (Z-LL)₂ probe confirmed that PfSPP is the target of (Z-LL)₂ (Fig. 4.1B). 10 μM of the (Z-LL)₂-based ABP was incubated with CHAPSO-extracts of mixed stage *P. falciparum* parasite lysates at 37 °C for 1 hr. Inhibitors such as (Z-LL)₂, LY411,575, AK8, and DAPT were preincubated with the lysates for 1 hr at 37 °C before addition of the probe to

compete for labeling. After labeling, samples were immunoprecipitated using streptavidin-agarose and western blot analysis was performed using an antibody to a cytosolic domain of PfSPP. Importantly the first lane of the blot shows successful IP-western of PfSPP indicating that PfSPP is targeted by (Z-LL)₂. Unbiotinylated (Z-LL)₂ effectively competes for labeling of PfSPP against the biotinylated (Z-LL)₂ probe providing further confirmation that (Z-LL)₂ is not non-specifically labeling PfSPP but likely binding to the active site. LY411,575 and AK8 do not compete for labeling which is commensurate with the published studies indicating that they bind at the substrate docking site rather than the active site where (Z-LL)₂ is thought to bind [133].

A

| Inhibitor | Organism | IC ₅₀ |
|---|----------------------|------------------|
| $(Z-LL)_2$  | <i>P. falciparum</i> | 1.8 μ M |
| | <i>T. gondii</i> | 0.95 μ M |
| | <i>T. brucei</i> | 1.8 μ M |
| LY411,575  | <i>P. falciparum</i> | 0.45 μ M |
| | <i>T. gondii</i> | 0.040 μ M |
| | <i>T. brucei</i> | 9.8 μ M |
| DAPT  | <i>P. falciparum</i> | >10 μ M |
| | <i>T. gondii</i> | >10 μ M |
| | <i>T. brucei</i> | >10 μ M |

| Inhibitor | Organism | IC ₅₀ | Inhibitor | Organism | IC ₅₀ |
|---|----------------------|------------------|---|----------------------|------------------|
| ES I Ac-LULVULSNUL-NH ₂ | <i>P. falciparum</i> | 9.8 μ M | AK4 Ac-LULLLULAAU-NH ₂ | <i>P. falciparum</i> | 0.075 μ M |
| | <i>T. gondii</i> | >10 μ M | | <i>T. gondii</i> | 1.5 μ M |
| | <i>T. brucei</i> | >10 μ M | | <i>T. brucei</i> | >10 μ M |
| ES II Ac-LULVULLLUL-NH ₂ | <i>P. falciparum</i> | 0.58 μ M | AK8 Ac-ULLLULLLAAU-NH ₂ | <i>P. falciparum</i> | 0.080 μ M |
| | <i>T. gondii</i> | 5.5 μ M | | <i>T. gondii</i> | 0.35 μ M |
| | <i>T. brucei</i> | >10 μ M | | <i>T. brucei</i> | 0.35 μ M |
| ES III Ac-ULLUVSNUL-NH ₂ | <i>P. falciparum</i> | >10 μ M | AK9 Ac-LULLLULLLAAU-NH ₂ | <i>P. falciparum</i> | 0.080 μ M |
| | <i>T. gondii</i> | >10 μ M | | <i>T. gondii</i> | 2.5 μ M |
| | <i>T. brucei</i> | >10 μ M | | <i>T. brucei</i> | 10 μ M |

B

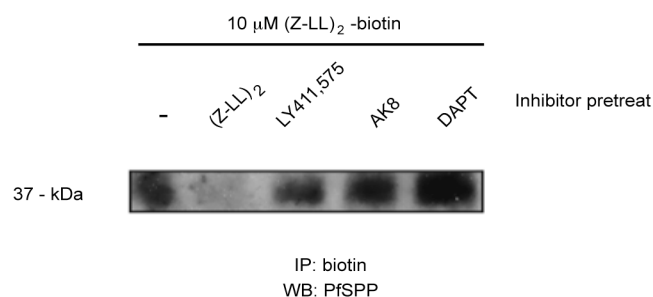


Figure 4.1: SPP/PS Inhibitor pharmacology against protozoan parasites and photolabeling of PfSPP with a (Z-LL)₂-based probe. (a) Structures and names of key SPP/Ps inhibitors are shown. (U=aminoisobutyric acid, L=Leucine, S=Serine, N=Asparagine, A=Alanine, Ac=Acetyl). **(b)** CHAPSO solubilized-membrane proteins were incubated with 10 μ M of (Z-LL)₂-biotin for 1 hr, then irradiated with UV-light. Labeled proteins were identified via IP-Western analysis using streptavidin agarose and anti-PfSPP for western blotting. Treatment of membrane proteins with 10 fold excess of non-biotinylated (Z-LL)₂ prevented labeling. No effect was observed with preincubation with non-active site-directed inhibitors (AK8, LY411,575) or with the gamma-secretase specific inhibitor DAPT. *In collaboration with Dany Shanmugam and Jeremy Mallari.*

Design of a heterologous SPP assay

A cell-based SPP assay would be a powerful pharmacological tool to functionally characterize various SPPs as well as evaluate potential SPP inhibitors. Therefore, we endeavored to design a robust cell-based heterologous SPP reporter activity assay (Fig. 4.2A). We designed the assay in the budding yeast *S. cerevisiae* because of the genetic tractability in this system. Additionally, *S. cerevisiae* lacks the gene for PS, therefore SPP activity is the direct result of any exogenously expressed SPP. Despite previous claims that there is no SPP in yeast, there exists an SPP-like protein (YKL100c; scSPP) in the yeast genome that is homologous to SPP. An scSPP knockout strain was made in the $\Delta pdr1,3$ strain, which lacks multidrug resistance pumps. Δspp is viable and has no gross phenotypic differences when compared to the wildtype strain. Next the $\Delta pdr1,3\text{-}\Delta spp$ strain was transformed with the following plasmids: a reporter consisting of glucocorticoid response element (GRE) fused to LacZ, a truncated glucocorticoid receptor fused to the transmembrane of human cytomegalovirus glycoprotein UL-40 (gpUL-40) on the N-terminus (a canonical SPP substrate) induced with galactose, and the recombinant parasite SPP. The fused substrate is membrane bound with the glucocorticoid receptor in the cytosol (Fig. 4.2A). Upon cleavage of the transmembrane domain by SPP, the glucocorticoid receptor is no longer anchored by the substrate and is released. It translocates into the nucleus where it binds the GRE and expresses LacZ which encodes β -galactosidase. SPP activity is determined by the addition of a chemiluminescent substrate which detects β -galactosidase (Fig. 4.2A).

To test the activity of other SPPs we used the $\Delta pdr1,3-\Delta spp$ strain containing the reporter and substrate plasmids and overexpressed PfSPP, TgSPP, TbSPP and human SPP. The expression of various SPPs (~40-50kDa) and GR526-gpUL40 (~70kDa) was detected using a western blot with anti-myc and anti-HA tag antibody, respectively (Fig. 4.2B and C). The activity of endogenous scSPP was measured by the assay described above by overexpression of the reporter and GR526 substrate vectors in wt and Δspp background. Luminescence data showed 4.5x activity of endogenous scSPP while the activity was abolished in the knockout of scSPP. The fold activity is a ratio of induced, induced + 50 μ M LY411,575 or induced + 50 μ M DAPT to uninduced. The results in Figure 4.2C show that all overexpressed SPPs are active aspartyl proteases that cleave the GR526-gpUL40 substrate with various activities. Differences in activity may be reflective of expression levels as well as activity towards the GR526-gpUL40 substrate. To further confirm that protease activity is due to SPP and not another protease, the SPP inhibitor LY411,575 was added at the time of induction and cells were incubated overnight (~16hrs). Each SPP was inhibited by LY411,575 and the SPP activities were reduced from 2.7- to 25-fold, illustrating that protozoan SPPs are indeed targetable by specific drug-like compounds. Under the same conditions, the PS-specific inhibitor DAPT showed no inhibition of SPP activity, confirming that our assay replicates the sensitivities to SPP inhibitors seen in parasite assays.

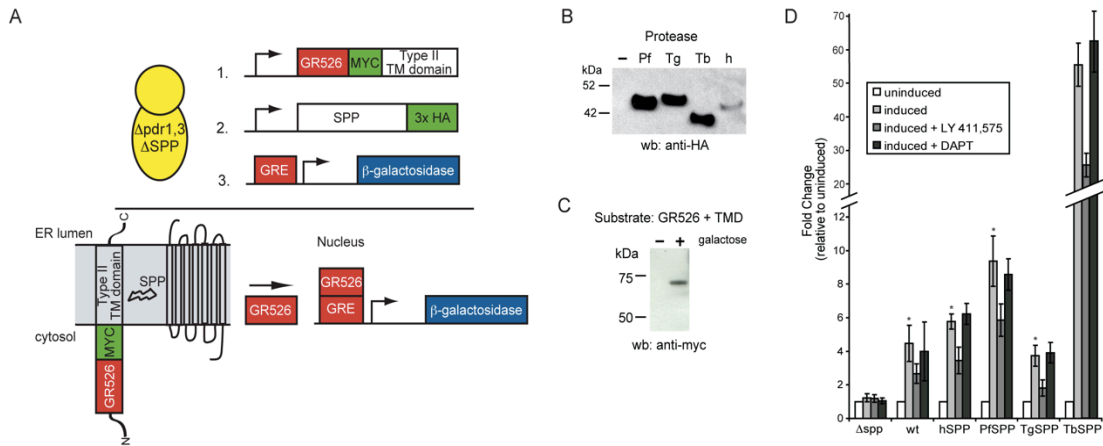


Figure 4.2: Yeast-based SPP assay. **(a)** Yeast strain (Δ pdr1,3- Δ spp) was transformed with three overexpression plasmids: a reporter with the glucocorticoid response element fused to LacZ, inducible glucocorticoid receptor 526 fused N-terminally to type II transmembrane domain of the model SPP substrate gpUL40 and signal peptide peptidase protease from various parasites. The SPP cleaves the substrate and releases GR526 which goes to the nucleus where it binds the GRE and the expression of LacZ is detected via a luminescent substrate (measures β -galactosidase activity). **(b)** Expression of HA-tagged human, *P. falciparum*, *T. gondii*, and *T. brucei* SPP in the Δ pdr1,3- Δ SPP yeast strain as detected by western blotting for HA. **(c)** gp-UL40 is detected only upon induction of galactose, as detected by anti-myc western blotting. **(d)** Δ pdr1,3 Δ SPP, in the absence of endogenous scSPP or protease, shows modest activity when the substrate is induced or in presence of LY411,575/DAPT. Δ pdr1,3 with the endogenous scSPP shows 4.5x activity. Δ pdr1,3 Δ SPP with an overexpressed protease shows successful cleavage, inhibition by 50 μ M LY 411,575 and no change under presenilin specific DAPT 50 μ M inhibitor. The fold activity is a ratio of induced, induced + 50 μ M LY411,575 or induced + 50 μ M DAPT to uninduced. The activity of SPPs are hSPP (5.8x), PfSPP (9.4x), TgSPP (3.7x) and TbSPP (56x). * = Statistically significant with a p-value <0.05. SPP activities were reduced to wt-scSPP (2.7x), hSPP (3.5x), PfSPP (5.8x), TgSPP (1.8x) and TbSPP (25x). In collaboration with Bhumi Patel.

SPP inhibitors target PfSPP in live Plasmodium falciparum parasites

To identify the target(s) of SPP inhibitors in live parasites, we attempted to generate resistant parasites to the compound. Identification of genetic changes in the resistant parasite lines may provide details as to the molecular target of the compounds in culture [137]. For this, we focused our effort on *P. falciparum*, which has recently proven amenable to this methodology [138,139]. In collaboration with the Novartis Institute for Tropical Diseases (NITD) we identified a series of small molecules based on the drug-like LY411,575 scaffold which were potent antimalarials, with IC₅₀s ranging from 20 nM to 160 nM. In addition, we assessed each inhibitor against PfSPP in our yeast assay and found they each inhibited the enzyme with varying potencies (data not shown). To elucidate the biological targets of the NITD series and LY411,575 compounds we selected for parasite resistance to each compound. Drug-resistant parasites were selected by the application of sub-lethal amounts of each inhibitor over a period of months, with drug concentration increasing concomitantly as parasite resistance increased. Resistant lines were generated for each drug and the resulting lines found to be more than 10-fold resistant to than the parental Dd2 clone. Analysis of this resistant line to antimalarials atovaquone, chloroquine, and artemisinin showed no significant differences in sensitivities to these compounds.

To identify the mutation, cDNA transcribed from RNA of resistant parasites was subjected to PCR, cloned and sequenced. Strikingly, sequencing analysis of the PfSPP coding sequence for each parasite line revealed a single non-synonymous mutation, L333F. From the PfSPP coding sequence we know that

the L333 residue resides in transmembrane domain 8, just upstream of the highly conserved PAL motif, a hydrophobic region necessary for activity in both SPP and PS. Unfortunately, no crystal structural yet exists for PfSPP, hindering predictions on the role of the L333 residue to catalytic activity of PfSPP [140].

To confirm the role of the L333F mutation in conferring resistance, we expressed the mutant PfSPP (L333F) in our yeast assay and analyzed the potency of NITD-731, our most potent antimalarial. The IC₅₀ in the mutant L333F PfSPP showed a more than 2-fold increase to that of wild-type PfSPP (Fig. 4.3A). This change was not due to different expression levels of either protein as the total luminescence of PfSPP and PfSPP L333F was unchanged (data not shown). Unfortunately, issues with cell permeability of the other inhibitors in the yeast assay precluded analysis of the L333F mutation in conferring resistance to these inhibitors.

We also wished to confirm the importance of this mutation in generating resistance in live parasites. To do this, the L333F PfSPP gene was amplified from cDNA of a resistant parasite line and ligated into an expression vector that would allow for transposase-mediated recombination into a parasite genome [141]. Transgenic parasites were then assayed for growth while in the presence of increasing drug concentration. Parasites expressing the L333F PfSPP showed statistically significant increased resistance to NITD-731 relative to those expressing solely a wild type allele (Fig. 4.3D). In both our heterologous assay and transgenic parasites we observed a decreased level of resistance conferred by L333F relative to the original drug-selected resistant parasite lines. This is

potentially due to the existence of other mutations in multi-drug resistance transporters in the resistant lines that synergize resistance to the drug to a level beyond what the isolated mutation provides. It is also likely a product of the coexpression of the mutant PfSPP and endogenous wild-type allele in our transgenic parasite lines. Together, the resistance conferred by the expression of L333F PfSPP suggests that the target of the inhibitors used to generate resistant parasites is PfSPP.

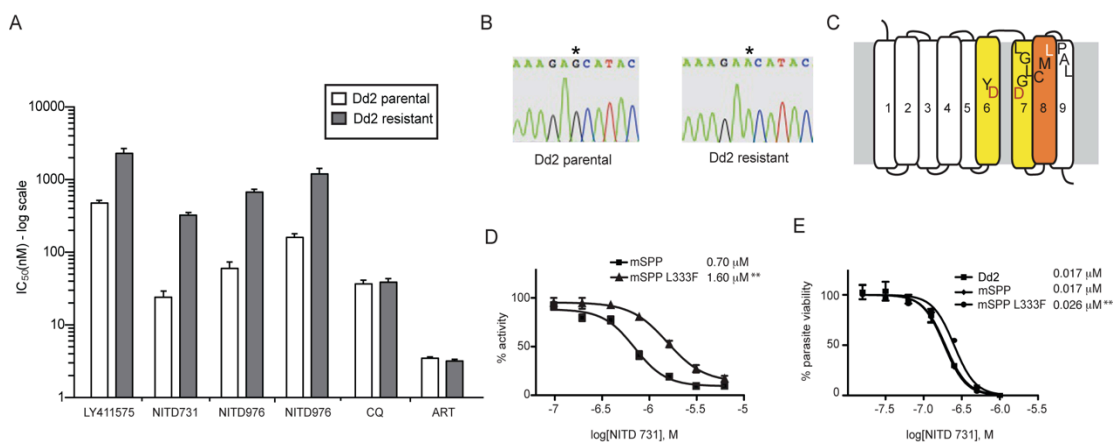


Figure 4.3: Generation of parasites resistant to potent PfSPP inhibitors (a) Parasites grown in sub-lethal concentrations of LY411,575 and three NITD inhibitors developed resistance to the compound, resulting in multi-fold increase in sensitivity (note log scale). The resistant parasites showed no concomitant resistance to other common anti-malarials (CQ=chlorquine, ART=artesunate. Only a single resistant line, NITD731r, is shown in the tests with resistance to CQ and ART). **(b)** Sequencing of the PfSPP gene in each resistant line revealed a G to A base mutation resulting in the non-synonymous amino acid change, L333F. **(c)** The location of the L333 amino acid maps to transmembrane domain 8, close to the highly conserved PAL motif. **(d)** The L333F PfSPP mutant was generated for use in the yeast activity assay and showed a greater than two-fold resistance to NITD731. **(e)** Introduction of the L333F transgene into Dd2 parental parasites confers slight resistance to inhibition of NITD731. The wild-type gene was also introduced as a control. (** Statistically significant with a p-value <0.01)

PfSPP has heightened function in the parasite ER during the trophozoite stage

Our results thus far suggested the importance for SPP in the biology of protozoan parasites and established its suitability as targetable protease. Beyond its necessity, information on the role of SPP in protozoans is lacking. To characterize PfSPP further, we assessed its endogenous localization by indirect immunofluorescence (IFA) utilizing our PfSPP antibody. Throughout the parasite life cycle, we observed strict perinuclear localization of PfSPP throughout the parasite's lifecycle, likely in the endoplasmic reticulum/golgi (ER/golgi) complex (Fig. 4.4A). Co-IFA performed with resident ER protease plasmepsin V confirmed this organellar localization (Fig. 4.4B) [142]. We observed no localization to the micronemes of merozoites, as had been previously suggested [131]. These results recapitulate previous findings in other organisms that show SPP is an ER/golgi-localized protease [121].

Expression levels of PfSPP increase throughout the ring and trophozoite stages and peak at late trophozoite, followed by a decline during schizogony. Gene expression in *P. falciparum* is tightly temporally coupled to protein function, which suggests the key functions for PfSPP are likely during the trophozoite stage [143]. To assess this we evaluated the sensitivities of parasites to SPP inhibitors during different stages of the erythrocytic cycle. Individual cultures of parasites were treated at ring, trophozoite, or schizont stages for 6 hrs prior to drug removal and continuation of culture until the next cycle in non-drug media. PfSPP inhibition was most potent against trophozoite stage parasites, with some sensitivity seen schizonts as well. The ER is the hub of protein synthesis for the

secretory pathway and is likely most active during the metabolically dynamic trophozoite stage [144]. Therefore, PfSPP inhibition may compromise the function of the ER, the effects of which are most profound during this stage.

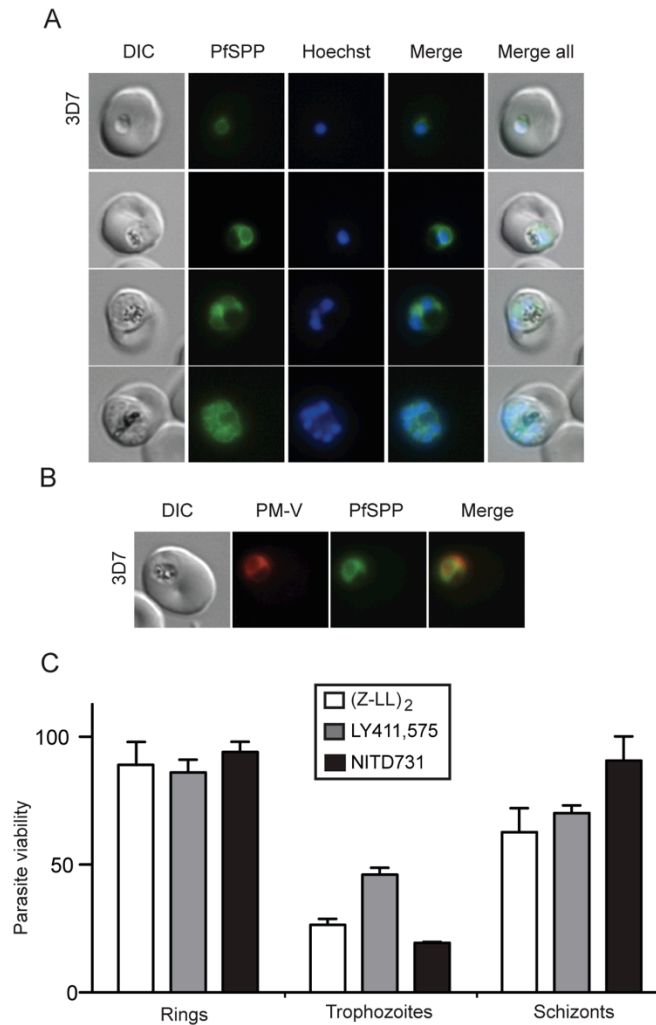


Figure 4.4: PfSPP localizes to the parasite ER and is important during the trophozoite stage. (a) Indirect immunofluorescence assays using an antibody raised to PfSPP shows localization of PfSPP in the ER throughout the lifecycle. Nuclei were visualized with Hoechst 3342. **(b)** PfSPP ER localization was confirmed by performing a co-IFA with plasmepsin V, an ER-resident protease, and PfSPP, and showed that staining overlapped for the two proteins. **(c)** Parasites were treated with SPP inhibitors for a 6 hour duration during the ring, trophozoite, or schizont stages with 6x the IC₅₀ of the drug indicated. Parasites show the most sensitivity to SPP inhibition during the trophozoite stage.

Inhibition of PfSPP sensitizes parasites to ER-stress

Recent work in mammalian cells has suggested a role for SPP in dislocation during ER-associated degradation (ERAD), a coordinated multi-component process by which terminally misfolded proteins within the ER are recruited to the ER membrane, dislocated through the lipid bilayer, and degraded by the ubiquitin-proteasome system in the cytosol [127,145]. To investigate a potential role for PfSPP in *P. falciparum* ERAD, we treated parasites simultaneously with both thapsigargin and SPP inhibitors and analyzed the effects of the drug combinations for evidence of synergy. Thapsigargin causes the release of calcium from the ER, compromising the ER's ability to produce properly folded proteins. The combination treatment of thapsigargin with the SPP inhibitors (Z-LL)₂, LY-411,575, and NITD731 produced synergistic parasitocidal effects beyond what would be expected by simply adding the effects of the individual compounds together. The results are presented as an isobologram of the varying ratios of the two compounds, where points below the line of additivity indicate synergy. No synergy was seen with atovaquone (Fig. 4.5A), an anti-malarial ubiquinone analogue whose mechanism of action involves the mitochondria. This suggests that the synergy between SPP inhibitors and thapsigargin is due to the disruption of the parasite's ability to respond to stress in the ER.

If PfSPP is involved in a parasite ERAD pathway, we reasoned that parasites would also see synergy between PfSPP inhibition and another protein within the ERAD network. Recently, the AAA (ATPase associated with diverse

cellular activities) ATPase p97 (or Cdc48; VCP, valosin-containing protein) was shown to be involved in the ERAD-mediated extraction of proteins from the ER and was necessary for their release as polyubiquitinated substrates into the cytosol [146]. To facilitate functional studies of mammalian p97, two groups identified small molecule inhibitors of p97 through high-throughput screening efforts: DBeQ, which reversibly inhibits p97 in an ATP-competitive fashion, and Eeyarestin 1 (Eey 1), an irreversible p97 inhibitor [147,148]. *P. falciparum* contains two putative p97 homologues, PF07_0047 and PFF0940c. PF07_0047 is targeted to the apicoplast where it possibly mediates translocation of nuclear-encoded proteins into the apicoplast, but the function of PFF0940c has not been investigated [149]. We reasoned that DBeQ may be a suitable inhibitor of PFF0940c because of the high level of identity between PFF0940c and mammalian p97 (66.7%). Treatment of the parasites showed that DBeQ is a potent antimalarial, with an IC_{50} in the nanomolar range (225 nM). We next investigated the simultaneous inhibition of PfSPP and p97 in parasites. The combined treatment with both SPP inhibitors and DBeQ showed that the SPP inhibitors potentiated the effectiveness of DBeQ, while DBeQ had little effect on the efficacy of SPP inhibitors, as illustrated on the downward and rightward grouping of the fractional inhibitory concentration (FIC) points in the isobolograms (Fig. 4.5B). Similar effects were seen with Eey1, suggesting the DBeQ and Eey 1 worked through a similar mechanism (Fig. 4.5B). This evidence suggests PfSPP and p97 may function in a parasite ERAD pathway, with PfSPP working upstream of p97.

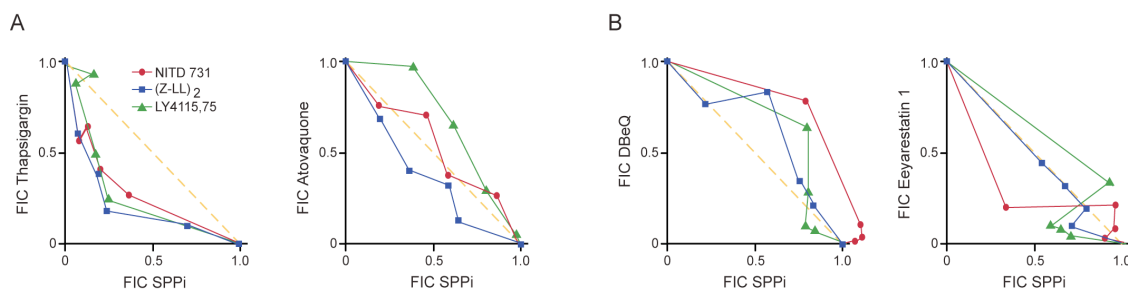


Figure 4.5: Inhibition of PfSPP synergizes with ER stress in *P. falciparum* and potentiates antimalarial effect of an inhibitor of the ERAD pathway. (a) Individual IC_{50} values were determined for each SPP inhibitor and thapsigargin singly and for each inhibitor in combination with thapsigargin at four different fixed ratios. The fractional IC_{50} (FIC; IC_{50} of drug in combination/ IC_{50} of drug alone) value was determined for each drug in each combination, and plotted on the isobologram. The x axis indicates the FIC of the SPP inhibitors. All three SPP inhibitors showed synergistic combinations with thapsigargin. The average ΣFIC for the SPP inhibitors with thapsigargin were 0.80, 0.72, and 0.79 for LY411,575, (Z-LL)₂, and NITD731, respectively, while the same inhibitors paired with atovaquone averaged ΣFIC s of 1.3, 0.95, and 1.0. The diagonal line represents a ΣFIC of 1, indicating additivity between the two drugs. Below the line (ΣFIC of <1) indicates a synergistic combination. **(b)** Isobolograms of the *in vitro* combinations between SPP inhibitors and the p97 inhibitors DBeQ and Eey 1. The isobolograms show that SPP inhibitors strongly potentiate the p97 inhibitors. The average FIC for DBeQ was 0.30, 0.65, and 0.36 and for Eeyarestatin was 0.12, 0.25, and 0.21 with LY411,575, (Z-LL)₂, and NITD731, respectively.

4.3 Discussion

Here we provide chemical-genetic evidence that protozoans SPPs are druggable anti-protozoan targets. We also show that in *P. falciparum*, inhibition of PfSPP leads to disruption of the parasite's ability to maintain ER homeostatic equilibrium, and that this may represent a potential exploitable vulnerability in protozoan parasites.

That an enzyme is essential to a pathological organism does not guarantee it is a suitable drug target, but we believe PfSPP is attractive for a variety of reasons, including: 1) an extensive drug-discovery "piggy-back" opportunity for potential inhibitors in already existing chemical libraries, 2) the availability of experimental tools such as activity assays, and 3) the extreme sensitivity of SPP-inhibition in protozoan parasites in contrast to human cells.

The demonstration that Abeta cleavage, an essential initiating event in the pathogenesis of Alzheimer's disease, is carried out by an intramembrane aspartyl protease spurred intense pharmaceutical medicinal chemistry efforts to develop inhibitors for this novel protease. Both PS and SPPs are part of the A22-family integral membrane aspartyl proteases; thus it is likely that there exist numerous potent PfSPP inhibitors in PS inhibitor-directed chemical libraries. Indeed, LY411,575 was a byproduct of a previous PS drug-discovery effort. Because these PS inhibitor libraries were developed with a prospective potential therapeutic use, they would potentially already have drug-like characteristics and known pharmacology, reducing costs barriers for development.

Worries about host toxicity for PfSPP inhibitors are mitigated by the fact that knockdown of SPP is non-lethal in human cell lines. Furthermore, (Z-LL)₂ showed little toxicity in non-cancer human cell lines, indicating the potential for high therapeutic indexes for SPP inhibitors [150].

How the L333 residue in PfSPP confers resistance to an LY-based inhibitor is difficult to answer because of a lack of knowledge regarding SPP structure and catalytic activity. The L333 residue lies at the end transmembrane domain 8 (TMD8) of PfSPP. In chemical crosslinking studies in PS, a nine transmembrane protease like PfSPP, the N-terminus of TMD8 has been shown to be able to interact with residues within the active site [151]. In addition, LY411,575 represents a class of inhibitors that are thought to bind a region of SPP that partially overlaps with the active site. This suggests the region that the L333F residue resides in contributes to or allosterically interacts with the active site.

Finally, our data also suggest PfSPP may have a role in the parasite's ERAD pathway and that the enzymatic machinery involved in ERAD may serve as a novel antimalarial chemotype. ERAD is activated in response to ER stressors that cause the accumulation of terminally misfolded proteins in the ER and is orchestrated by a number of proteins in a process involving transcriptional and translational regulation. The transcription factors that initiate the transcriptional up-regulation of the components of protein folding, trafficking, and degradation machinery during the initial unfolded protein response have not been identified in *P. falciparum*, suggesting that these parasites have limited, if any,

transcriptional regulatory mechanisms in response to ER stress [152]. In addition, the make-up of the ERAD pathway in *P. falciparum* is reduced in complexity compared to metazoans, where the network topology of ERAD is extensive and partially redundant; multiple members of the pathway found in yeast and humans are absent in *P. falciparum*, such as the TRAP and Bap31 proteins, which associate with Sec61. This lack of complexity and redundancy may help to explain the sensitivity of parasites to ER-stressors such as thapsigargin and to SPP and p97 inhibition.

During combined treatment with SPP and p97 inhibitors we observed directional effects of the inhibitors on each other; while SPP inhibitors potentiated the efficacy of p97 inhibitors, p97 inhibition on masked SPP inhibitor potency. This may suggest that p97 functions downstream of PfSPP and that inhibition of p97 has a negligible effect on upstream PfSPP inhibition. This sequential action would be expected based on the localization of SPP in the parasite ER membrane and p97 in the cytosol. Other potential ERAD-based inhibitors, such as for protein disulfide isomerase, which has been shown to associate with SPP during ERAD in mammalian cells and which may act in a parallel pathway with SPP, may allow for synergistic pairings [129].

Our collective data here suggest that SPP may be a valid anti-protozoan drug target, in addition to the parasite's ERAD pathway at large. Our most potent SPP inhibitor is lethal to CQ-resistant parasites, and has an IC_{50} in the range of currently used antimalarials such as artemisinin and atovaquone. The recent emergence of artemisinin resistant parasites has exacerbated the need to

identify new anti-malarials. Inhibition of PfSPP alone or in combination with another ERAD-focused anti-malarial may represent a valid strategy both for drug treatment and to combat resistance.

4.4 Experimental Procedures

Parasite culture

Briefly, 3D7 parasites were cultured in RPMI 1640 (Invitrogen) supplemented with Albumax II (Invitrogen). For synchronization, schizont stage parasites were magnet purified using a SuperMACS™ II Cell Separation Unit (Miltenyi Biotech).

IC₅₀ determination

For IC₅₀ determinations, synchronized parasites were plated at 1% parasitemia and 6% hematocrit in 96-well plates at a total volume of 50 mL. Serial dilutions of 2x concentration of the respective compound were added to the wells to bring the total volume up to 100 mL and 0.5% parasitemia and 3% hematocrit. Compounds were assayed for a 72 h period, after which 2x Vybrant DyeCycle Green DNA (Invitrogen) in PBS was added for a final concentration of 10 mM and incubated at 37 °C for 30 min. DNA content, as an indicator of parasitemia, was analyzed on an Accuri C6 Flow Cytometer with C-Sampler. IC₅₀ curves were generated using GraphPad Prism (GraphPad Software).

Labeling of parasite lysates with (Z-LL)₂ activity-based probe

For parasite labeling, mixed stage parasites were harvested and released from erythrocytes with 1% saponin followed by centrifugation at 1,500xg for 5 min and 3 washes in cold PBS. Parasite lysates were prepared by freeze-thaw in the presence of 1% CHAPSO in 25 mM HEPES-KOH, pH 7.6, 100 mM KOAc, 2 mM Mg(OAc)₂, 1 mM DTT, and protease inhibitor cocktail (EDTA-free) (Roche). Membrane and cell debris was clarified by centrifugation at 16,000 x g for 30 min at 4 °C. Labeling was performed with indicated concentrations of the ABP for 1 hr at 37 °C followed by UV crosslinking (365 nm) for 1 hr on ice. Competition of labeling was carried out by preincubating lysates for 1 hr at 37 °C. For immunoprecipitation, lysates were passed through 7K MWCO desalting columns (Pierce) after UV crosslinking then incubated overnight with streptavidin Ultralink Resin (Pierce). Proteins were visualized by standard western blotting and VECTASTAIN ABC kit (Vector Labs).

Yeast strains

w303 pump mutants (MATa can1-100, his3-11, 15, leu2-3,112, trp1-1, ura3-1, ade2-1, pdr1::kanMX, pdr3::hygMX) was used to make a Δ spp by recombination using a pAG304ccdb under a Trp selection. pLZGreLacZ was used as the reporter strain containing the glucocorticoid receptor with a leu marker. GR526-gpUL40 was made using glucocorticoid receptor amino acids 1-526 fused to the TMD domain of Human cytomegalovirus glycoprotein UL40 (NKFSNTRIGFTCAVMAPRTLILTVGLLCMTITSLL) by 2xmyc tag and inserted into pAG426GALccdb. The pLZGrelacZ and GR526-gpUL40 were transformed

in both wildtype w303 and w303, Δ spp pump mutant strains to determine endogenous scSPP and Δ spp activities. Parasite SPPs (PfSPP (recodonized for yeast expression), TbSPP, TgSPP) were cloned into pAG423GALccdbHA (his marker) and human SPP was cloned into pAG423GPDccdbHA vectors using recombination. The vectors were transformed into yeast using standard Li/Ac protocol and selected on appropriate (-leu, -ura or -leu, -ura, -his) plates.

Briefly, yeast cells were grown overnight in S-raffinose (-leu,-ura or -leu,-ura,-his) media to prevent expression of the substrate. They were then diluted to OD ~0.2 and induced with 2% galactose overnight (~16hrs). A sample of uninduced cell served as a control. Appropriate amounts of chemical compounds were diluted in 500ul of yeast cells at the time of induction. Due to solubility issues, each compound was diluted into 1:1 DMSO:water solution and added to cells at a nonlethal DMSO concentration of 4.25ul/500ul - 0.8%. Cells were then adjusted to OD ~0.3 and 100 μ l of cells were incubated with 100 μ l GAL-Screen reagent (Applied Biosystems) for 1 hour at 27°C on a 96well plate. The luminescence was read using Berthold microplate luminometer. The fold activity was calculated as induced/uninduced luminescence count and each experiment was done in triplicates.

Resistant parasite generation

Parasites were treated with sub-lethal concentration of inhibitor, increasing as resistance increased. Inhibitor resistance was generated for a period of 4 months. Resistant parasites were cloned by limiting dilution. Parasites were

saponin treated, spun down, RNA extracted using RNEasy Kit (Qiagen), converted to cDNA using Superscript I Reverse Transcriptase Kit, and cloned into pAG423ccdbHA using Spe and Xho restriction sites. The cDNA from parasites the parasite lines were subjected to three independent PCR reactions. PfSPP L333F was made by standard site directed mutagenesis techniques using the wildtype recodonized PfSPP as a template.

Parasite transfections

P. falciparum vectors expressing PfSPP-HA and PfSPP L333F-HA were cloned in the piggyBacII vector via NotI and XhoI restriction sites. For transfections, 100 µg of the piggyBacII PfSPP vector and 50 µg in 50 µl of water and 50 µl of 2x cytomix were combined with 250 µl of packed red blood cells, that had been previously was 3x in 1 mL of cytomix. The solution was brought up to 400 µl with 1x cytomix (120 mM KCl, 0.15 mM CaCl₂, 2 mM EGTA, 5 mM MgCl₂, 10 mM K₂HPO₄, 25 mM HEPES, adjusted to pH 7.6 with KOH). The solution was electroporated using a Bio-Rad GenePulser Xcell II, with settings 0.31 kV and 950 µF, in 0.2 mm cuvettes. Electroporated cells were washed 2x in complete media and added to magnet purified schizonts in a total of 5 mL complete media. Selection for transgenic parasites was carried out by application of 2.5 nM WR99210 to cultures.

Chapter 5: Conclusions and Future Directions

In this work, I have characterized the biological function and drug target potential of three essential proteases in *P. falciparum*. In the first two sections of this work I developed and utilized novel chemical tools to provide the first conclusive evidence for the role of an exopeptidase, PfA-M1, in hemoglobin metabolism. Inhibition of this enzyme is lethal to parasites, possibly by depriving them of essential amino acids normally acquired from PfA-M1-mediated Hb digestion. I also find that the Pf-LAP aminopeptidase likely has a significant role outside of hemoglobin degradation. In the third part of this work, I chemically validate SPP as a novel protozoan drug target. I also present the first evidence that inhibiting the parasites' limited ERAD pathway may represent a therapeutic opportunity, and that inhibition of PfSPP likely interferes with the function of this pathway. In the following section these results will be explored in greater depth along with suggestions on experiments to expand this work.

5.1 A bestatin-based chemical biology strategy reveals distinct roles for M1 and M17 family aminopeptidases

Characterization of Pf-LAP

In Chapter 3 I utilized a suite of inhibitors to characterize MAP activity in *P. falciparum*. In addition to presenting evidence that PfA-M1 is a DV-localized hemoglobinase, the data also suggested that Pf-LAP has functions other than hemoglobin digestion. This is based on the cytosolic localization of Pf-LAP and

the fact that parasites are susceptible to Pf-LAP inhibition prior to the initiation of this process. One possible function of Pf-LAP could be in the final trimming of various short peptides generated by the proteasome into free amino acids. Involvement of leucyl aminopeptidases in non-lysosomal protein turnover has been demonstrated in human cells [110]. In addition, proteasome inhibitors block parasite development at the same stage in the erythrocytic cycle as PNAP. One facile method to examine the potential interconnectedness of Pf-LAP and the proteasome would be via fixed-ratio isobologram analysis, as presented in Chapter 4. If Pf-LAP and the proteasome cooperate in cytosolic protein turnover, I predict that dual inhibition of the two components should produce additive or synergistic killing of parasites.

Another approach to answer whether Pf-LAP has functional homology to mammalian LAPs would be by a mass-spectrometry-based method, similar to that used in Chapter 3. In this instance, we would compare changes in the amount of small peptides (2 to 6 amino acids) between untreated and PNAP-treated samples. Peptides that increase in abundance in the treated samples would potentially be Pf-LAP substrates. To characterize whether these peptides are derived from the proteasome, we could analyze an additional sample in which parasites are concomitantly treated with both proteasome inhibitor and PNAP. If peptides identified in the PNAP-only treated condition are products of the proteasome, they should not appear in samples treated with a proteasome inhibitor.

Malarial aminopeptidases as putative drug targets

Previous work on the development of aminopeptidase inhibitors has produced compounds with only modest effectiveness against parasites in cultures and in mouse models, and until recently, bestatin remained the most potent aminopeptidase inhibitor against parasites in culture. As presented in Chapter 3, the identification of aminopeptidase-directed inhibitors that are lethal to parasites in nanomolar concentrations represents a major advance in the targeting of these enzymes in parasites, and confirms the attractiveness of PfA-M1 and Pf-LAP as drug targets.

One potentially efficacious antimalarial strategy could be to simultaneously target other hemoglobin proteases, such as the plasmepsins, falcipains, or DPAP1 along with PfA-M1. Targeting enzymes functioning in series within a given catabolic pathway may result in a synergistic combination, resulting in the need for less of each drug when used in combination than individually to achieve the same effects. Indeed, previous work by the Bell group has shown the bestatin is synergistic when used in combination with aspartyl protease inhibitors [113]. Of course, previous issues encountered with falcipain and plasmepsin protease inhibition would still be relevant (genetic redundancy, poor *in vitro* potency), but these complications may be less problematic when coupled with the inhibition of essential downstream proteases. Intriguingly, the Bogyo and Klemba groups have recently provided evidence that the DV-localized essential protease DPAP1 is targetable by small molecule drug-like inhibitors that are highly potent in culture [153]. Unfortunately the inhibitors were toxic in a mouse model, but less

potent DPAP1 inhibitors with better toxicity profiles did show promise in slowing parasite growth in the animals. In addition, DPAP1 inhibitors produce the same DV morphology as PfA-M1 inhibition does, indicating hemoglobin degradation as the likely role for DPAP1 (M. Klemba, personal communication). Thus, a viable strategy may be to target PfA-M1 and DPAP1, which would overcome issues of functional redundancy encountered with plasmepsin and falcipain inhibition; both DPAP1 and PfA-M1 are single copy essential enzymes. This dual targeting strategy would inhibit almost all exopeptidase activity in the DV. In addition, the application of combined therapy would to minimize the chances for the emergence of resistant parasites.

Peptides are often not ideal therapeutics due to their rapid inactivation by serum or gastrointestinal proteases. The bestatin-based MAP inhibitors PNAP and BTA are more suitable as drugs because they are beta-peptides, and as such, are resistant to proteolytic cleavage. Further modification to the inhibitor scaffold to increase hydrophobicity, such as C-terminal esterification, which removes the charge on the C-terminus, may help to increase its permeability. The suitability of bestatin-based MAP inhibitors as drugs is demonstrated by the fact that bestatin is approved for oral administration in Japan for patients with nonlymphocytic leukemia [154].

Specificity studies may be complicated by the existence of 13 M1 and 3 LAP family MAPs in humans. However, none of the human M1 or LAP aminopeptidases share more than 30% identity with the parasite orthologs. Studies on various other mammalian MAP orthologs show significant variation in

inhibitor activity, giving an indication that achieving selectivity is possible. The human aminopeptidase ortholog most similar to PfA-M1 has extensive variation at the N- and C-terminal domains, indicating that inhibitor access to the active site may be quite altered. Unfortunately, no structural information yet exists for the human M1 or LAP enzymes. The relative lack of toxicity associated with bestatin use and paucity of identity between the malarial and human enzymes give hope that cross-targeting may be negligible.

5.2 Chemical validation of signal peptide peptidases as potential anti-protozoan targets

The protozoan signal peptide peptidase represents a novel drug target

Protozoan pathogens, including *T. brucei*, *T. gondii*, and *P. falciparum*, express only one copy of the signal peptide peptidase gene. In Chapter 4, I present data that shows that the gene products from each organism encode active proteases that when expressed in yeast are amenable to inhibition by small molecules that are also lethal to parasites in a dose-dependent manner. Furthermore, continuous cultivation of these parasites in the presence of a sub-lethal concentration of the inhibitor produces *P. falciparum* parasites with mutations in its PfSPP gene. This resulting amino acid change confers resistance to the inhibitors both *in vitro* and in culture, indicating the inhibitor target in live parasites is indeed PfSPP. Collectively, this data indicates the suitability of SPP as an anti-protozoan target.

Recent work by the Mota lab assessed the suitability of SPP inhibition for

prevention of Plasmodium development in the liver *in vitro* and *in vivo*. Prevention of liver stage development would lead to true causal prophylaxis and would interrupt transmission because development of the proceeding infectious blood stage gametocytes would be blocked. The inhibitor LY411,575 was shown to block hepatic cell development of *P. berghei* in a dose-dependent fashion, and led to a statistically significant decrease in cerebral malaria in mice with a 55% higher mortality in the control group of animals compared to the LY411,575-treated ones [155]. A statistically significant difference in development in cerebral malaria was also observed in LY411,575-treated animals versus the controls. LY411,575 is limited in the concentrations that can be used because of complications caused by its concomitant inhibition of GS activity, mainly the blocking of GS processing of NOTCH protein, which leads to severe gut toxicity (a major shortcoming of GS inhibitor-mediated Alzheimer's therapies). Therefore, inhibitors that show better specificity for SPP of GS will be vital. While the effectiveness of SPP inhibition in killing erythrocytic stages *in vivo* is still unknown, a dual inhibitor with potency against the exo-erythrocytic and erythrocytic stages would represent a valuable tool in the antimalarial arsenal.

That it was possible to generate parasites resistant to the inhibitors *in vitro* should not disqualify PfSPP as a drug target. Selection of resistance was accomplished via the continuous application of the SPP drugs to cultures over a period of months. In theory, this type of exposure would likely guarantee the development of resistance to most single-target compounds due to the natural mutation frequency in *P. falciparum* [137]. Today, single agent therapy for

malaria is highly recommended against, and the introduction of any new antimalarial agent, regardless of target, would surely be in combination with another therapeutic to prevent the emergence of resistance.

The function of PfSPP in the parasite endoplasmic reticulum

The work presented in Chapter 4 suggests that PfSPP may be necessary for the maintenance of protein homeostasis, potentially in the parasite's ERAD pathway. Parasites show extreme sensitivity to SPP inhibition when combined with a compound (thapsigargin) that induces ER protein misfolding. In addition, this also corroborates evidence in mammalian cells that has shown SPP is required for protein dislocation from the ER during ERAD, although no precise role has been hypothesized [127,129].

As a multipass transmembrane protein, it is tempting to think of SPP as the channel through which ERAD substrates translocate into the cytosol, which has not yet been conclusively identified [156]. However this scenario is complicated by the aspartyl protease active site that fills the hydrophilic intramembrane cavity of SPP. ERAD substrates that pass through the pore would likely result in one of two fates: proteolytically cleavage by SPP or otherwise clogging of the pore by ERAD substrates not cleaved by SPP. There is of yet no evidence for proteolytic processing of ERAD substrates prior to dislocation.

It may be possible that a particular domain exists within SPP to recognize destabilized and unfolded transmembrane peptide ERAD substrates independent

of its protease activity. SPP preferentially associates with truncated transmembrane peptides, and this interaction is abrogated by (Z-LL)₂ [130,157]. Intriguingly, although the active site inhibitor blocks the interaction, the stabilization was reproduced with an active site “dead” mutant of SPP and therefore independent of catalytic activity. In this scenario, SPP may play a key intermediate in the hand-off of transmembrane ERAD substrates to, potentially to p97. This is analogous to rhomboid mitochondria intramembrane protease PcP1, which cooperates with the AAA ATPase mAAA to dislocate and degrade Ccp1 from the mitochondrial inner-membrane [158]. ERAD substrates destined for the proteasome emerge from the ER polyubiquitinated. Assessing ubiquitination levels in the absence and presence of SPP inhibitors may help to narrow down SPP’s role in the temporal scheme of the ERAD network.

The development of an ERAD cell-based assay may aid in the elucidation of the role of PfSPP and other putative members of this pathway. I am currently attempting to generate *T. gondii*-based ERAD assays using unstable GFP-tagged proteins as reporters for ERAD function. One assay will utilize the P30 protein of *T. gondii* fused to a destabilization domain (DD). P30 is a surface antigen in *T. gondii* that is trafficked via the ER. Upon destabilization by removal of the small ligand Shield 1, the P30-DD-GFP should be removed from the ER and degraded by the ERAD pathway. Another strategy would be to utilize a known unstable protein that upon synthesis in the ER membrane undergoes ERAD. Many of these proteins have been well characterized (e.g. TCR- α , null-Hong Kong α_1 -antitrypsin) and have been used as model substrates to assess

the integrity of ERAD *in vivo* [159,160]. In this reporter system impairment of ERAD function is indicated by an accumulation of the GFP substrate within the ER. A working functional assay such as this would allow the analysis of ERAD in real-time by light microscopy, or a quantifiable static assessment by western blot or flow cytometry. We will use this assay to assess whether PfSPP (and p97) inhibition disrupts ERAD activity in parasites.

Clues to the biological function of PfSPP may also be obtained by the identification of its downstream proteolytic substrates. Proteomics-based substrate identification has proven beneficial in the identification of substrates for numerous proteases, and has helped to advance understanding of their roles. At least two potential methods exist that may be utilized for enabling substrate identification of substrates [161]. The first is a comparative gel-based approach, in which proteins whose 1D-SDS-PAGE migration patterns differ significantly between two samples are subjected to LC-MS/MS analysis. In this case, the comparison would be between parasites treated with SPP inhibitors and those left untreated. Another method involves the use of tagged inactive protease with active site mutation that allows trapping of the substrate with the inactive protease, which allows for purification of the protease and substrate together. The Golde lab has validated this methodology for SPP in mammalian cells, but its feasibility *P. falciparum* has not been tested. Validation of putative substrates could be carried out by analysis in our heterologous yeast assay.

Inhibiting the protozoan ERAD pathway as an antimalarial strategy

While residing in the host erythrocyte *P. falciparum* establishes a complicated protein secretory network to facilitate protein trafficking to destinations both inside and outside the parasite. This specialized secretory system is likely highly dependent fully functional ER to facilitate high rates of protein folding and secretion. Therefore, protein quality control in the ER and the mechanisms that relieve the ER of misfolded proteins is an essential component of a high-functioning ER. Combined results in Chapter 4 for suggest that parasites are highly susceptible to perturbations in ER function and the ERAD pathway specifically, and that targeting components therein may serve as a therapeutic strategy. Inhibitors of p97, an ATPase chaperone involved in protein folding and unfolding, are potent against *P. falciparum* in nanomolar concentrations, are potentiated by PfSPP inhibitors, and have no toxicity to non-cancerous human cell lines [147,162]. This family of proteins has two representatives in *P. falciparum*, PF07_0047 and PFF0940c. The gene encoding PF07_0047 contains a transit peptide that localizes GFP to the apicoplast. It has been hypothesized the certain components of the *P. falciparum* protein ERAD machinery have been duplicated and are used for protein import into the apicoplast, a relic plastid gained by a secondary endosymbiotic event [149]. The coding region of PFF0940c contains no identifiable localization sequences, and is likely cytosolic. Parasites treated with the p97 inhibitors die within one 48 hr lifecycle, as opposed the delayed death phenotype observed with apicoplast-targeting inhibitors [163]. Thus it is likely the effects produced by the p97 inhibitors are derived from inhibition of the cytosolic p97 ATPase, likely

PFF0904c.

Parasites show remarkable sensitivity to non-optimized inhibitors of p97, but the high homology between human and parasite p97 makes it of therapeutic interest to develop specific inhibitors to the parasite enzyme. One approach to discover selective inhibitors would be through the development of an *in vitro* p97 assay amenable to high-throughput screening methods. The Deshaies lab recently developed a p97 ATPase assay that relies on using luciferase to measure the amount of ATP that remained after incubation with p97. This assay would likely be suitable for testing recombinant Plasmodium p97 as well, allowing for the facile comparison of cross-targeting of inhibitors.

References

1. Hay SI, Okiro EA, Gething PW, Patil AP, Tatem AJ, et al. (2010) Estimating the global clinical burden of *Plasmodium falciparum* malaria in 2007. *PLoS Med* 7: e1000290.
2. Breman JG (2001) The ears of the hippopotamus: manifestations, determinants, and estimates of the malaria burden. *Am J Trop Med Hyg* 64: 1-11.
3. Weatherall DJ, Miller LH, Baruch DI, Marsh K, Doumbo OK, et al. (2002) Malaria and the red cell. *Hematology Am Soc Hematol Educ Program*: 35-57.
4. Chima RI, Goodman CA, Mills A (2003) The economic impact of malaria in Africa: a critical review of the evidence. *Health Policy* 63: 17-36.
5. Kitron U, Spielman A (1989) Suppression of transmission of malaria through source reduction: antianopheline measures applied in Israel, the United States, and Italy. *Rev Infect Dis* 11: 391-406.
6. Najera JA, Gonzalez-Silva M, Alonso PL (2011) Some lessons for the future from the Global Malaria Eradication Programme (1955-1969). *PLoS Med* 8: e1000412.
7. White NJ (2011) A vaccine for malaria. *N Engl J Med* 365: 1926-1927.
8. Sa JM, Chong JL, Wellems TE (2011) Malaria drug resistance: new observations and developments. *Essays Biochem* 51: 137-160.
9. Mita T, Tanabe K, Kita K (2009) Spread and evolution of *Plasmodium falciparum* drug resistance. *Parasitol Int* 58: 201-209.
10. Dondorp AM, Fairhurst RM, Slutsker L, Macarthur JR, M DJ, et al. (2011) The threat of artemisinin-resistant malaria. *N Engl J Med* 365: 1073-1075.
11. Kappe SH, Vaughan AM, Boddey JA, Cowman AF (2010) That was then but this is now: malaria research in the time of an eradication agenda. *Science* 328: 862-866.
12. Wu Y, Wang X, Liu X, Wang Y (2003) Data-mining approaches reveal hidden families of proteases in the genome of malaria parasite. *Genome Res* 13: 601-616.
13. Blackman MJ (2000) Proteases involved in erythrocyte invasion by the malaria parasite: function and potential as chemotherapeutic targets. *Curr Drug Targets* 1: 59-83.
14. Roiko MS, Carruthers VB (2009) New roles for perforins and proteases in apicomplexan egress. *Cell Microbiol* 11: 1444-1452.
15. Francis SE, Sullivan DJ, Jr., Goldberg DE (1997) Hemoglobin metabolism in the malaria parasite *Plasmodium falciparum*. *Annu Rev Microbiol* 51: 97-123.
16. Miller LH, Dvorak JA, Shiroishi T, Durocher JR (1973) Influence of erythrocyte membrane components on malaria merozoite invasion. *J Exp Med* 138: 1597-1601.
17. Holder AA, Guevara Patino JA, Uthapibull C, Syed SE, Ling IT, et al. (1999) Merozoite surface protein 1, immune evasion, and vaccines against asexual blood stage malaria. *Parassitologia* 41: 409-414.

18. Harris PK, Yeoh S, Dluzewski AR, O'Donnell RA, Withers-Martinez C, et al. (2005) Molecular identification of a malaria merozoite surface sheddase. *PLoS Pathog* 1: 241-251.
19. Mitchell GH, Thomas AW, Margos G, Dluzewski AR, Bannister LH (2004) Apical membrane antigen 1, a major malaria vaccine candidate, mediates the close attachment of invasive merozoites to host red blood cells. *Infect Immun* 72: 154-158.
20. Howell SA, Withers-Martinez C, Kocken CH, Thomas AW, Blackman MJ (2001) Proteolytic processing and primary structure of *Plasmodium falciparum* apical membrane antigen-1. *J Biol Chem* 276: 31311-31320.
21. Baker RP, Wijetilaka R, Urban S (2006) Two *Plasmodium* rhomboid proteases preferentially cleave different adhesins implicated in all invasive stages of malaria. *PLoS Pathog* 2: e113.
22. Lew VL, Tiffert T, Ginsburg H (2003) Excess hemoglobin digestion and the osmotic stability of *Plasmodium falciparum*-infected red blood cells. *Blood* 101: 4189-4194.
23. Sherman IW (1977) Amino acid metabolism and protein synthesis in malarial parasites. *Bull World Health Organ* 55: 265-276.
24. Ersmark K, Samuelsson B, Hallberg A (2006) Plasmepsins as potential targets for new antimalarial therapy. *Med Res Rev* 26: 626-666.
25. Rosenthal PJ, Sijwali PS, Singh A, Shenai BR (2002) Cysteine proteases of malaria parasites: targets for chemotherapy. *Curr Pharm Des* 8: 1659-1672.
26. Goldberg DE, Slater AF, Cerami A, Henderson GB (1990) Hemoglobin degradation in the malaria parasite *Plasmodium falciparum*: an ordered process in a unique organelle. *Proc Natl Acad Sci U S A* 87: 2931-2935.
27. Goldberg DE, Slater AF, Beavis R, Chait B, Cerami A, et al. (1991) Hemoglobin degradation in the human malaria pathogen *Plasmodium falciparum*: a catabolic pathway initiated by a specific aspartic protease. *J Exp Med* 173: 961-969.
28. Rosenthal PJ, McKerrow JH, Aikawa M, Nagasawa H, Leech JH (1988) A malarial cysteine proteinase is necessary for hemoglobin degradation by *Plasmodium falciparum*. *J Clin Invest* 82: 1560-1566.
29. Subramanian S, Hardt M, Choe Y, Niles RK, Johansen EB, et al. (2009) Hemoglobin cleavage site-specificity of the *Plasmodium falciparum* cysteine proteases falcipain-2 and falcipain-3. *PLoS One* 4: e5156.
30. Bonilla JA, Bonilla TD, Yowell CA, Fujioka H, Dame JB (2007) Critical roles for the digestive vacuole plasmepsins of *Plasmodium falciparum* in vacuolar function. *Mol Microbiol* 65: 64-75.
31. Eggleston KK, Duffin KL, Goldberg DE (1999) Identification and characterization of falcilysin, a metallopeptidase involved in hemoglobin catabolism within the malaria parasite *Plasmodium falciparum*. *J Biol Chem* 274: 32411-32417.
32. Millholland MG, Chandramohanadas R, Pizarro A, Wehr A, Shi H, et al. (2011) The malaria parasite progressively dismantles the host erythrocyte cytoskeleton for efficient egress. *Mol Cell Proteomics*.
33. Aly AS, Matuschewski K (2005) A malarial cysteine protease is necessary for *Plasmodium* sporozoite egress from oocysts. *J Exp Med* 202: 225-230.

34. McCoubrie JE, Miller SK, Sargeant T, Good RT, Hodder AN, et al. (2007) Evidence for a common role for the serine-type *Plasmodium falciparum* serine repeat antigen proteases: implications for vaccine and drug design. *Infect Immun* 75: 5565-5574.
35. Delplace P, Bhatia A, Cagnard M, Camus D, Colombet G, et al. (1988) Protein p126: a parasitophorous vacuole antigen associated with the release of *Plasmodium falciparum* merozoites. *Biol Cell* 64: 215-221.
36. Hodder AN, Drew DR, Epa VC, Delorenzi M, Bourgon R, et al. (2003) Enzymic, phylogenetic, and structural characterization of the unusual papain-like protease domain of *Plasmodium falciparum* SERA5. *J Biol Chem* 278: 48169-48177.
37. Crabb BS, Rug M, Gilberger TW, Thompson JK, Triglia T, et al. (2004) Transfection of the human malaria parasite *Plasmodium falciparum*. *Methods Mol Biol* 270: 263-276.
38. Meissner M, Krejany E, Gilson PR, de Koning-Ward TF, Soldati D, et al. (2005) Tetracycline analogue-regulated transgene expression in *Plasmodium falciparum* blood stages using *Toxoplasma gondii* transactivators. *Proc Natl Acad Sci U S A* 102: 2980-2985.
39. Smukste I, Stockwell BR (2005) Advances in chemical genetics. *Annu Rev Genomics Hum Genet* 6: 261-286.
40. Banaszynski LA, Chen LC, Maynard-Smith LA, Ooi AG, Wandless TJ (2006) A rapid, reversible, and tunable method to regulate protein function in living cells using synthetic small molecules. *Cell* 126: 995-1004.
41. Dvorin JD, Martyn DC, Patel SD, Grimley JS, Collins CR, et al. (2010) A plant-like kinase in *Plasmodium falciparum* regulates parasite egress from erythrocytes. *Science* 328: 910-912.
42. Dluzewski AR, Rangachari K, Wilson RJ, Gratzer WB (1986) *Plasmodium falciparum*: protease inhibitors and inhibition of erythrocyte invasion. *Exp Parasitol* 62: 416-422.
43. Klemba M, Gluzman I, Goldberg DE (2004) A *Plasmodium falciparum* dipeptidyl aminopeptidase I participates in vacuolar hemoglobin degradation. *J Biol Chem* 279: 43000-43007.
44. Dalal S, Klemba M (2007) Roles for two aminopeptidases in vacuolar hemoglobin catabolism in *Plasmodium falciparum*. *J Biol Chem* 282: 35978-35987.
45. Arastu-Kapur S, Ponder EL, Fonovic UP, Yeoh S, Yuan F, et al. (2008) Identification of proteases that regulate erythrocyte rupture by the malaria parasite *Plasmodium falciparum*. *Nat Chem Biol* 4: 203-213.
46. Lyon JA, Haynes JD (1986) *Plasmodium falciparum* antigens synthesized by schizonts and stabilized at the merozoite surface when schizonts mature in the presence of protease inhibitors. *J Immunol* 136: 2245-2251.
47. Chandramohanadas R, Davis PH, Beiting DP, Harbut MB, Darling C, et al. (2009) Apicomplexan parasites co-opt host calpains to facilitate their escape from infected cells. *Science* 324: 794-797.

48. Greenbaum DC, Baruch A, Grainger M, Bozdech Z, Medzihradszky KF, et al. (2002) A role for the protease falcipain 1 in host cell invasion by the human malaria parasite. *Science* 298: 2002-2006.
49. Turk B (2006) Targeting proteases: successes, failures and future prospects. *Nat Rev Drug Discov* 5: 785-799.
50. McKerrow JH, Sun E, Rosenthal PJ, Bouvier J (1993) The proteases and pathogenicity of parasitic protozoa. *Annu Rev Microbiol* 47: 821-853.
51. Ettari R, Bova F, Zappala M, Grasso S, Micale N (2010) Falcipain-2 inhibitors. *Med Res Rev* 30: 136-167.
52. Sijwali PS, Koo J, Singh N, Rosenthal PJ (2006) Gene disruptions demonstrate independent roles for the four falcipain cysteine proteases of *Plasmodium falciparum*. *Mol Biochem Parasitol* 150: 96-106.
53. Omara-Opyene AL, Moura PA, Sulsona CR, Bonilla JA, Yowell CA, et al. (2004) Genetic disruption of the *Plasmodium falciparum* digestive vacuole plasmepsins demonstrates their functional redundancy. *J Biol Chem* 279: 54088-54096.
54. Lee BJ, Singh A, Chiang P, Kemp SJ, Goldman EA, et al. (2003) Antimalarial activities of novel synthetic cysteine protease inhibitors. *Antimicrob Agents Chemother* 47: 3810-3814.
55. Luan Y, Xu W (2007) The structure and main functions of aminopeptidase N. *Curr Med Chem* 14: 639-647.
56. Sato Y (2004) Role of aminopeptidase in angiogenesis. *Biol Pharm Bull* 27: 772-776.
57. Foulon T, Cadel S, Cohen P (1999) Aminopeptidase B (EC 3.4.11.6). *Int J Biochem Cell Biol* 31: 747-750.
58. Sato Y (2003) Aminopeptidases and angiogenesis. *Endothelium* 10: 287-290.
59. Danziger RS (2008) Aminopeptidase N in arterial hypertension. *Heart Fail Rev* 13: 293-298.
60. Greenbaum D, Medzihradszky KF, Burlingame A, Bogyo M (2000) Epoxide electrophiles as activity-dependent cysteine protease profiling and discovery tools. *Chem Biol* 7: 569-581.
61. Liu Y, Jiang N, Wu J, Dai W, Rosenblum JS (2006) Polo-like kinases inhibited by wortmannin: Labeling site and downstream effects. *J Biol Chem*.
62. Kumar S, Zhou B, Liang F, Wang WQ, Huang Z, et al. (2004) Activity-based probes for protein tyrosine phosphatases. *Proc Natl Acad Sci U S A* 101: 7943-7948.
63. Vocadlo DJ, Bertozzi CR (2004) A strategy for functional proteomic analysis of glycosidase activity from cell lysates. *Angew Chem Int Ed Engl* 43: 5338-5342.
64. Adam GC, Cravatt BF, Sorensen EJ (2001) Profiling the specific reactivity of the proteome with non-directed activity-based probes. *Chem Biol* 8: 81-95.
65. Giannousis PP, Bartlett PA (1987) Phosphorus amino acid analogues as inhibitors of leucine aminopeptidase. *J Med Chem* 30: 1603-1609.
66. Chan WW, Dennis P, Demmer W, Brand K (1982) Inhibition of leucine aminopeptidase by amino acid hydroxamates. *J Biol Chem* 257: 7955-7957.

67. Saghatelian A, Jessani N, Joseph A, Humphrey M, Cravatt BF (2004) Activity-based probes for the proteomic profiling of metalloproteases. *Proc Natl Acad Sci U S A* 101: 10000-10005.
68. Wilkes SH, Prescott JM (1985) The slow, tight binding of bestatin and amastatin to aminopeptidases. *J Biol Chem* 260: 13154-13162.
69. Rich DH, Moon BJ, Harbeson S (1984) Inhibition of aminopeptidases by amastatin and bestatin derivatives. Effect of inhibitor structure on slow-binding processes. *J Med Chem* 27: 417-422.
70. Burley SK, David PR, Lipscomb WN (1991) Leucine aminopeptidase: bestatin inhibition and a model for enzyme-catalyzed peptide hydrolysis. *Proc Natl Acad Sci U S A* 88: 6916-6920.
71. Tsuge H, Ago H, Aoki M, Furuno M, Noma M, et al. (1994) Crystallization and preliminary X-ray crystallographic studies of recombinant human leukotriene A4 hydrolase complexed with bestatin. *J Mol Biol* 238: 854-856.
72. Addlagatta A, Gay L, Matthews BW (2006) Structure of aminopeptidase N from *Escherichia coli* suggests a compartmentalized, gated active site. *Proc Natl Acad Sci U S A* 103: 13339-13344.
73. Sekine K, Fujii H, Abe F (1999) Induction of apoptosis by bestatin (ubenimex) in human leukemic cell lines. *Leukemia* 13: 729-734.
74. Ezawa K, Minato K, Dobashi K (1996) Induction of apoptosis by ubenimex (Bestatin) in human non-small-cell lung cancer cell lines. *Biomed Pharmacother* 50: 283-289.
75. Penning TD (2001) Inhibitors of leukotriene A4 (LTA4) hydrolase as potential anti-inflammatory agents. *Curr Pharm Des* 7: 163-179.
76. Huisgen R, Mloston G, Polborn K (1996) 1,3-Dipolar Activity in Cycloadditions of an Aliphatic Sulfine(.) (1). *J Org Chem* 61: 6570-6574.
77. Kaval N, Ermolat'ev D, Appukkuttan P, Dehaen W, Kappe CO, et al. (2005) The application of "click chemistry" for the decoration of 2(1H)-pyrazinone scaffold: generation of templates. *J Comb Chem* 7: 490-502.
78. Snow RW, Guerra CA, Noor AM, Myint HY, Hay SI (2005) The global distribution of clinical episodes of *Plasmodium falciparum* malaria. *Nature* 434: 214-217.
79. Miller LH, Baruch DI, Marsh K, Doumbo OK (2002) The pathogenic basis of malaria. *Nature* 415: 673-679.
80. O'Donnell RA, Hackett F, Howell SA, Treeck M, Struck N, et al. (2006) Intramembrane proteolysis mediates shedding of a key adhesin during erythrocyte invasion by the malaria parasite. *J Cell Biol* 174: 1023-1033.
81. Skinner-Adams TS, Stack CM, Trenholme KR, Brown CL, Grembecka J, et al. (2010) *Plasmodium falciparum* neutral aminopeptidases: new targets for anti-malarials. *Trends Biochem Sci* 35: 53-61.
82. Liu J, Istvan ES, Gluzman IY, Gross J, Goldberg DE (2006) *Plasmodium falciparum* ensures its amino acid supply with multiple acquisition pathways and redundant proteolytic enzyme systems. *Proc Natl Acad Sci U S A* 103: 8840-8845.
83. Curley GP, O'Donovan SM, McNally J, Mullally M, O'Hara H, et al. (1994) Aminopeptidases from *Plasmodium falciparum*, *Plasmodium chabaudi chabaudi* and *Plasmodium berghei*. *J Eukaryot Microbiol* 41: 119-123.

84. Kolakovich KA, Gluzman IY, Duffin KL, Goldberg DE (1997) Generation of hemoglobin peptides in the acidic digestive vacuole of *Plasmodium falciparum* implicates peptide transport in amino acid production. *Mol Biochem Parasitol* 87: 123-135.
85. Allary M, Schrevel J, Florent I (2002) Properties, stage-dependent expression and localization of *Plasmodium falciparum* M1 family zinc-aminopeptidase. *Parasitology* 125: 1-10.
86. Ragheb D, Bompiani K, Dalal S, Klemba M (2009) Evidence for catalytic roles for *Plasmodium falciparum* aminopeptidase P in the food vacuole and cytosol. *J Biol Chem* 284: 24806-24815.
87. Azimzadeh O, Sow C, Geze M, Nyalwidhe J, Florent I (2010) *Plasmodium falciparum* PfA-M1 aminopeptidase is trafficked via the parasitophorous vacuole and marginally delivered to the food vacuole. *Malar J* 9: 189.
88. Stack CM, Lowther J, Cunningham E, Donnelly S, Gardiner DL, et al. (2007) Characterization of the *Plasmodium falciparum* M17 leucyl aminopeptidase. A protease involved in amino acid regulation with potential for antimalarial drug development. *J Biol Chem* 282: 2069-2080.
89. Harbut MB, Velmourougane G, Reiss G, Chandramohanadas R, Greenbaum DC (2008) Development of bestatin-based activity-based probes for metallo-aminopeptidases. *Bioorg Med Chem Lett* 18: 5932-5936.
90. Barglow KT, Cravatt BF (2007) Activity-based protein profiling for the functional annotation of enzymes. *Nat Methods* 4: 822-827.
91. Salisbury CM, Cravatt BF (2007) Activity-based probes for proteomic profiling of histone deacetylase complexes. *Proc Natl Acad Sci U S A* 104: 1171-1176.
92. Cohen MS, Hadjivassiliou H, Taunton J (2007) A clickable inhibitor reveals context-dependent autoactivation of p90 RSK. *Nat Chem Biol* 3: 156-160.
93. Suda H, Aoyagi T, Takeuchi T, Umezawa H (1976) Inhibition of aminopeptidase B and leucine aminopeptidase by bestatin and its stereoisomer. *Arch Biochem Biophys* 177: 196-200.
94. Lowther WT, Matthews BW (2002) Metalloaminopeptidases: common functional themes in disparate structural surroundings. *Chem Rev* 102: 4581-4608.
95. Nankya-Kitaka MF, Curley GP, Gavigan CS, Bell A, Dalton JP (1998) *Plasmodium chabaudi chabaudi* and *P. falciparum*: inhibition of aminopeptidase and parasite growth by bestatin and nitrobestatin. *Parasitol Res* 84: 552-558.
96. Gavigan CS, Dalton JP, Bell A (2001) The role of aminopeptidases in haemoglobin degradation in *Plasmodium falciparum*-infected erythrocytes. *Mol Biochem Parasitol* 117: 37-48.
97. Naughton JA, Nasizadeh S, Bell A (2010) Downstream effects of haemoglobinase inhibition in *Plasmodium falciparum*-infected erythrocytes. *Mol Biochem Parasitol* 173: 81-87.
98. Nishizawa R, Saino T, Takita T, Suda H, Aoyagi T (1977) Synthesis and structure-activity relationships of bestatin analogues, inhibitors of aminopeptidase B. *J Med Chem* 20: 510-515.
99. Schechter I, Berger A (1967) On the size of the active site in proteases. I. Papain. *Biochem Biophys Res Commun* 27: 157-162.

100. McGowan S, Porter CJ, Lowther J, Stack CM, Golding SJ, et al. (2009) Structural basis for the inhibition of the essential *Plasmodium falciparum* M1 neutral aminopeptidase. *Proc Natl Acad Sci U S A* 106: 2537-2542.
101. Rostovtsev VV, Green LG, Fokin VV, Sharpless KB (2002) A stepwise Huisgen cycloaddition process: copper(I)-catalyzed regioselective "ligation" of azides and terminal alkynes. *Angew Chem Int Ed Engl* 41: 2596-2599.
102. Wang Q, Chan TR, Hilgraf R, Fokin VV, Sharpless KB, et al. (2003) Bioconjugation by copper(I)-catalyzed azide-alkyne [3 + 2] cycloaddition. *J Am Chem Soc* 125: 3192-3193.
103. Speers AE, Adam GC, Cravatt BF (2003) Activity-based protein profiling in vivo using a copper(I)-catalyzed azide-alkyne [3 + 2] cycloaddition. *J Am Chem Soc* 125: 4686-4687.
104. McGowan S, Oellig CA, Birru WA, Caradoc-Davies TT, Stack CM, et al. (2010) Structure of the *Plasmodium falciparum* M17 aminopeptidase and significance for the design of drugs targeting the neutral exopeptidases. *Proc Natl Acad Sci U S A* 107: 2449-2454.
105. Skinner TS, Manning LS, Johnston WA, Davis TM (1996) In vitro stage-specific sensitivity of *Plasmodium falciparum* to quinine and artemisinin drugs. *Int J Parasitol* 26: 519-525.
106. Klemba M, Beatty W, Gluzman I, Goldberg DE (2004) Trafficking of plasmepsin II to the food vacuole of the malaria parasite *Plasmodium falciparum*. *J Cell Biol* 164: 47-56.
107. Gluzman IY, Francis SE, Oksman A, Smith CE, Duffin KL, et al. (1994) Order and specificity of the *Plasmodium falciparum* hemoglobin degradation pathway. *J Clin Invest* 93: 1602-1608.
108. Wang F, Krai P, Deu E, Bibb B, Lauritzen C, et al. (2011) Biochemical characterization of *Plasmodium falciparum* dipeptidyl aminopeptidase 1. *Mol Biochem Parasitol* 175: 10-20.
109. Martin RE, Kirk K (2007) Transport of the essential nutrient isoleucine in human erythrocytes infected with the malaria parasite *Plasmodium falciparum*. *Blood* 109: 2217-2224.
110. Saric T, Graef CI, Goldberg AL (2004) Pathway for degradation of peptides generated by proteasomes: a key role for thimet oligopeptidase and other metallopeptidases. *J Biol Chem* 279: 46723-46732.
111. Botbol V, Scornik OA (1979) Intermediates in the degradation of abnormal globin. Bestatin permits the accumulation of the same peptides in cell-free extracts as in intact reticulocytes. *J Biol Chem* 254: 11254-11257.
112. Gantt SM, Myung JM, Briones MR, Li WD, Corey EJ, et al. (1998) Proteasome inhibitors block development of *Plasmodium* spp. *Antimicrob Agents Chemother* 42: 2731-2738.
113. Gavigan CS, Machado SG, Dalton JP, Bell A (2001) Analysis of antimalarial synergy between bestatin and endoprotease inhibitors using statistical response-surface modelling. *Antimicrob Agents Chemother* 45: 3175-3181.
114. Ragheb D, Dalal S, Bompiani KM, Ray WK, Klemba M (2011) Distribution and biochemical properties of an M1-family aminopeptidase in *Plasmodium*

- falciparum indicate a role in vacuolar hemoglobin catabolism. *J Biol Chem* 286: 27255-27265.
115. Androulakis S, Schmidberger J, Bate MA, DeGori R, Beitz A, et al. (2008) Federated repositories of X-ray diffraction images. *Acta Crystallogr D Biol Crystallogr* D64: 810-814.
 116. Maric S, Donnelly SM, Robinson MW, Skinner-Adams T, Trenholme KR, et al. (2009) The M17 leucine aminopeptidase of the malaria parasite *Plasmodium falciparum*: importance of active site metal ions in the binding of substrates and inhibitors. *Biochemistry* 48: 5435-5439.
 117. Weiss LM, Dubey JP (2009) Toxoplasmosis: A history of clinical observations. *Int J Parasitol* 39: 895-901.
 118. Fevre EM, Picozzi K, Jannin J, Welburn SC, Maudlin I (2006) Human African trypanosomiasis: Epidemiology and control. *Adv Parasitol* 61: 167-221.
 119. Sibley LD (2011) Invasion and intracellular survival by protozoan parasites. *Immunol Rev* 240: 72-91.
 120. McKerrow JH, Rosenthal PJ, Swenerton R, Doyle P (2008) Development of protease inhibitors for protozoan infections. *Curr Opin Infect Dis* 21: 668-672.
 121. Weihofen A, Binns K, Lemberg MK, Ashman K, Martoglio B (2002) Identification of signal peptide peptidase, a presenilin-type aspartic protease. *Science* 296: 2215-2218.
 122. Martoglio B, Golde TE (2003) Intramembrane-cleaving aspartic proteases and disease: presenilins, signal peptide peptidase and their homologs. *Hum Mol Genet* 12 Spec No 2: R201-206.
 123. Ponting CP, Hutton M, Nyborg A, Baker M, Jansen K, et al. (2002) Identification of a novel family of presenilin homologues. *Hum Mol Genet* 11: 1037-1044.
 124. Grigorenko AP, Moliaka YK, Soto MC, Mello CC, Rogaev EI (2004) The *Caenorhabditis elegans* IMPAS gene, *imp-2*, is essential for development and is functionally distinct from related presenilins. *Proc Natl Acad Sci U S A* 101: 14955-14960.
 125. Casso DJ, Tanda S, Biehs B, Martoglio B, Kornberg TB (2005) *Drosophila* signal peptide peptidase is an essential protease for larval development. *Genetics* 170: 139-148.
 126. Krawitz P, Haffner C, Fluhrer R, Steiner H, Schmid B, et al. (2005) Differential localization and identification of a critical aspartate suggest non-redundant proteolytic functions of the presenilin homologues SPPL2b and SPPL3. *J Biol Chem* 280: 39515-39523.
 127. Loureiro J, Lilley BN, Spooner E, Noriega V, Tortorella D, et al. (2006) Signal peptide peptidase is required for dislocation from the endoplasmic reticulum. *Nature* 441: 894-897.
 128. Stagg HR, Thomas M, van den Boomen D, Wiertz EJ, Drabkin HA, et al. (2009) The TRC8 E3 ligase ubiquitinates MHC class I molecules before dislocation from the ER. *J Cell Biol* 186: 685-692.
 129. Lee SO, Cho K, Cho S, Kim I, Oh C, et al. (2010) Protein disulphide isomerase is required for signal peptide peptidase-mediated protein degradation. *EMBO J* 29: 363-375.

130. Schrul B, Kapp K, Sinning I, Dobberstein B (2010) Signal peptide peptidase (SPP) assembles with substrates and misfolded membrane proteins into distinct oligomeric complexes. *Biochem J* 427: 523-534.
131. Li X, Chen H, Bahamontes-Rosa N, Kun JF, Traore B, et al. (2009) Plasmodium falciparum signal peptide peptidase is a promising drug target against blood stage malaria. *Biochem Biophys Res Commun* 380: 454-459.
132. Weihofen A, Lemberg MK, Ploegh HL, Bogyo M, Martoglio B (2000) Release of signal peptide fragments into the cytosol requires cleavage in the transmembrane region by a protease activity that is specifically blocked by a novel cysteine protease inhibitor. *J Biol Chem* 275: 30951-30956.
133. Kornilova AY, Bihel F, Das C, Wolfe MS (2005) The initial substrate-binding site of gamma-secretase is located on presenilin near the active site. *Proc Natl Acad Sci U S A* 102: 3230-3235.
134. Wolfe MS (2011) gamma-Secretase inhibitors and modulators for Alzheimer's disease. *J Neurochem*.
135. Sato T, Ananda K, Cheng CI, Suh EJ, Narayanan S, et al. (2008) Distinct pharmacological effects of inhibitors of signal peptide peptidase and gamma-secretase. *J Biol Chem* 283: 33287-33295.
136. Wong GT, Manfra D, Poulet FM, Zhang Q, Josien H, et al. (2004) Chronic treatment with the gamma-secretase inhibitor LY-411,575 inhibits beta-amyloid peptide production and alters lymphopoiesis and intestinal cell differentiation. *J Biol Chem* 279: 12876-12882.
137. Nzila A, Mwai L (2010) In vitro selection of Plasmodium falciparum drug-resistant parasite lines. *J Antimicrob Chemother* 65: 390-398.
138. Rottmann M, McNamara C, Yeung BK, Lee MC, Zou B, et al. (2010) Spiroindolones, a potent compound class for the treatment of malaria. *Science* 329: 1175-1180.
139. Nam TG, McNamara CW, Bopp S, Dharia NV, Meister S, et al. (2011) A Chemical Genomic Analysis of Decoquinone, a Plasmodium falciparum Cytochrome b Inhibitor. *ACS Chem Biol* 6: 1214-1222.
140. Wolfe MS (2010) Structure, mechanism and inhibition of gamma-secretase and presenilin-like proteases. *Biol Chem* 391: 839-847.
141. Balu B, Shoue DA, Fraser MJ, Jr., Adams JH (2005) High-efficiency transformation of Plasmodium falciparum by the lepidopteran transposable element piggyBac. *Proc Natl Acad Sci U S A* 102: 16391-16396.
142. Klemba M, Goldberg DE (2005) Characterization of plasmepsin V, a membrane-bound aspartic protease homolog in the endoplasmic reticulum of Plasmodium falciparum. *Mol Biochem Parasitol* 143: 183-191.
143. Bozdech Z, Llinas M, Pulliam BL, Wong ED, Zhu J, et al. (2003) The transcriptome of the intraerythrocytic developmental cycle of Plasmodium falciparum. *PLoS Biol* 1: E5.
144. Cooke BM, Lingelbach K, Bannister LH, Tilley L (2004) Protein trafficking in Plasmodium falciparum-infected red blood cells. *Trends Parasitol* 20: 581-589.
145. Bagola K, Mehnert M, Jarosch E, Sommer T (2011) Protein dislocation from the ER. *Biochim Biophys Acta* 1808: 925-936.

146. Rabinovich E, Kerem A, Frohlich KU, Diamant N, Bar-Nun S (2002) AAA-ATPase p97/Cdc48p, a cytosolic chaperone required for endoplasmic reticulum-associated protein degradation. *Mol Cell Biol* 22: 626-634.
147. Chou TF, Brown SJ, Minond D, Nordin BE, Li K, et al. (2011) Reversible inhibitor of p97, DBeQ, impairs both ubiquitin-dependent and autophagic protein clearance pathways. *Proc Natl Acad Sci U S A* 108: 4834-4839.
148. Wang Q, Li L, Ye Y (2008) Inhibition of p97-dependent protein degradation by Eeyarestatin I. *J Biol Chem* 283: 7445-7454.
149. Spork S, Hiss JA, Mandel K, Sommer M, Kooij TW, et al. (2009) An unusual ERAD-like complex is targeted to the apicoplast of *Plasmodium falciparum*. *Eukaryot Cell* 8: 1134-1145.
150. Bland FA, Lemberg MK, McMichael AJ, Martoglio B, Braud VM (2003) Requirement of the proteasome for the trimming of signal peptide-derived epitopes presented by the nonclassical major histocompatibility complex class I molecule HLA-E. *J Biol Chem* 278: 33747-33752.
151. Kornilova AY, Kim J, Laudon H, Wolfe MS (2006) Deducing the transmembrane domain organization of presenilin-1 in gamma-secretase by cysteine disulfide cross-linking. *Biochemistry* 45: 7598-7604.
152. Gosline SJ, Nascimento M, McCall LI, Zilberstein D, Thomas DY, et al. (2011) Intracellular eukaryotic parasites have a distinct unfolded protein response. *PLoS One* 6: e19118.
153. Deu E, Leyva MJ, Albrow VE, Rice MJ, Ellman JA, et al. (2010) Functional studies of *Plasmodium falciparum* dipeptidyl aminopeptidase I using small molecule inhibitors and active site probes. *Chem Biol* 17: 808-819.
154. Urabe A, Mutoh Y, Mizoguchi H, Takaku F, Ogawa N (1993) Ubenimex in the treatment of acute nonlymphocytic leukemia in adults. *Ann Hematol* 67: 63-66.
155. Parvanova I, Epiphany S, Fauq A, Golde TE, Prudencio M, et al. (2009) A small molecule inhibitor of signal peptide peptidase inhibits *Plasmodium* development in the liver and decreases malaria severity. *PLoS One* 4: e5078.
156. Braakman I, Bulleid NJ (2011) Protein folding and modification in the mammalian endoplasmic reticulum. *Annu Rev Biochem* 80: 71-99.
157. Crawshaw SG, Martoglio B, Meacock SL, High S (2004) A misassembled transmembrane domain of a polytopic protein associates with signal peptide peptidase. *Biochem J* 384: 9-17.
158. Tatsuta T, Augustin S, Nolden M, Friedrichs B, Langer T (2007) m-AAA protease-driven membrane dislocation allows intramembrane cleavage by rhomboid in mitochondria. *EMBO J* 26: 325-335.
159. Soetandyo N, Wang Q, Ye Y, Li L (2010) Role of intramembrane charged residues in the quality control of unassembled T-cell receptor alpha-chains at the endoplasmic reticulum. *J Cell Sci* 123: 1031-1038.
160. DeLaBarre B, Christianson JC, Kopito RR, Brunger AT (2006) Central pore residues mediate the p97/VCP activity required for ERAD. *Mol Cell* 22: 451-462.
161. Doucet A, Overall CM (2008) Protease proteomics: revealing protease in vivo functions using systems biology approaches. *Mol Aspects Med* 29: 339-358.

162. Wang Q, Mora-Jensen H, Weniger MA, Perez-Galan P, Wolford C, et al. (2009) ERAD inhibitors integrate ER stress with an epigenetic mechanism to activate BH3-only protein NOXA in cancer cells. *Proc Natl Acad Sci U S A* 106: 2200-2205.
163. Ekland EH, Schneider J, Fidock DA (2011) Identifying apicoplast-targeting antimalarials using high-throughput compatible approaches. *FASEB J* 25: 3583-3593.